Summary

Geological and structural evolution of tectonically active areas of the central Calabrian Arc

UNIVERSITÀ DELLA CALABRIA

Scuola di Dottorato "Archimede" in Scienze, Comunicazione e Tecnologie

UNIVERSITÀ DELLA CALABRIA

UNIVERSITA' DELLA CALABRIA

Dipartimento di Biologia, Ecologia e Scienze della Terra (DiBEST)

Scuola di Dottorato

"ARCHIMEDE" IN SCIENZE, COMUNICAZIONI E TECNOLOGIE

Indirizzo

Scienze della Terra

CICLO

XXVIII

TITOLO TESI

Geological and structural evolution of tectonically active areas of the central Calabria Arc

Settore Scientifico Disciplinare : Geo/02 Geologia Stratigrafica e Sedimentologica

Direttore: Ch.mo Prof. Pietro Pantano

Firma

Supervisore: Dott. ~~Francesco~~ Muto

Firma

Cotutor Dott/ssa Maria Filomena Loreto

Firma

Cotutor Ch.mo Prof. Salvatore Critelli

Firma

Dottorando: Dott. Fabrizio Brutto

Firma

A.A. 2012-2015

ABSTRACT

The Catanzaro Trough is a Neogene-Quaternary basin developed between the Serre and the Sila Massif, filled by up to 2000 m of Upper Miocene to Quaternary sedimentary succession, belonging to the central Calabrian Arc and extended from offshore, Sant'Eufemia Basin (SE Tyrrhenian Sea), to the onshore, Catanzaro Basin.

By joining on land geo-structural with marine geophysical data, we performed a detailed analysis of processes that during last 5 My have controlled the evolution of western portion of the Catanzaro Trough. The fieldwork study, focused on the onshore area, has allowed to acquire more than 700 fault planes, classified on the base of kinematics and fault directions, whereas the geophysical data (sub-bottom, multi- and mono-channel seismic profiles), coming from some scientific cruises within the Sant'Eufemia Gulf (SE Tyrrhenian Sea), gave us the opportunity to reconstruct the tectono-stratigraphic evolution of the offshore area.

The combination amongst abrupt sea level changes, transpressional and trans/extensional tectonics and back-arc Tyrrhenian subsidence during SE-drifting of Calabrian Arc controlled sedimentary basin hosted by the Catanzaro Trough, as the result we have recognized three tectonic events formed in the Upper Miocene- Zanclean, Piacezian-Lower Pleistocene, and Middle-Upper Pleistocene.

The data analysis provide information about stratigraphy and tectonics in the strata and also give some indication of the tectono-stratigraphic architecture. Sedimentary basin, in fact, looks to be mainly controlled by the activity of NW–SE and NE–SW oriented fault systems.

The NW-SE oriented faults showing strike slip and oblique kinematics can be considered responsible for the opening of a WNW–ESE paleo-strait connecting the Tyrrhenian Sea with the Ionian Sea during multi-phases tectonics that have acted in the study area since Miocene. The integrated geo-structural and geophysical data show a change from left-lateral to right-lateral kinematics during Piacezian-Lower Pleistocene, as the result of a change of the stress field.

Since Middle Pleistocene, the study area experienced an extensional phase, WNW-ESE oriented, controlled mainly by NE-SW and subordinately N-S oriented normal faults, which split obliquely the western Catanzaro Trough, producing up-faulted and down-faulted blocks, arranged as graben-type systems, extending from onshore to offshore area.

In agreement with and Jacques et al., (2001) and Presti et al., (2013), the NE-SW and N-S trend normal faults play a relevant role as part of recent seismotectonic processes controlling the Late Quaternary geodynamic of the central Calabrian Arc, representing the source of the main destructive earthquakes occurred in the area.

Thanks to these multidisciplinary approach we are able to provide a more reliable and detailed structural frame of the central Calabria segment, providing new elements about recent activity of faults, and giving a further contribution for the seismogenetic potential assessment of an area historically considered with the highest earthquake and tsunami risk throughout Italy.

KEY WORDS: Calabrian Arc, strike slip faults, extensional tectonics, seismotectonic.

RIASSUNTO

La stretta di Catanzaro è un bacino sedimentario caratterizzato da una successione sedimentaria compresa tra il Miocene ed il Quaternario, che raggiunge uno spessore di 2000m,. Questo bacino è collocato nell' Arco Calabro centrale, compreso tra il Massiccio delle Serre e quello della Sila e si estende dall'offshore tirrenico, bacino di Sant'Eufemia (Mar Tirreno meridionale), sino all'onshore calabrese, rappresentato dal bacino di Catanzaro.

La realizzazione di questo progetto ha comportato necessariamente un approccio multidisciplinare, dove l'integrazione di informazioni di carattere strutturale, geologico, geofisico e sismotetettonico è risultato di fondamentale importanza per la definizione dell' evoluzione tettonica neogenica-quaternaria dell'area.

La combinazione dei dati geologico-strutturali acquisiti nell'onshore calabrese (più di 700 piani di faglia distribuiti su circa 40 stazioni di misura strutturali, classificati in base alla cinematica e all'orientazione) ed i dati geofisici (profili sismici multicanale, monocanale e ad alta risoluzione) provenienti da alcune crociere scientifiche condotte all'interno del Golfo di Sant'Eufemia, hanno permesso un'analisi dettagliata dei processi che hanno controllato la Stretta di Catanzaro negli ultimi 5 milioni di anni, sia nella sua porzione onshore che offshore.

I dati ottenuti da questa analisi combinata ha mostrato come il bacino sedimentario della Stretta di Catanzaro è controllato principalmente da due sistemi di faglia orientati NW-SE e

NE-SW. L'analisi dei dati ha permesso di definire come il sistema NW-SE sia caratterizzato da una cinematica trascorrente, con una chiara componente estensionale, il quale ha gestito nelle prime fasi evolutive, legate all'apertura del paleo-stretto, agendo come zona di trasferimento ed accomodamento tensionale tra l 'Arco Calabro settentrionale e quello meridionale.

Lo studio integrato di dati geofisici e geologici testimoniano un'inversione cinematica durante il Piaceziano, in cui la trascorrenza sinistra viene sostituita da una cinematica destra, a causa probabilmente di un cambio del campo tensionale agente all'interno della Stretta di Catanzaro.

Dal Pleistocene medio, il quadro strutturale è ulteriormente complicato dall'attivazione del sistema con cinematica normale orientato NE-SW a subordinatamente N-S, ed estensione orientata WNW-ESE, i quali bordano una serie di strutture, tipo graben, che segmentano la Stretta di Catanzaro in vari sottobacini, un esempio è rappresentato dal Bacino di Lamezia.

In accordo con Jacques et al., (2001) e Presti et al., (2013), i sistemi di faglia NE-SW e N-S giocano un ruolo rilevante nel quadro sismotettonico dell'area del tardo Quaternario; questi lineamenti strutturali rappresentano, infatti, le sorgenti sismiche dei più distruttivi terremoti avvenuti nell'Arco Calabro centrale.

Grazie ad un approccio multidisciplinare, è stato possibile fornire una descrizione più realistica e dettagliata del segmento centrale dell'Arco Calabro. contribuendo così a migliorare la conoscenza scientifica di un'area considerata ad elevato rischio sismogenetico e tsunamigenico.

KEY WORDS: Arco Calabro, faglie trascorrenti, faglie estensionali, sismo tettonica.

Introduction and aim of the work

Strike-slip faults systems can be considered as the faults system that mainly affect the Earth's crust. Geometrical characteristics and abundance of these faults depend by several factors, anyway them presence is considered as the kinematic consequence of large-scale motion of plates (Wilson, 1965).

Strike-slip systems frequently control opening of sedimentary basins that, hence, show a complex geometry, due to the along strike fault perturbation which can form pull-apart and fault wedge basins. In these systems where the extension faults are obliquely associated to the margin of main transcurrent faults, we can observe transtensional basins *sensu stricto* (Ingersoll & Busby 1996) characterized by highly geo-structural complexity (Allen et al., 1996, Ingersoll, 2012).

Basins formed by transtensional zones are commonly characterized by en echelon arrays of normal faults obliquely oriented to the boundaries of the deformational zone (Allen et al., 1996, Waldrom, 2005). One or both margins of this transtensional zone may be a normal faults system, as studied by Beauchamp (1998) in the High Atlas Triassic-Jurassic basins, or a strike-slip fault, such as the Plio-Quaternary Loreto region within the Baja California (Zanchi, 1994). In the world, numerous examples of large sedimentary basins controlled by strike-slip faults system can be quoted, as the Dead Valley (Christie-Blick & Biddle, 1985) and submarine basins underlying the Gulf of Aqaba (Ben-Avraham, 1985), the Cayman trough (Leroy et al 1996) and Gulf of California (Pesaud et al., 2003) and the Scotia-Antarctic plate boundary zone (Bohoyo et al., 2007). Transcurrent tectonic setting also are common in obliquely convergent settings where interplate strain is partitioned into arc-parallel strike-slip zones within the fore-arc, arc or back-arc region (Fitch, 1972; Beck, 1983; Jarrard 1986; Sylvester, 1988; Diament et al., 1992; Hanus et a., 1996; Sieh & Natawidjaja 2000; Cunnigham et al., 2007). Strike-slip systems, in this geological setting, rotate and act as element of accommodation.

The Calabrian Arc (Southern Apennines, Mediterranean Sea; Fig. i.1) can be considered one of the most interesting subduction systems due to the high level of structural complexity where strike slip faults play a relevant role during the evolution of the region which, since Tortonian time, favor the southwestward drifting of the arc and its fragmentation blocks (Ghisetti et al., 1979; Turco et al., 1990; Finetti & De Ben, 1986; Van Dijk et al. 2000). This tectonic setting produces extensional faults along the Tyrrhenian side, frequently organized in

graben-like systems, forming a normal faults belt running for about 370 km of length from the Crati Valley to the Hyblean Plateau (Monaco and Tortorici 2000; Tortorici et al., 2003).

Deep sedimentary basins are hosted by both longitudinal extensional fault and transversal strike-slip fault systems. Indeed, in the central Calabrian Arc the deep Catanzaro Trough (Fig. i.1) is bounded by a large strike-slip faults zone crossing the entire emerged arc from the Ionian to the Tyrrhenian Sea (Finetti & De Ben, 1986; Tansi et al. 2007, Del Ben et al., 2008; Milia et al., 2009), dividing the arc in two main parts. Despite the several studies and models (Van Dijk & Scheepers, 1995, and reference therein; Knott & Turco , 1991; Guarnieri, 2006; Milia et al., 2009), the controlling factors of the origin of transversal strike-slip zones still under debate.

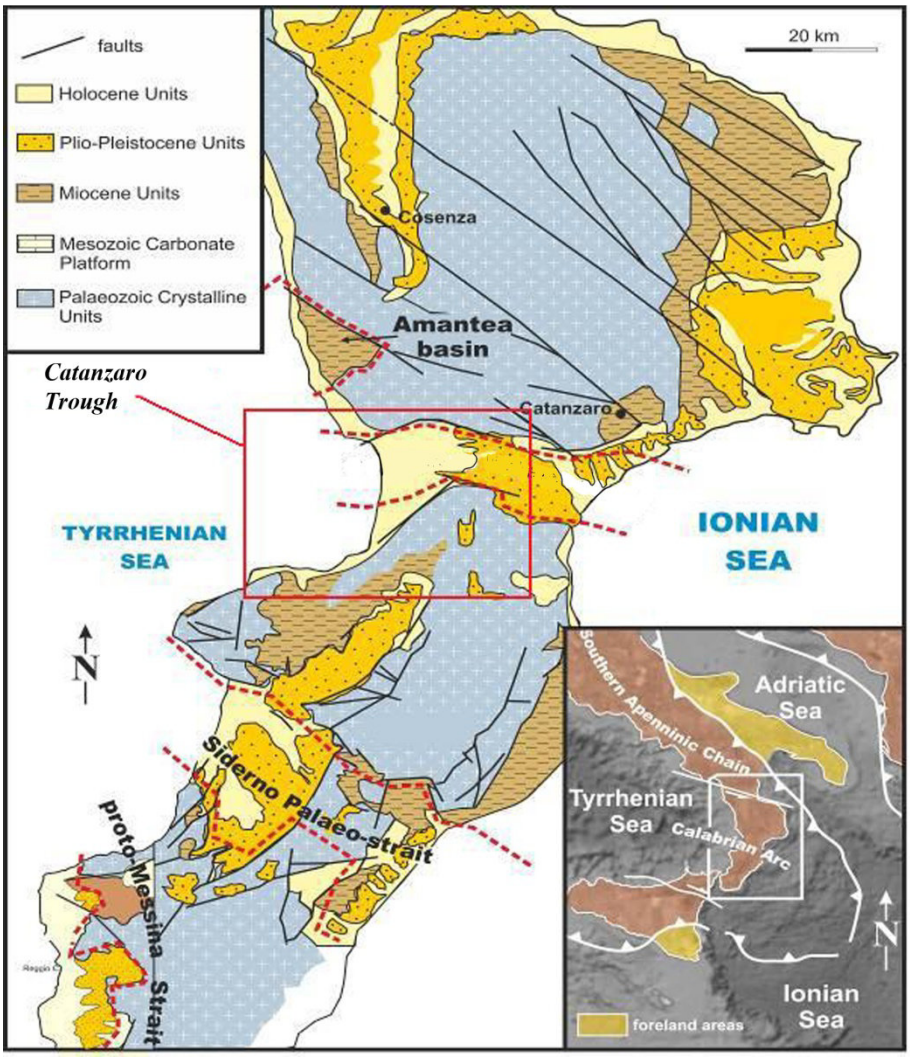

Figure i.1: Simplified geological map of Calabrian arc (modified from Tansi et al., 2007)

The aim of this work is to define the Plio-Quaternary evolution of Catanzaro Trough and the role of transverse and longitudinal faults, as part of the differential evolution between northern and southern sector of the Calabrian Arc.

We have used an innovative multidisciplinary approach, combining onshore with offshore, and geological with geophysical data, to assess the complex structural framework of the study area, and to understand the role played by the Catanzaro Trough as element of accommodation during the evolution of Calabrian Arc.

The fieldwork study, focused on the onshore area, has allowed to acquired more than 700 fault planes, which have been classified on the base of kinematics and fault directions. While, geophysical data (Multibeam data, Multichannel and Sparker profiles; SE Tyrrhenian Sea) were acquired during two oceanographic surveys, carried out in the Sant'Eufemia Gulf aboard the R/V OGS-Explora (summer of 2010) and the CNR R/V Bannock (Trincardi et al. 1987). Further insights have been obtained using seismic profiles and Marta and Marisa drilling wells, deriving from Eni (Ente Nazionale Idrocarburi ex Agip S.p.A) investigations (ViDEPI project) occurred in the onshore and offshore of study area.

Part of this study was focused on the Catanzaro Trough seismotectonic. We have collected data, including historical earthquakes inversion (Srovich and Pettenati, 2007), some well constrained first-motion focal mechanisms (Guerra et al 2006) and all the available crustal focal mechanisms computed for the study region by using waveform inversion methods (Li et al., 2007; D'Amico et al., 2010, 2011; Presti et al., 2013). In this collected data, we also included two new focal mechanisms computed through the CAP waveform inversion method provided by D'Amico from Physics Department University of Malta.

i.2 Research activities

The research activities were organized in different phases during three years:

1. *reference study:* the study of references was concentrated to reconstruct the scientific background relating to geological and structural setting of Calabrian Arc, part of this study is oriented to group the main research topics: e.g. structural geology, geophisics, Quaternary geology and, active and recent tectonic, regarding structural models of similar study areas;
2. *acquisition of topographic and technical maps:* we have used three type of topographic and technical maps with different scale:

- 1:10000 edited by Cassa del Mezzogiorno with technical assistance of Italian Military Geographic Institute (IGM);
- 1:5000 and 1:25000 Regional Technical Chart of Calabria Region, georeferenced in UTM system;
- 1:25000 geologic map edited by Cassa del Mezzogiorno;

3. *study of aerial photos*: derived from photogrammetric surveys conducted in 1983 (scale 1: 33000) and 1990 (1:33000) by the Italian Military Geographic Institute (IGM) in Florence (Piccarretta and Ceraudo, 2000, Ceraudo, 2003);
4. *field trip acquisition data:* we acquired new structural datasets, mainly brittle elements, collected along the onshore segment of Catanzaro Trough, related to the main faults system. The structural data were organized in ca. 40 of stations measurement, distributed above basement rocks and Neogene-Quaternary deposits;
5. *interpretation of geophysical and wells data:*
    - *Onshore data analysis and wells study:* we used geophysical and wells documentation collected by Eni s.p.a. (italian oil company) at the beginning of the 80' and provided to users in the frame of the VIDEPI Project (Visibility of Petroleum Exploration Data in Italy). The public technical documents related to the Italian exploration activities were realized by UNMIG-National mining office for hydrocarbons and georesources of Ministry of Economic Development, (unmig.sviluppoeconomico.gov.it/videpi/);
    - *Offshore data analysis* Interpretation of geophysical data (Sparker, multichannel seismic – MCS, sub-bottom profiles – Chirp and high resolution morpho-bathymetry), obtained during two scientific cruise in the Sant'Eufemia Gulf (ISTEGE Project and 1987 oceanographic cruise aboard the R/V Bannock); Interpretation of well data and seismic lines (ViDEPI Eni project);
6. *research activities, performed in Department of Earth Sciences - Durham University from November 2014 to April 2015, was supervisored by* the Dr. Nicola De Paola. The goal has been to elaborate structural data, coming from geological surveying acquired along Catanzaro Trough, geological field mapping and analysis of Catanzaro Through basin evolution.

7. *integrated study of active faults* by using:
    - ITaly HAzards from CApable faulting (ITHACA) is a database aimed at collecting and analyzing all available information on active tectonic structures in Italy, with particular regard to tectonic processes able to generate natural hazards. The project deals with active capable faults, which are defined as faults that have significant potential for displacement at or near the ground surface;
    - Database of Individual Seismogenic Sources (DISS) is a georeferenced repository of tectonic, fault, and paleoseismological information expressly devoted, but not limited, to potential applications in the assessment of seismic hazard at regional and national scale;
    - historical earthquakes inversion (Srovich and Pettenati, 2007);
    - first-motion focal mechanisms (Guerra et al 2006);
    - available crustal focal mechanisms computed for the study region by using waveform inversion methods (Li et al., 2007; D'Amico et al., 2010, 2011, Presti et al., 2013);
    - finally, we also include two new focal mechanisms computed through the CAP waveform inversion method provided by D'Amico from Physics Department University of Malta.

CHAP.1 Geographic setting

The study area, named Catanzaro Trough, is located in the western portion of central Calabria, along the Tyrrhenian side. With reference to 1:25000 Regional Technical Chart of Calabria Region, the study area is located in the following sections (Fig. 1.1):

- 570; II Filadelfia section;
- 574; I Lamezia Terme, II Curinga and IV Castiglione Marittimo sections;
- 575; I Catanzaro, II Catanzaro Lido, III Girifalco and IV Pianopoli sections;
- 580; IV Squillace section.

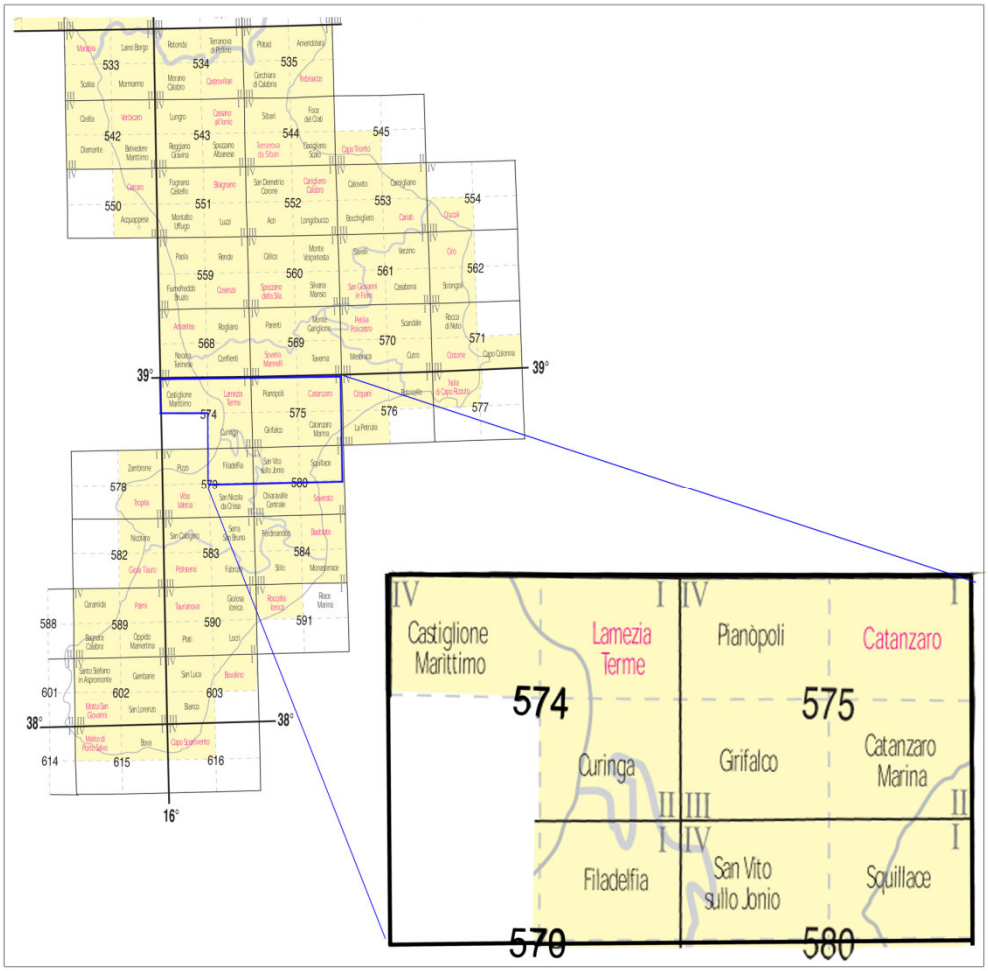

Figure 1.1: 1:25000 Regional Technical Chart of Calabria Region. The used sections are underlined with a blue line and show in the inset.

Morphologically, the territory passes eastwards from the Tyrrhenian coastal plain, commonly called Piana di Sant'Eufemia, to sweet hilly landscape, observed within the central Catanzaro Strait. In this area the hills reach more than 400 meters high; whereas both to north

and to south the area is bordered by two mountains belts, Sila and Serre uplands. Moving from the Catanzaro Trough to the two uplands, the morphology shows an alternation of steep scarps and flight of wave-cut surfaces and/or thin-depositional platforms, representing the palaeoshorelines and the erosional surfaces or marine terraces respectively.

The area is characterized by small, highly irregular rivers, named 'fiumare' for their often dry streams. Through the northern and southern mountain ranges, the river channels show V-shaped river with steep gradients of flow. When they reach the sedimentary sequences within the Catanzaro Trough the streams display a sudden decreasing of channel slope, forming gentle valleys.

The most important river in the area is the Amato river, which rises on Sila upland. Next to the Catanzaro Trough, Amato river, as well as other minor torrents, change its drainage pattern, passing before flowing onto Sant'Eufemia Gulf from ca. N-S to NE-SW oriented trends. Eastward, Corace river represents the main river of the area, even this rises on Sila upland and flowing down in the Ionian sea, showing along all of its watercourses ca. same N-S drainage pattern.

CHAP. 2 Geological setting

2.1 Geodynamic of the Mediterranean region

Geological and geophysical studies, carried out in the last decades, have stated that the central Mediterranean region is characterized by three structural domains: the foreland, the hinterland and the orogenic domain (Ben Avraham 1990, Lentini et al., 1994, 2006, Van Dijk & Scheepers 1995, Finetti et al., 1996, Critelli, 1999; Critelli et al., 2013).

The foreland domain includes the currently undeformed continental areas consisting of the Apulian and African plates, the two foreland areas are separated since late Paleozoic by the inferred oceanic crust of part of the Ionian basin (Fig. 2.1; Lentini et al., 2006, Finetti et al., 2005). The hinterland domain is represented by Corsica-Sardinia block and the back-arc Tyrrhenian basin opening since the Serravallian time (Fig. 2.1). This latter is characterized by the oceanic crust covered in the eastern part by Miocene- Holocene deposits. Finally the orogenic domain is composed by the Apennine-Maghrebian belt and by the Calabrian-Peloritan Arc that superimposed to the Apennines in the southern part (Fig. 2.1; Gueguen et al., 1998, Faccenna et al., 2005, Carminati et al., 2005, Lentini et al., 2006, Milia et al., 2009).

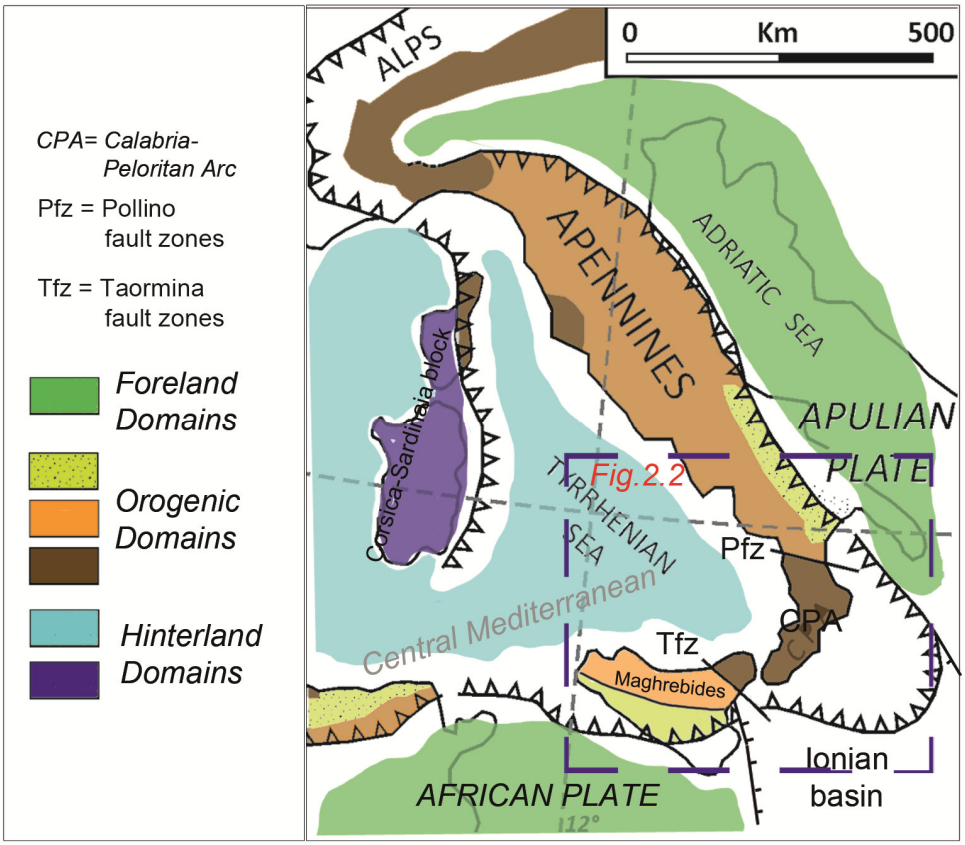

Figure 2.1: Sketch map of western- central Mediterranean region (modified from Perri & Ohta, 2014).

2.2 Tectono-stratigraphic features of CPA

The western Catanzaro Trough represents a Neogene- Quaternary sedimentary basin belonging to a well-developed *arc-shaped* structure, the Calabrian Arc (Amodio-Morelli et al., 1976; Tortorici, 1982).

Calabrian Arc is a fragment of Alpine chain connecting the southern Apennine with Maghrebide Block. The SE-ward roll-back of the Ionian slab beneath the orogenic arc, controlled by the Nubian - Euroasian plates convergence (Fig. 2.2), caused rapid opening of the back-arc basin and the migration of the Calabrian block (Malinverno & Ryan 1986, Faccenna et al. 2005). This last is driven by opposite vertical axis rotation along the WNW-ESE oriented northern and southern edges (Mattei et al., 2007), the Pollino and Taormina Lines (Fig. 2.2) respectively (Amodio-Morelli et al., 1976, Ghisetti & Vezzani, 1982, Langone et al., 2006).

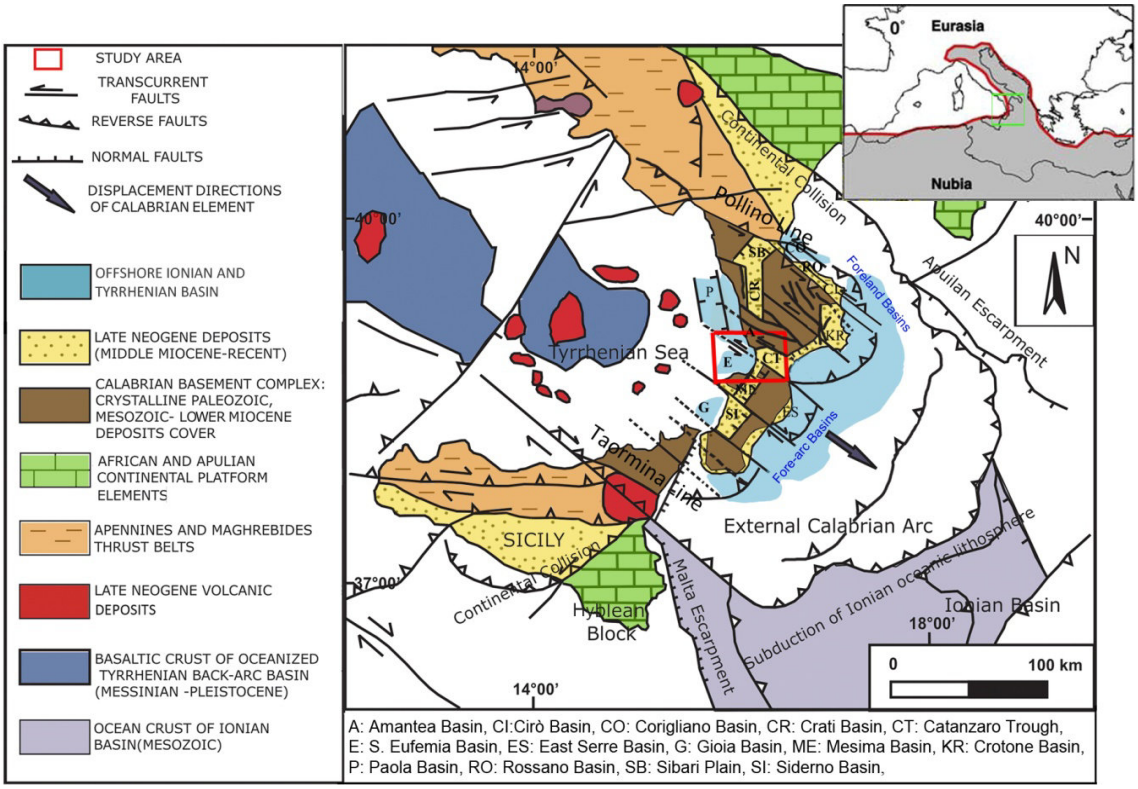

Figure 2.2: The geological framework of the Central Mediterranean region (modified from Van Dijk et al., 2000).

The result of the rapid trench migration is the opening of the Tyrrhenian back-arc basin during Upper Miocene -Pleistocene age (Fig. 2.3; Finetti et al., 1986, Neri et al., 1996, 2012), and the fragmentation of CPA into structural highs and transversal marine sedimentary basins (Ghisetti 1979, Tansi et al., 2007, Tripodi et al., 2013), including Catanzaro Trough.

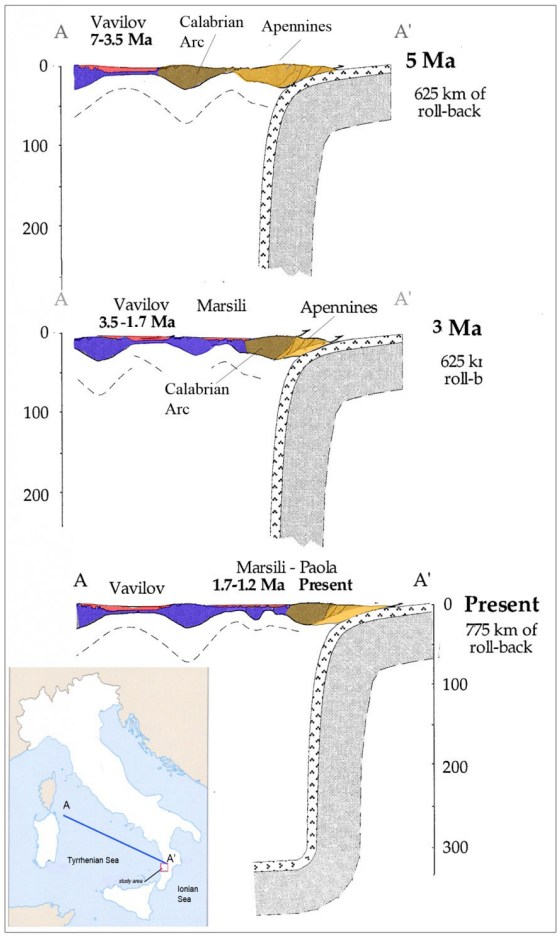

Figure 2.3: Cross section showing Plio-Quaternary slab retreat of southern Tyrrhenian sea (modified from Gueguen et al., 1998)

According several authors, the Ionian slab has partially or completely undergone detachment (Wortel & Spakman, 1992, Guarnieri et al., 2006). Neri et al., 2009 state that the subducting oceanic crust is apparently continuous over depth only beneath the central part of the Calabrian Arc, while the detachment should have already occurred in correspondence of the Arc edges, namely Pollino and Taormina Lines. The relict of this once large subduction zone is presently limited to an extremely narrow (<200 km), deep (>400 km) and steep (70°) NW dipping Wadati-Benioff zone (Selvaggi and Chiarabba, 1995). In response to the Ionian slab detachment, the whole of the CPA undergoes a general tectonic rebound (uplift), at a rate of 0.5–1.2 mm/yr in the last 1–0.7 Ma, when the propagating tear passes underneath the plate margin segment (Monaco et al., 1996, Wortel & Spakman, 2000). All these observations suggest that the rollback in the Tyrrhenian- Calabrian system is almost stopped or significantly slowed down.

The active tectonic regime in Calabria is characterized by a NW–SE oriented extension, with T-axes about perpendicular to the chain axis, suggesting that the dominance of

compression driven by the Nubian-Eurasian plate convergence no longer holds there. The GPS velocity running from the Corsica-Sardinia block to the CPA, shows that there are no evidences of active extension in the Tyrrhenian basin. On the contrary, a NW–SE shortening (at a level of 1.4 ± 0.6 mm yr−1) is likely to be accommodated there. The whole NW–SE extension affecting the CPA is of the order of 3.0 ± 0.6 mm yr−1, 2.0 mm yr−1 of which are accommodated on land (D' Agostino et al., 2004, Serpelloni et al., 2007, 2010).

The CPA comprise a number of superimposed Jurassic-Cretaceous ophiolitic sequences, and Hercynian and pre-Hercynian continental basement rocks that are in part affected by varying grades of later Alpine retrograde metamorphism (Amodio Morelli *et al.*, 1976; Atzori *et al.*, 1984; Del Moro *et al.*, 1986; Bonardi et al., 2001, Butler et al., 2004, Iannace et al., 2007). The Paleozoic metamorphic and plutonic terranes of the CPA represent the remnants of Caledonian, Hercynian and Alpine orogens (*e.g.* Amodio Morelli *et al.*, 1976; Schenk, 1981; Zanettin Lorenzoni, 1982; Atzori *et al.*, 1984; Del Moro *et al.*, 1986; Zeck, 1990; Messina *et al.*, 1994, Piluso and Morten 2004, Cirrincione et la., 2011), which during Oligocene to early Miocene times have undergone a drifting from the southern Iberian plate to Adria-Africa lithosphere (Critelli et al., 1999).

Erosional remnants of the CPA (Critelli et al, 2013) is characterized by the two main superimposed metamorphic and crystalline units, belonging to Calabrian Terranes (*sensu* Tansi et al., 2007), which lie, in turn, on Mesozoic Carbonates Units of the Apennine-Maghrebide chain since the Early Miocene (Critelli, 1999; Rossetti et al., 2004; Iannace et al., 2007; Vignaroli et al., 2012). These basement units are juxtaposed by means of low angle overthrusted contacts, which are dissected and folded by later high angle faults of Middle Miocene- Recent age, ordered in different fault systems and patterns, partly related to transcurrent faulting (Van Dijk et al., 2000).

Basically, the crystalline basement outcropping in the CPA is made of:

- Jurassic to Early Cretaceous ophiolite-bearing sequences with foliated slates, black metapelites and metasilts, and red mudrocks and thin levels of laminate marble (Bousquet, 1963, Vezzani, 1968, Ogniben, 1973, Amodio-Morelli, 1976, Tortorici, 1982, Critelli et al., 2013), these units are referred to the *Liguride Complex* (sensu Ogniben, 1969, Knott, 1987), outcropping in the northwestern portion of the study area, here named *Metapelitic and Ophiolitic Units*.
- Paleozoic igneous- metamorphic sequences, belonging to *Calabride Terranes* (Messina et al.,, 1991a, 1991b), are, in turn, tectonically superposed of the Tethyan Ocean-derived units (Liguride Complex) and made of mylonitic augen-gneiss,

micaschist, and subordinately marbles and high-grade metamorphic rocks (biotite-sillimanite-garnet gneiss), intruded by plutonic bodies (Ogniben, 1969, Amodio-Morelli et al., 1976, Messina et al., 1994).

The difficulty to correlate the tectono-stratigraphic units of northern with those of southern Calabrian Terranes, revealed by the outcrops, has led to consider CPA as the result of juxtaposition of two sectors, divided by Catanzaro Trough and characterized by different structural setting and geodynamic evolution (Bonardi et al., 1980, 2001, Scandone e al., 1982, Tortorici et al., 1982, Boccaletti et al., 1984b, Dercourt et al., 1985). There is a general scientific agreement on the existence of three main differences between the two sectors, with reference to the southern CPA:

- Lack of Apenninic units underlying Calabrian Terranes;
- Lack of Ophiolite-Bearing units;
- Lack of Alpine metamorphism characterizing the crystalline basement.

2.2.2 Geological features of northern CPA

The northern sector, extended from Pollino Line to Catanzaro Trough, is made of two mountain chain Catena Costiera and Sila Massif (Piluso and Morten 2004) which show an overall similar tectonic evolution and can be described as the superposition of three major structural elements (Fig. 2.4) representing different paleogeographic domains:

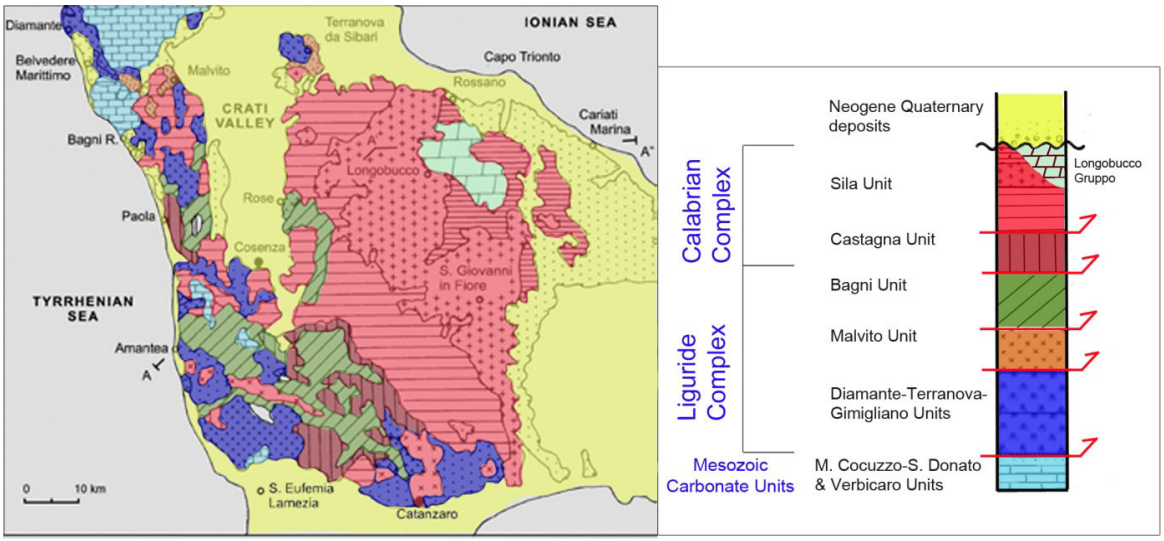

Figure 2.3: Sketch map of the simplified tectonostratigraphic terranes of the northern Calabrian Arc (modified from Critelli 1999)

1. the lowermost Mesozoic ‘Apennines’ Carbonate units (Fig. 2.4; Van Dijk, 2000), corresponding to a continental platform composed by dolomitic partly epimetamorphic limestone of Triassic age, correlated by Van Dijk (2000) to the Monte Cocuzzo-San Donato-Campotenese Unit, overlain by the Triassic- Jurassic platform and the basinal transition limestone and dolostone belonging to Verbicaro Unit (Ietto & Barillaro 1993, Iannace et al., 1995, Perrone 1996, Liberi et al., 2006);

2. the intermediate Liguride complex, composed of ophiolite-bearing sequences belonging to the neo-Tethys realm (De Roever 1972, Dietrich and Scandone 1972, Lanzafame et al., 1979, Beccaluva et al., 1982, Guerrera et al., 1993, Cello et al., 1996) has been subdivided into several tectonometamorphic units: the Diamante–Terranova unit, consisting of metabasites (derived from pillow lavas and breccias, hyaloclastites and rare serpentinite bodies) overlain by metasediments comprising calcschists, phyllites and quarzites of Jurassic-Lower Cretaceous age (Cello et al., 1996). The Gimigliano–Monte Reventino unit: comprises basal mafic and ultramafic rocks passing stratigraphically to quartzites, quartz-mica-schists, marbles, and calcschists (Colonna and Piccarreta, 1975, 1977), the (upper) Malvito unit, composed of Jurassic-Lower Cretaceous metabasites (mostly pillow lavas) and of a sedimentary cover of radiolarian cherts and Calpionella limestones, locally reaching albite-lawsonite metamorphic facies conditios (Fig. 2.4; Amodio Morelli et al. 1976, Cello et al., 1991, 1996); the Bagni unit, consisting of Hercynian phyllites and a Triassic (?)-Lower Cretaceous sedimentary cover, showing a lower greenschist facies metamorphic overprint (Cello et al., 1996).

3. the uppermost Calabride complex, consisting of a nearly continuous continental lithospheric section, created during the Hercynian (Graessner and Schenk 2001, Piluso and Morten 2004) has been characterized by two tectonometamorphic Units: Sila Units is the uppermost Alpine thrust Nappe, consisting in its deeper part of granulites-facies gneisses (Monte Gariglione Unit), as well as the overlying amphibolite- facies upper-crustal gneisses and low-grade Palaeozoic rocks, (Mandatoriccio and Bocchigliero Units): intruded by Late Hercynian granitoids of Sila Batholith (Messina et al., 1991a, 1994, Caggianelli et al., 2000, Graessner and Schenk, 2001). The Longobucco sequence represent the Mesozoic sedimentary cover (Messina et al., 1994). The second tectonometamorphic sequence, the Castagna Unit, established by Dubois and Glangeaud (1965), represents a pervasively mylonitised horizon consisting of medium-high grade metamorphic rocks (para- and orthogneiss, micaschist,

marble and amphibolite gneiss) intruded by late-Hercynian granitoids (Bonardi et al., 2001, Sacco, 2011)

2.2.1 Geological features of southern CPA

Southern CPA, extended from Catanzaro Trough to Taormina line, is characterized by three mountain chain Serre, Aspromonte Massifs and Peloritain Mountains.

2.2.1.1 Serre Massif

The Serre Massif is composed by two nappes that can be distinguished on the basis of the different Hercynian and Alpine overprints (Fig. 2.5):

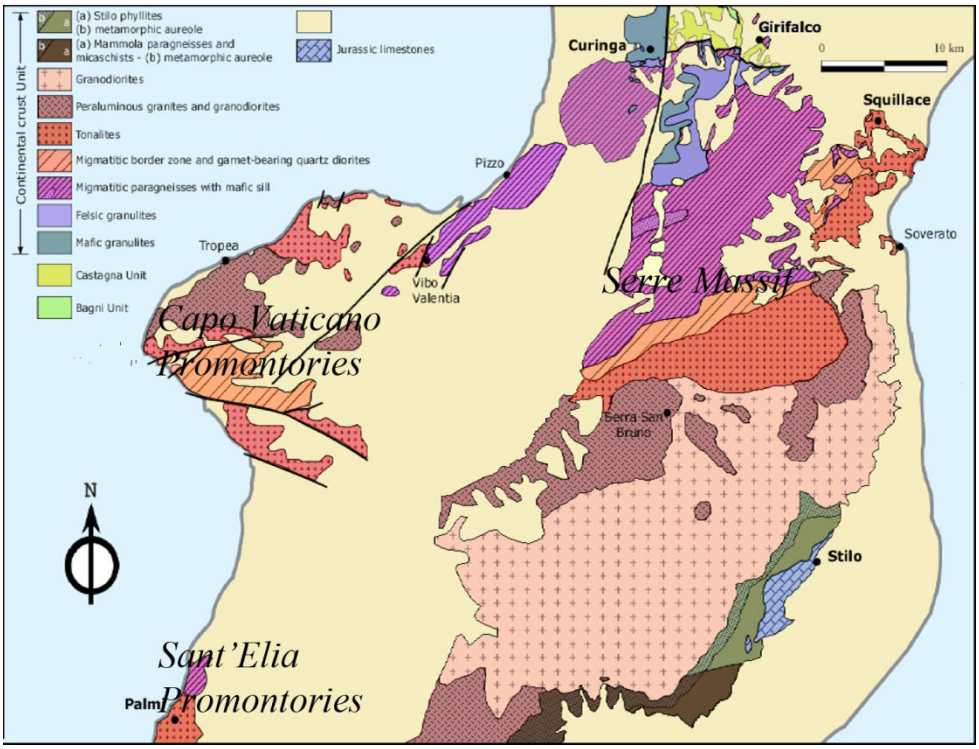

Figure 2.5: Geological sketch map of the Serre Massif, Capo Vaticano and Sant'Elia promontories (modified from: Borsi et al., 1976; Fornelli et al., 1994; Grässner & Schenk, 1999; Rottura et al., 1991, Festa et al., 2004).

1. the upper nappe, related to the Polia Copanello Unit has a considerable thickness and represents a nearly continuous section of the Hercynian crust (Schenk, 1980) well recognizable both in northern and in central Calabria. It is composed of granulite facies metamorphic rocks, overlain by thick granitoid sheets in the intermediate level, followed upwards by medium to low-grade metamorphic rocks. The main metamorphism, responsible also for partial melting in the lower crust, was synchronous to intrusion of granitoids and took place during the late stages of the Hercynian orogeny (Graessner et al., 2000);

2. the lower nappe related to the Castagna Unit, have a minor thicknesses and are composed of Hercynian medium-grade milonitic metamorphic rocks. The Alpine metamorphic overprint locally affected both nappes along some shear zones. In the northern Serre area the intermediate nappe mainly consists of orthogneisses with some paragneisses and micaschists (Paglionico and Piccarreta, 1976, Langone and Prosser 2006).

2.2.1.2 Aspromonte Massif and Peloritain Mountains

According Pezzino et al. (1990, 2008), Ortolano et al. (2005), Cirrincione et al. (2008) and Fazio et al. (2008) the Aspromonte Massif shows the presence of three polyphase metamorphic complexes (Fig. 2.6): the uppermost Stilo Unit (SU) at the top, the intermediate Aspromonte-Peloritani Unit (APU), and the underlying Madonna di Polsi Unit (MPU). The last two units (APU and MPU), characterised by different metamorphic histories, are tectonically overlapped along a thick mylonitic shear horizon. Farther to the south, the high-grade metamorphic rocks of the APU extend across the Strait of Messina up to the Peloritani Mountain belt and represent the highest unit of the nappe-edifice cropping out in Sicily. This unit overlies the Variscan phyllite sequence of the Mandanici Unit and a terrigenous-carbonate Mesozoic cover, called Alì sequence (Lentini & Vezzani, 1975).

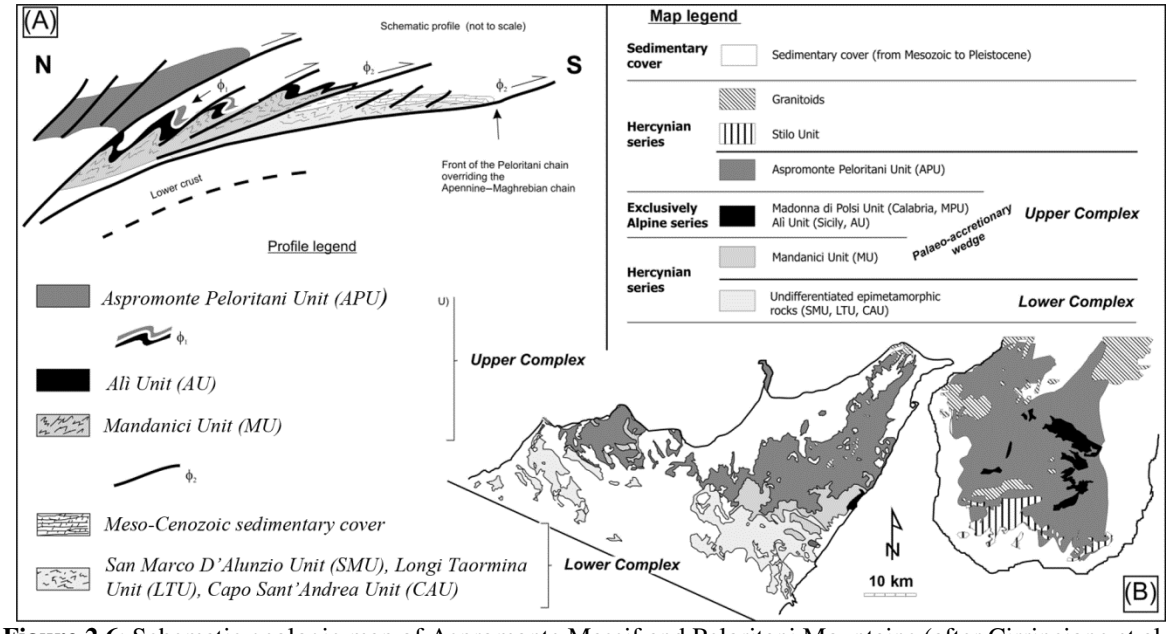

Figure 2.6: Schematic geologic map of Aspromonte Massif and Peloritani Mountains (after Cirrincione et al., 2011).

Extending the model proposed by Pezzino et al. (2008) to crystalline basement rocks outcropping in Sicily: the entire Peloritani belt may be subdivided into two complexes (Fig. 2.6) with different tectono-metamorphic histories (Atzori et al., 1994; Cirrincione & Pezzino,

1994; Cirrincione et al., 2011). The lower complex (San Marco D'Alunzio Unit, Longi Taormina Unit, Capo Sant'Andrea Unit), exposed in the southern part of the Peloritani belt, comprises volcano-sedimentary Cambrian–Carboniferous sequences, which were affected by Variscan sub-greenschist to greenschist facies metamorphism and which are covered by unmetamorphosed Mesozoic–Cenozoic sediments. The upper complex, in the north-eastern part of the belt, consists of two units (Mandanici Unit and Aspromonte–Peloritani Unit), showing Variscan greenschist to amphibolite facies metamorphism, which in part are also affected by a younger alpine greenschist facies metamorphic overprint (Cirrincione & Pezzino, 1991; Atzori et al., 1994). Fragments of a metamorphosed Mesozoic–Cenozoic cover, namely Alì series (AU) in the Peloritani Mountains, corresponds to the MPU in the Aspromonte Massif. The AU is interposed between the Mandanici Unit and the Aspromonte–Peloritani Unit.

2.3 Structural and geological backgrounds of Catanzaro Trough

2.3.1 Structural features of Catanzaro Trough

We here focus the work on the western Catanzaro Trough along the Tyrrhenian side of central Calabria, the study area represents a linkage zone between northern and southern sectors of Calabrian Arc which experienced different tectonic phases, resulting confined by both longitudinal and transversal faults systems (Ghisetti, 1979, Monaco & Tortorici, 2000).

The longitudinal faults system are characterized by high angle NE-SW and N-S oriented structural lineaments, these structures is part of the Siculo-Calabrian rift zone (Monaco et al., 1997, Monaco and Tortorici 2000), a ca N-S elongated basins which extend from the Calabrian arc until eastern Sicily, for a length of about 370 km. Them tectonic activity is also witnessed by the high concentration of the largest historical earthquakes along the Siculo-Calabrian rift zone (Fig. 2.7; Monaco & Tortorici, 2000, Galli & Bosi 2002). The strong uplift of Sila, Serre and Aspromonte Massifs caused elevated marine terraces all along the Tyrrhenian coast of Calabria (Westaway, 1993, Mihauchy et al., 1994, Tortorici et al., 2003, Bianca et al., 2011).

The transversal faults system border the northern and southern edges of Catanzaro Trough (Van Dijk et al. 2000; Tansi et al., 2007, Milia et al., 2009)

The northern margin is characterized by a regional NW-SE-trending left-lateral strike-slip faults system. These structural lineaments consist of three right-stepping *en ´echelon*

major fault segments, S-dipping, where the southern segment is represented by Lamezia-Catanzaro Fault (Fig. 2.7; sensu Tansi et al., 2007), recognizable by means of evident morphological escarpments with triangular and trapezoidal facets.

The southern margin of studied basin is bordered by the WNW-ESE oriented, NNE dipping Maida –Staletti Fault zone and by Capo Vaticano Promontory (see figure 2.7 for location; Ghisetti, 1979, Langone et al., 2006, Caggianelli et al., 2013).

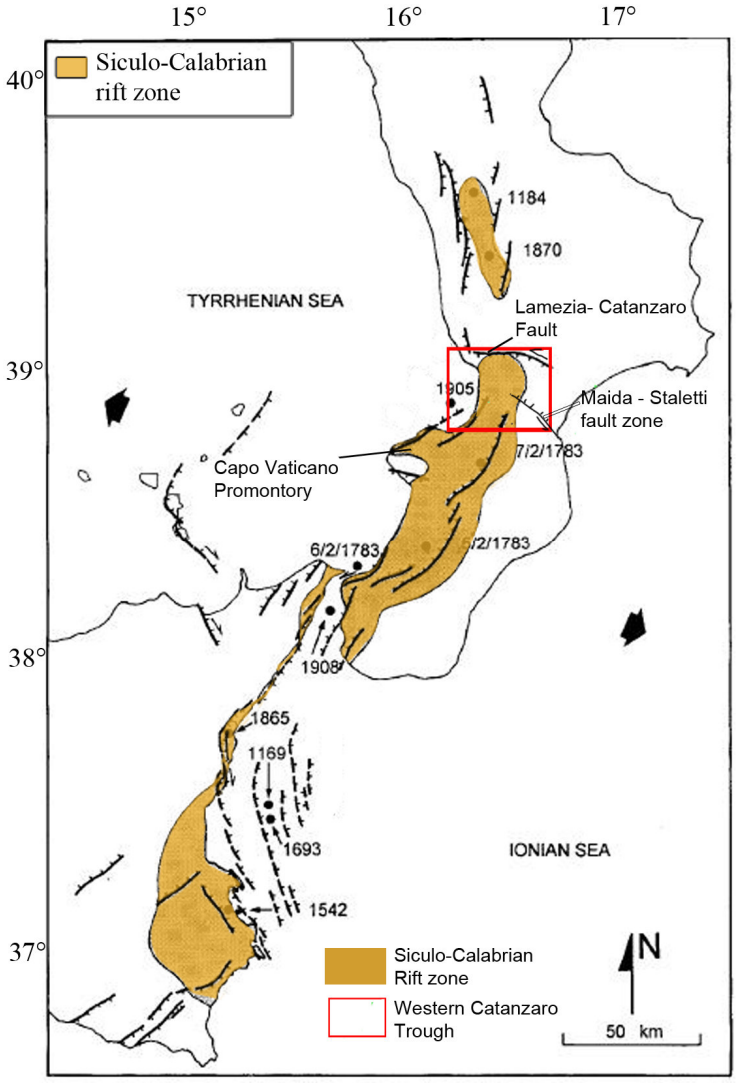

Figure 2.7: Historical earthquakes and faults along the Siculo-Calabrian Rift zone (modified from Monaco & Tortorici, 2000)

2.3.2 Geological features of Catanzaro Trough

The sedimentary sequences infilling the Catanzaro Trough encompasse the Lower Pliocene- Quaternary basin-fill succession (Catanzaro Basin according to Longhitano et al., 2014 and Chiarella et al., 2012a) unconformably overlies the Middle- Upper Miocene deposits (Ferrini & Testa, 1997, Cavazza & De Celles, 1998, Cianflone & Dominici, 2011). Both of them cover transgressively the igneous-metamorphic basement (Bousquet, 1963, Vezzani, 1968, Ogniben, 1973, Amodio-Morelli, 1976, Tortorici, 1982, Messina et al., 1994, Critelli et al., 2013).

The lowermost deposits of the Catanzaro Basin are represented by ca. 350 m thick mudstones and marls, considered time correlative with the Zanclean Trubi Formation which is extensively exposed in many areas of southern Italy (for example, the Crotone Basin; Zecchin et al., 2012, 2013). The Trubi Formation is paraconformably overlain by a ca. 200 m thick succession composed of weakly cemented sandstones and mudstones deposited in a marine shelf environment; the age of this unit is upper Pliocene–Pleistocene (Cavazza et al., 1997; Cavazza & Ingersoll, 2005).

This sequence is bounded at the top by the lower Pleistocene stratigraphic interval, which consists of ca. 100 m thick succession dominantly characterized by mixed siliciclastic/ bioclastic sands and sandstones and, subordinately, of mudstones (Chiarella, 2011; Chiarella et al., 2012a, Longhitano et al., 2014).

Since the Middle Pleistocene, an intense ESE-WNW oriented regional extensional phase occurred. The most evident consequence of the widespread Quaternary uplift is the occurrence of a spectacular flight of marine terraces, mainly developed along the western Calabria coastline (Capo Vaticano promontory, the Capo Suvero area, and the Coastal Range), resulted of the interaction between tectonic uplift and Quaternary cyclic sea-level changes (see also Tortorici et al.. 2002, 2003).

CHAP. 3 Geological field study of Catanzaro Trough

3.1 Geological features of Catanzaro Trough

The western Catanzaro Trough represents a Neogene- Quaternary sedimentary basin belonging to a well-developed *arc-shaped* structure, the Calabrian Arc (Amodio-Morelli et al., 1976; Tortorici, 1982), extended along Tyrrhenian side from offshore, Sant'Eufemia Basin (SE Tyrrhenian Sea) to the onshore area, Catanzaro Basin, and confined on land both north and south by Sila and Serre Massif, respectively.

In the onshore area we have focused part of this work to collect new geological insights about Catanzaro Trough. The field work study led us to create a geological and structural map (Attachment 1) and to define the stratigraphy characterizing this basin (Fig. 3.2).

The sedimentary sequences infilling the Catanzaro Trough is characterized by the Upper Miocene- Quaternary basin-fill succession unconformably overlies the Middle Miocene and Messinian evaporite deposits, all together cover the igneous-metamorphic basement (Fig. 3.2, Ferrini & Testa, 1997, Cianflone & Dominici, 2011).

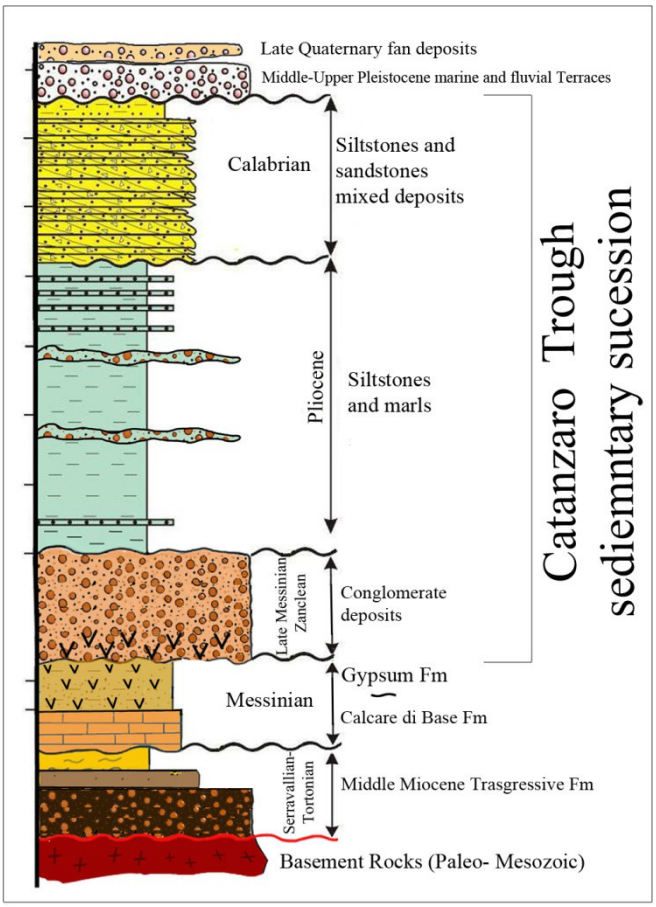

Figure 3.2: Stratigraphy of the study area (modified from Chiarella et al, 2011)

Catanzaro Trough underwent to several sedimentary changes from Middle Miocene to Pleistocene, indeed some parts of the back-arc zone were affected by extensional tectonics superimposed on Middle Miocene – Middle Pleistocene strike-slip deformations (Colella & D'Alessandro, 1988, Argnani & Trincardi, 1993, Van Dijk et al., 2000, Tripodi et al., 2013).

3.2 Middle - Upper Miocene deposits

The Middle-Upper Miocene transgressive sequence is a sedimentary cycle confined in marginal outcropping of western Catanzaro Trough and representing, with crystalline rocks, a inherited substratum on which the Catanzaro Trough sedimentary deposits were developed.

3.2.1 Serravallian- Tortonian sequence

At the bottom, this sequence shows up to 60 -70 m thick of Serravallian- Tortonian fluvial and deltaic conglomerates, formed by brown to reddish massive conglomerates (Fig. 3.3a), observed in the northeastern and northwestern edge of the study area, close to the Corace River where the succession reach the maximum thickness and Capo Suvero area, respectively. This succession is characterized by stratified conglomerates with alternate sandstones, showing a SW-dipping, with a 35° sloping strata (Fig. 3.3b). Clasts present different lithologies, essentially gneisses and igneous rocks with very poor contents of bioclastic rocks. supported by a reddish arcosic matrix, lacking of any palaeontological content. Muto and Perri (2002) define these deposits in the Amantea Basin as "*first depositional unit*".

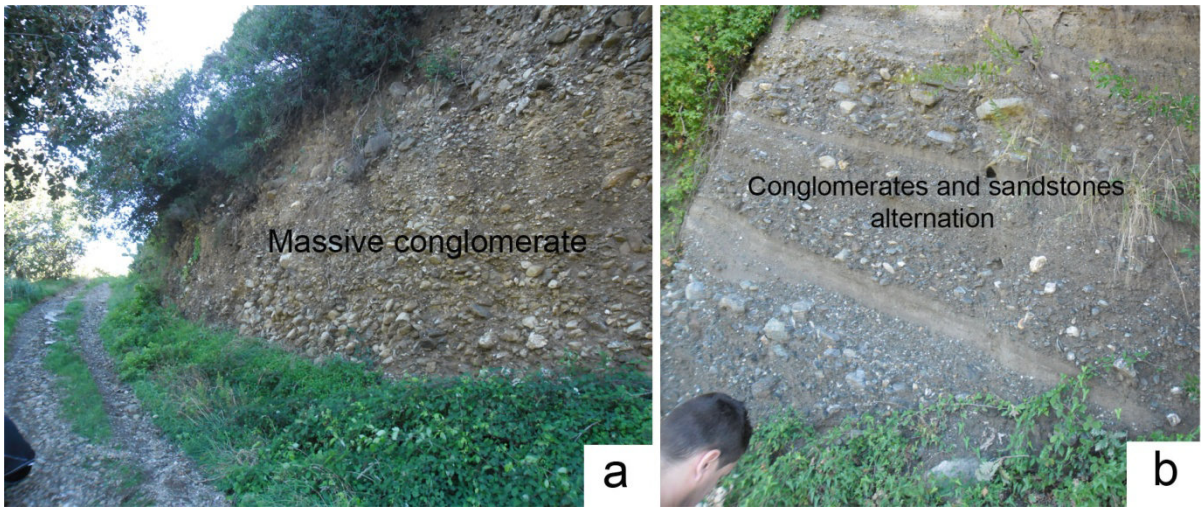

Figure 3.3: Serravallian- Tortonian conglomerate outcropping within Capo Suvero promontory a) massive grain-substained and b) stratified structure.

These deposits pass upward to Tortonian shelf deposits, characterized by grey bioclastic to silicoclastic sandstones and marls (Fig. 3.4).

Within the northwestern margin of Catanzaro Trough mixed arenites outcrops above basal conglomerates, these deposits were already observed within of Amantea Basin (*second depositional unit:* Colella, 1995; Muto & Perri, 2002) which represent hinterlandward coastal onlap of bioclastic ramp-type platform calcarenites (Fig. 3.4a; Mattei et al., 1999).

The mixed arenites are followed by marls and clays. Clays contains diatomites related to Tripoli Fm (Azzaro et al., 1988; Zecchin et al., 2012) and is located stratigraphically above the Tortonian pelagic marls, related to the Ponda Fm (Fig. 3.4b), and below carbonate beds represented by Messinian Calcare di Base Fm (Roda, 1964; Massari et al., 2010; Zecchin et al., 2012).

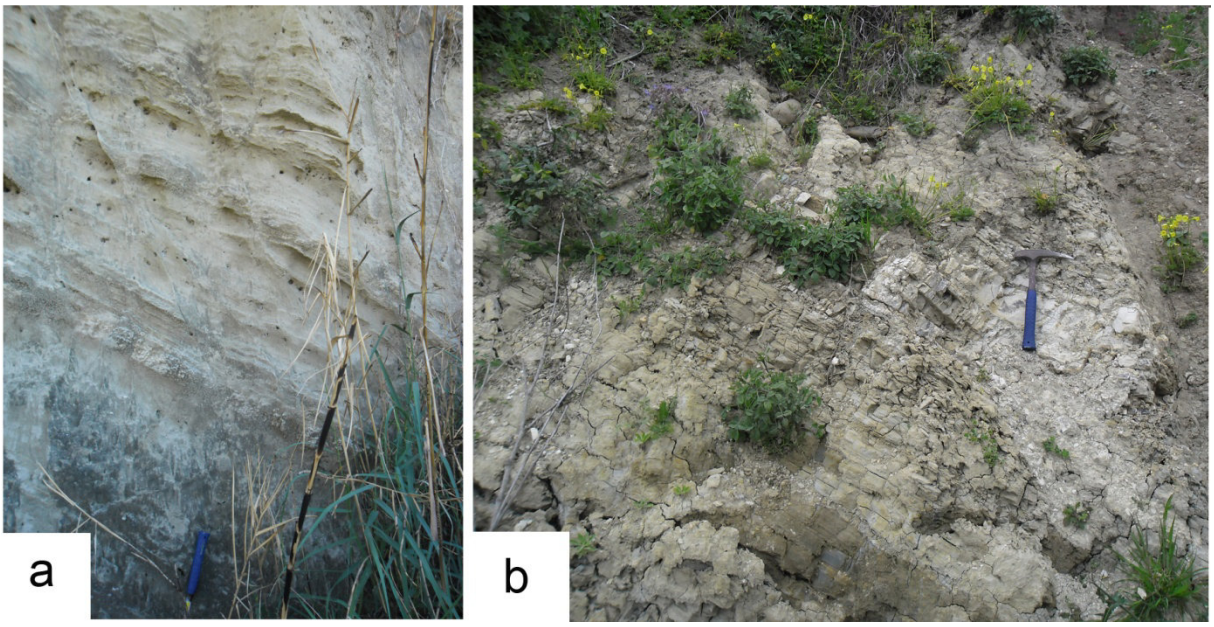

Figure 3.4: Tortonian shelf deposits, characterized by a) sandstones from grey bioclastic to siliciclastic and b) marls

Close to the Gizzeria Village, Tortonian and Messinian deposits are involved in a deep landslides which cover the real stratigraphic relationships. Indeed near this area the strata are tilted and in some cases are verticalized in response to downslope movement (Fig. 3.5).

Figure 3.5: Verticalized layers outcropping close to the Capo Suvero Promontory

3.2.2 Messinian sequence

Messinian sequence is bounded at the bottom by an abrupt erosional surface, due to severe sea level changes (Messinian Salinity Crisis). Evaporitic layers are made of a thin and discontinuous limestone–gypsum sequence conformably overlying the Serravallian–Tortonian sequence (Cavazza and DeCelles 1998; Roveri et al., 2001; Govers et al., 2009, Manzi et al., 2010).

The Calcare di Base Fm is the lower sedimentary succession of this sequence with stratified carbonate deposits and grey marls, up to 60 m thick, outcropping locally along the northern part of study area, above the inherited structural highs bordering the basin edge during the deposition of the Messinian formation. This succession could be related to shallow water Lower Evaporites deposits (Roveri et al., 2008, Manzi et al., 2010), even though they are poorly diffused in the area.

The Calcare di Base Fm. overlies stratigraphically the diatomitic clays and locally includes fault-scarp breccias with large blocks (Fig. 3.6a) and thin marl layers (Fig. 3.6b), the last probably describe a temporary deepening of the basin edge.

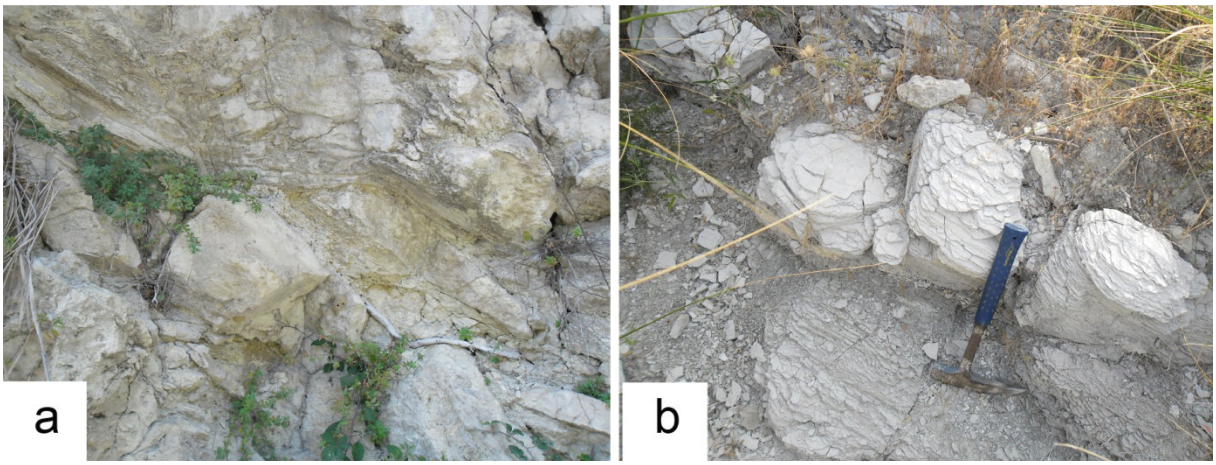

Figure 3.6: Calcare di Base outcropping in the northern area is characterized by: a) fault-scarp breccias with large blocks and b) thin marl layers.

Resedimented, deepwater (Resedimented Lower Gypsum, RLG; Roveri et al., 2008) evaporites outcrop more diffusely in the central Catanzaro Trough. The drastic decreasing of sea level produces partially the cannibalization of the Calcare di Base and almost completely Primary Lower Gypsum (PLG, Roveri et al., 2008). In fact, RGL contains PLG slided selenite blocks (Fig. 3.7), which passes upward by means of an intra-Messinian unconformity to gypsum-rudites, gypsum-arenites and gypsum-pelites, referred to Upper Evaporites (Cianflone & Dominici, 2011).

Figure 3.7: Resedimented Lower Gypsum (RGL) contains Primary Lower Gypsum PLG slided selenite blocks.

Upper Evaporites are characterized by ca. 50m thick of deposits, which show an alternation of gypsum pelites and gypsum arenites overlying Lower Evaporites, passing upward to fluvial and alluvial facies (Fig. 3.8b) with rounded metric boulders of branching selenites (Fig. 3.8c; Cianflone & Dominici, 2011, Lugli et al., 2005). Between Marcellinara and Settingiano villages, channel-bar facies outcrop diffusely along the northern portion of Catanzaro Trough..

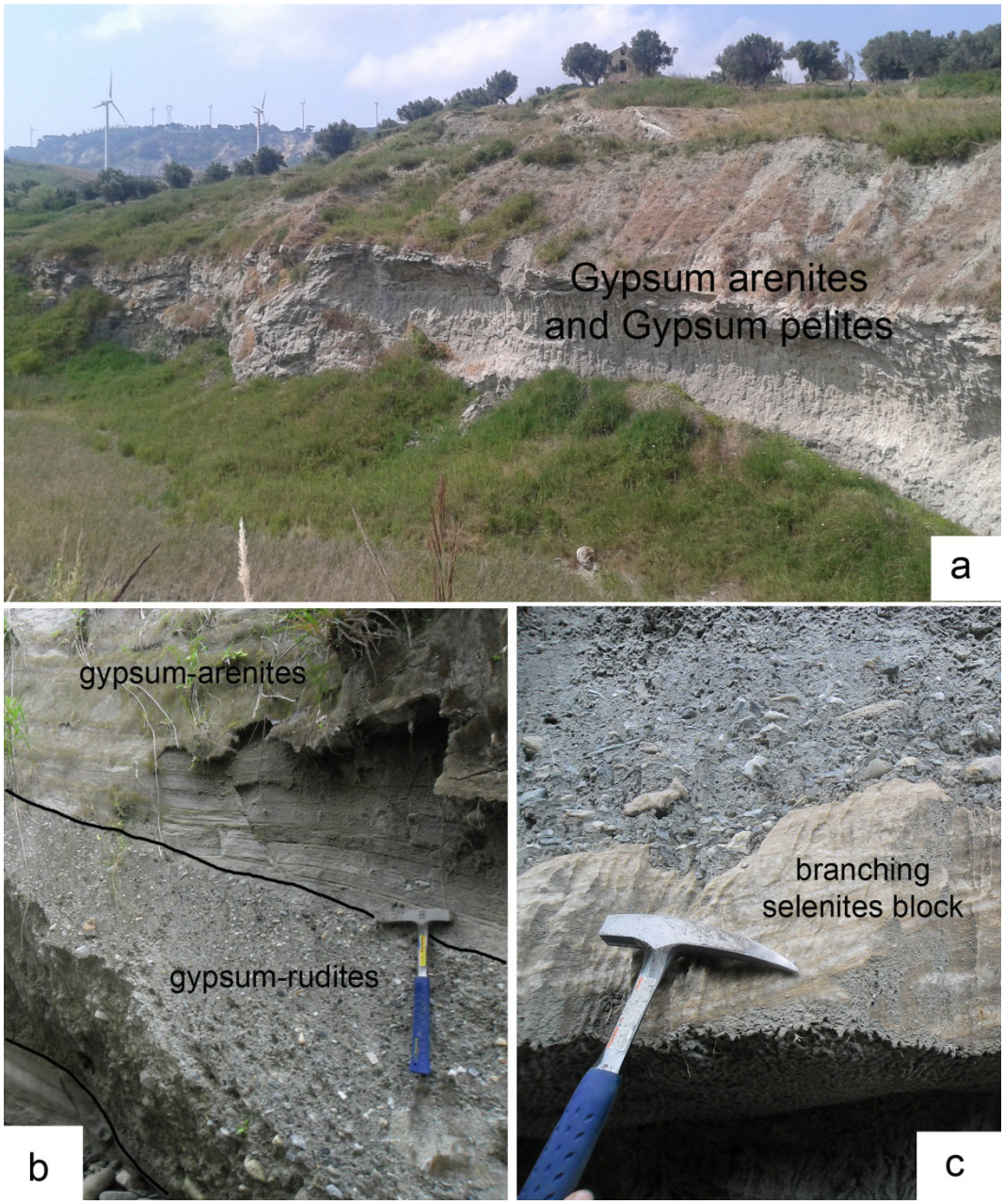

Figure 3.8: a) Gypsum- arenites and gypsum- pelites outcropping in a quarry between Marcellinara and Settingiano villages, b) alternation of gypsum-rudites and gypsum- pelites c) branching selenite block observed within channel-bars facies outcropping along Riato River.

3.3 Sedimentary units of Catanzaro Trough

The Catanzaro Trough underwent several sedimentary changes starting from Late Messinian, indeed it was affected by extensional tectonics, about N- S oriented and partially driven Middle Miocene – Lower Pleistocene strike-slip deformations (Van Dijk et al., 2000).

3.3.1 Late Messinian- Lower Pliocene conglomerates sequence

The lowermost sedimentary unit of Catanzaro Trough was represented by a continental succession up to 200 m thick, overlying gypsum-rich conglomerates belonging to Upper Evaporites (Fig. 3.9).

This sedimentary succession shows a drastic decrease of the intrabasinal evaporitic and carbonate alimentation in favour of metamorphic and plutonic detritus supplied by the Calabrian-Peloritan Arc units (Roveri et al., 2008, Cianflone & Dominici, 2011).

These deposits are represented mainly by Messinian to Lower Pliocene massive and stratified conglomerates, passing upward to sandstones. Conglomerates, mainly clast-supported, outcrop diffusely along the northern and southern margins of the basin, composed of granites and medium-to-low grade metamorphic rocks with minor evaporitic rocks.

Conglomerates outcropping close to the Sarrottino village correspond in time to the Carvane formation (Roda, 1964, Barone et al., 2008), representing second post-evaporitic unit (p-ev2) of Roveri et al. (2001). Within Marta well (wells documentation coming from Eni s.p.a. in the frame of ViDEPI project, this unit is more than 370 m thick and can be related to Pelliciano Mount and Carvane Fms.

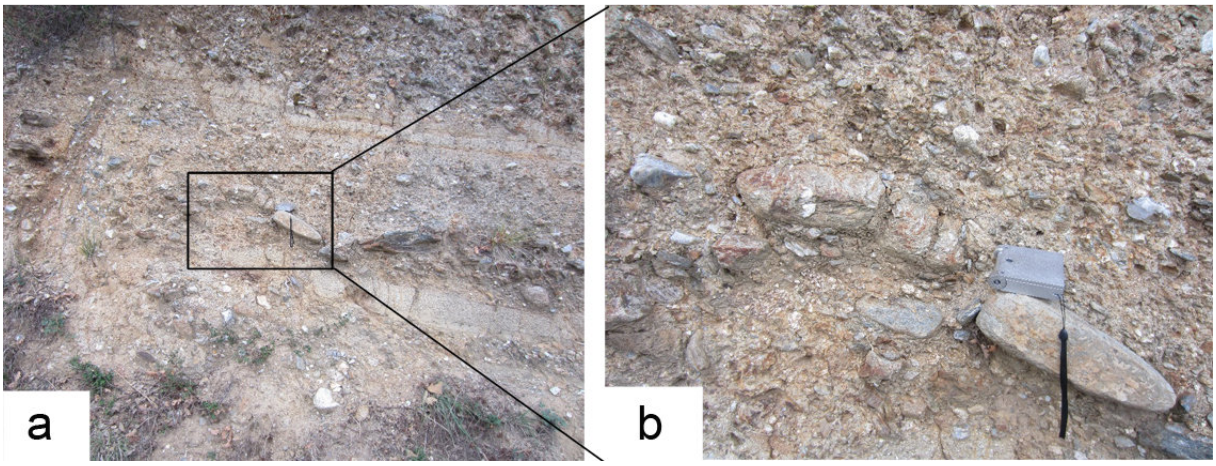

Figure 3.9: Alternation of Upper Messinian conglomerates and sandstones. High fractured and low sorted conglomerates showing an high number of metamorphic clasts

Although the Upper Messinian- Lower Pliocene conglomerates, outcropping along the southern edge, appear less thick and less widespread than the northern one, they shows major variability in term of composition, in fact clasts are composed by metamorphic, igneous and sedimentary- evaporitic rocks (Fig. 3.10a, b), the last observed close to the Cortale village (Fig. 3.10c, d).

Locally the evaporates-rich conglomerates are interbedded by marls and calcarenites layers, showing a sudden deepening of the basin margin.

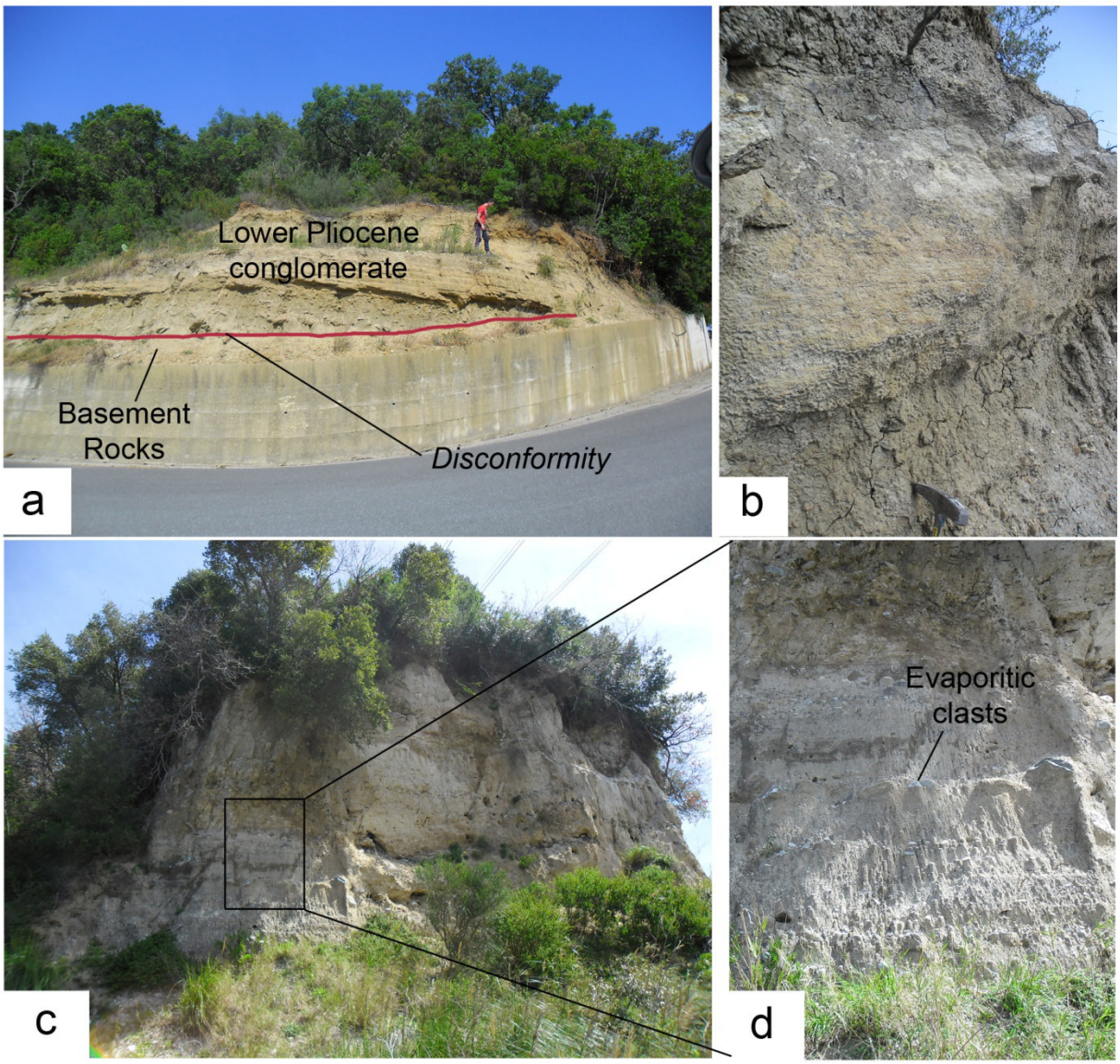

Figure 3.10: different conglomerates outcropping to the south of western Catanzaro Trough: a) and b) crystalline-rich conglomerates; c) and d) evaporites-rich conglomerates.

3.3.2 Pliocene limestone-marl sequence

The 300 thick limestone-marl alternations (Fig. 3.11a), associated to the Trubi Formation (Zanclean) outcrop widely in the study area and show, in the Eni wells, affinity with the lowest portion of Crotone Clay. These deposits cover Messinian sedimentary succession, and pass upward to a ca 50 m thick succession composed of weakly cemented sandstones and mudstones deposited in a marine shelfal environment related to the Monte Narbone Formation (Piacezian) (Di Stefano & Lentini, 1995; Cavazza & Ingersoll, 2005).

Close to the Maida village, at the bottom Trubi Fm shows marls and clay of variable colour from light grey to white. According to Saccà et al. (2004) the relative abundance of foraminifera contributed to define the depositional environment, circa-littoral deep-bathyal sea and the benthic association. This suggests the authors to relate these marls and clays to the Zanclean time. The previous outcropping pass upward to marls and sands alternations; the sand layers are of light brown colour with ripple structures (Fig. 3.11b).

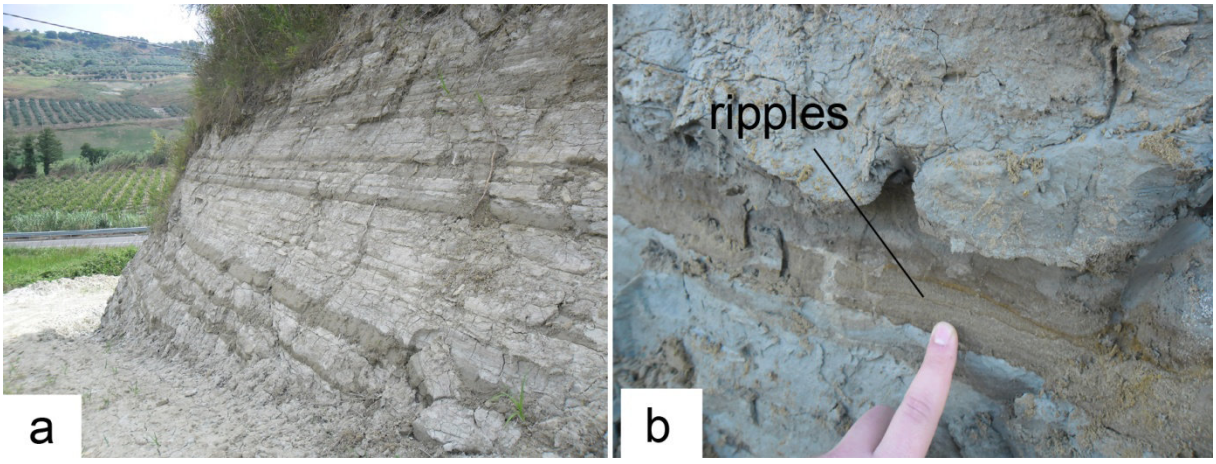

Figure 3.11: a) marls and sands alternations, b) particular of the outcropping showing the presence of ripples within the sands layers

Near Chiana Munda hill we have observed a ca. 80 m thick sands containing thin silts layers (Fig. 3.12). This outcrop is overlain, in turn, by grey to white marls and silts, which we can locate stratigraphically in the upper part of Pliocene sedimentary succession (Piacezian?-Lower Pleistocene?).

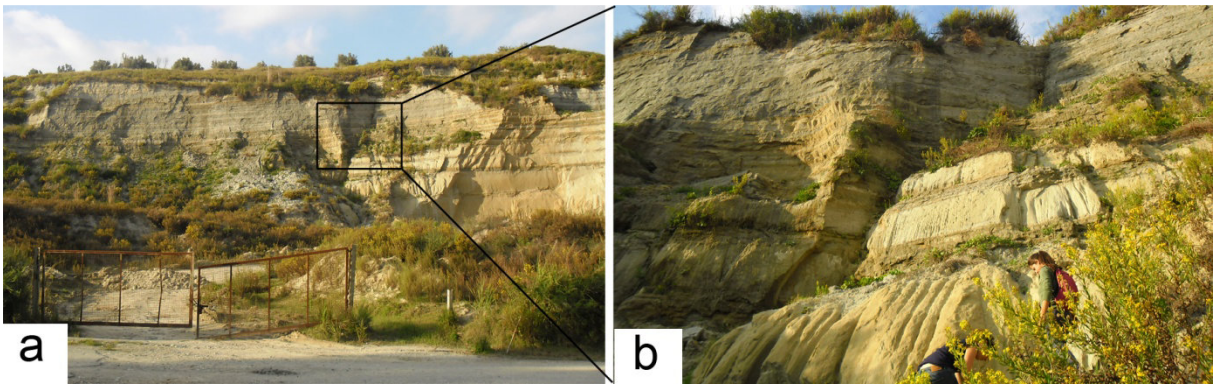

Figure 3.12: sands with minor marls layers outcropping near Chiana Munda hill

3.3.3 Lower Pleistocene mixed silici-bioclastic sands, sandstones sequence

The early Pleistocene unconformity the (EPSU; Zecchin et al., 2012, 2015) marks the opening of the Catanzaro fault-bounded palaeo-strait (sensu Longhitano et al., 2012, 2014). The EPSU separates the fine-grained Pliocene deposits from the Calabrian strait-fill succession, consisting of ca. 100 m mixed silici-bioclastic sands, sandstones and, subordinately, mudstones (Fig. 3.13; Chiarella et al., 2012a; Longhitano et al., 2014).

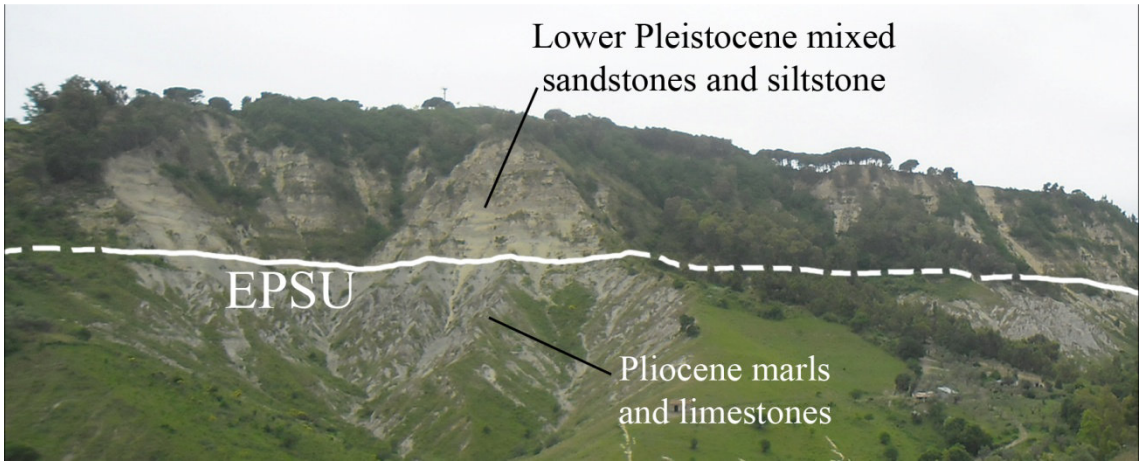

Figure 3.13: Plio-Pleistocene Uncomformity (EPSU; Zecchin et al., 2015) bounding the top of Pliocene marls and limestones.

Mixed sediments derive from the combination of an extrabasinal (siliciclastic) with an intrabasinal (bioclastic) fraction (Chiarella, 2011). The lower Pleistocene stratigraphic interval includes the Vena di Maida, the Pianopoli and the lowermost interval of the Basile Unit. These units consist dominantly of mixed, fine to coarse-grained sandstone and, subordinately, mudstone.

The two sandstone units present varied internal organization and their heterogeneity differ based on the occurrence of small to medium trough (3D) cross-strata in the Vena di

Maida unit, and planar (2D) cross-strata in the Pianopoli unit (Fig. 3.14; Chiarella et al., 2011, 2012a; Longhitano et al., 2014).

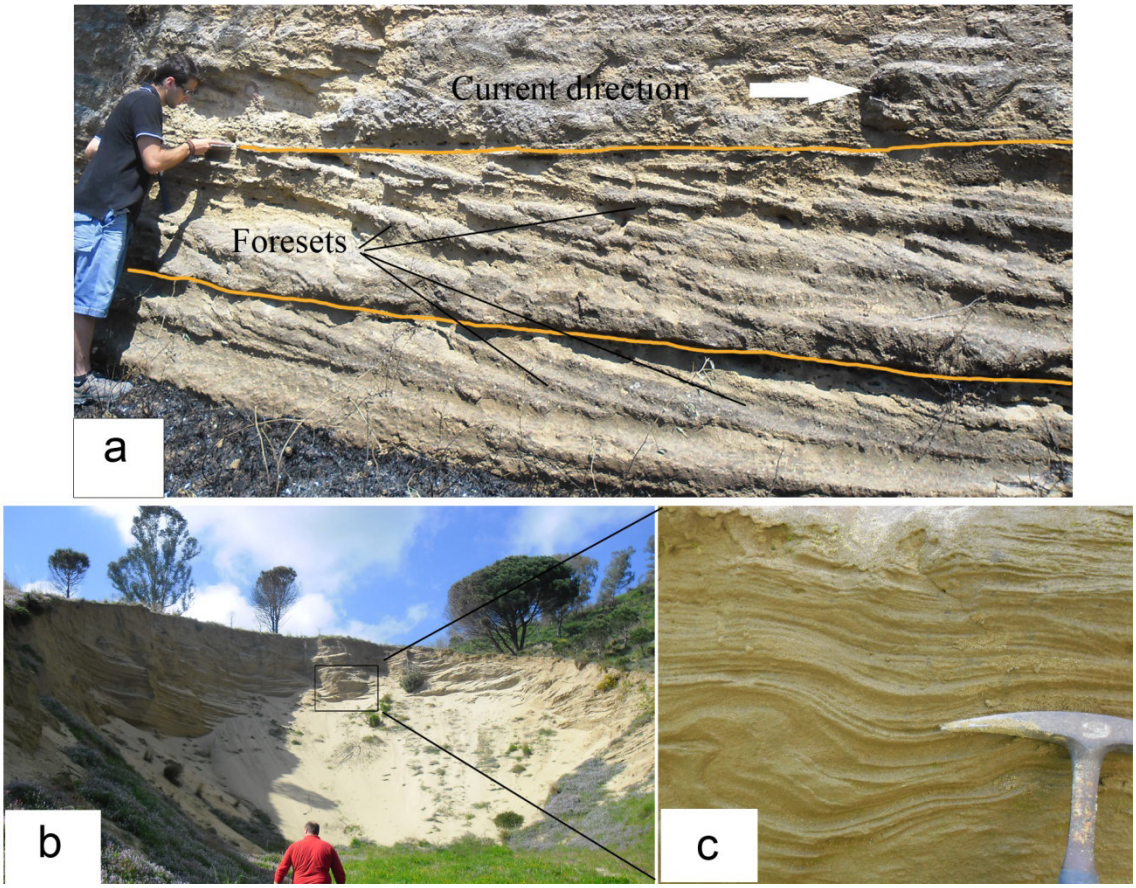

Figure 3.14: a) Tidal deposits showing foresets organized in trough cross-strata close to Girifalco Village, b) and 3D cross-stratified sands outcropping near Pianopoli village c) detail imaging likely bedform along the current tidal cross-stratification

Near San Pietro a Maida village we can observe a very short outcropping which shows a 5 m thick calcarenites, characterized by the presence of *balanus*, corals and ostreas, without cross-stratification. The sedimentary sequence overlies Polia Copanello Unit and part of Lower Pliocene conglomerates (Fig. 3.15).

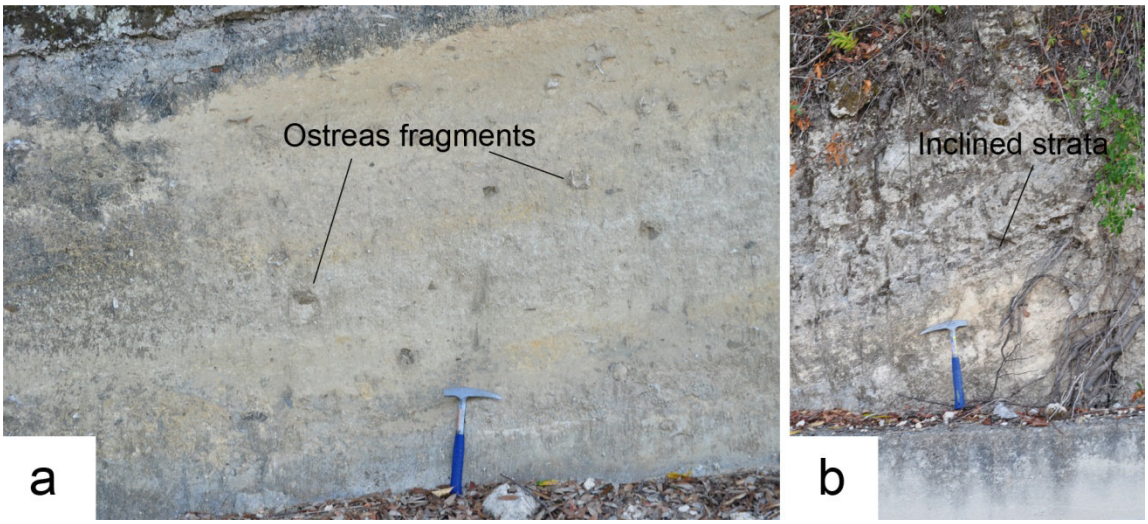

Figure 3.15: a) Calcarenites characterized by the presence of *balanus*, corals and ostreas, b) inclined stratification visible along the outcropping.

3.3.4 Middle-Upper Pleistocene Terrace sequence

The marine terraces distribution both in space and in time still ongoing debated: Tortorici et al. (2003) focused their studies on chronology and on the evaluation of the rates of uplift and, recognized seven distinct order of Capo Vaticano marine terraces. This study was supported by numerical dating derived from Optically Stimulated Luminescence (OSL) age estimates (Bianca et al., 2011). Their number and their distribution are very different from those reported in the Miyauchi et al. (1994) and Cucci & Tertulliani (2006) studies, both of them distinguished 12 orders of marine terraces.

The Marine terraces, mainly widespread along the Tyrrhenian coastline (Capo Vaticano promontory, Capo Suvero area and Costal Range), consist of a Middle-Late Pleistocene flight of wave-cut surfaces and/or thin-depositional platforms. Usually, they are bounded landwards by well developed inner edges representing the paleoshorelines related to the main sea level highstands (Tortorici et al., 2003).

The Quaternary terraced deposits are generally made up of siliciclastic sands and coarse sandstones with a fossiliferous content mostly represented by poor microfaunas. Even if rarely, within of these sequences, levels of gravel and boulders are observable (Fig. 3.16).

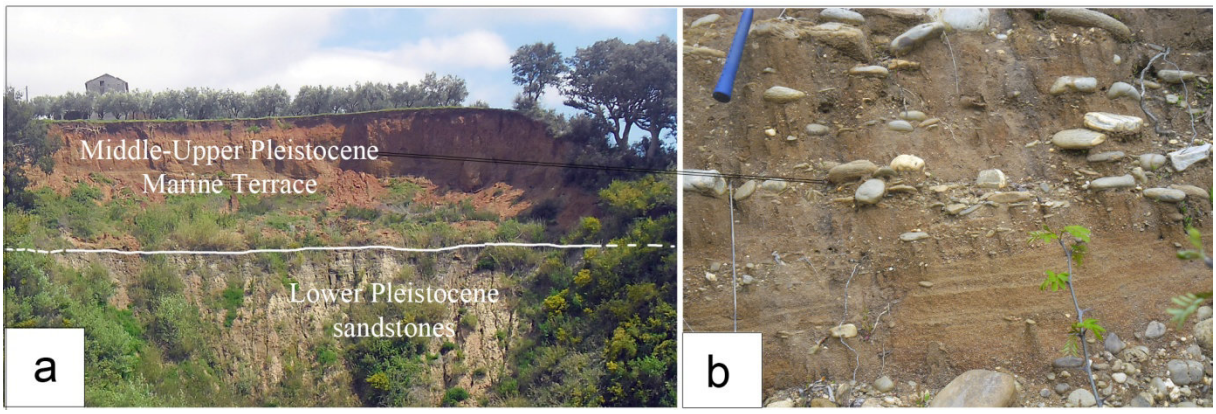

Figure 3.16: a) Erosional contact between Lower Pleistocene biocalcarenites and sand-wave deposits and Middle Upper Pleistocene Marine Terrace, b) Outcropping of Middle Upper Pleistocene Marine Terrace.

Within the Western Catanzaro Trough we have recognized at least six of the seven order of marine terraces, using the classification of Bianca et al. (2011) and Tortorici et al. (2002). The mapping of these morphological features allowed us to define a summit surface (Bianca et al., 2011) represents the highest and oldest order of the Middle-Upper Pleistocene marine terraced sequence. The eroded top surface reach the 700 m high both within the Serre Massif and the Capo Suvero area (Fig. 3.17). The Terrace VII, the lowest order of marine terraces, ascribed to the stage 3.3 (60 kyr) of the eustatic curve (Tortorici et al., 2002, 2003), is not observed in the area. The Terrace IV has been related to the OIS 5.5 (125 kyr) using TL age estimations (Balescu et al., 1997), widespread both within southwestern studied and Capo Suvero areas.

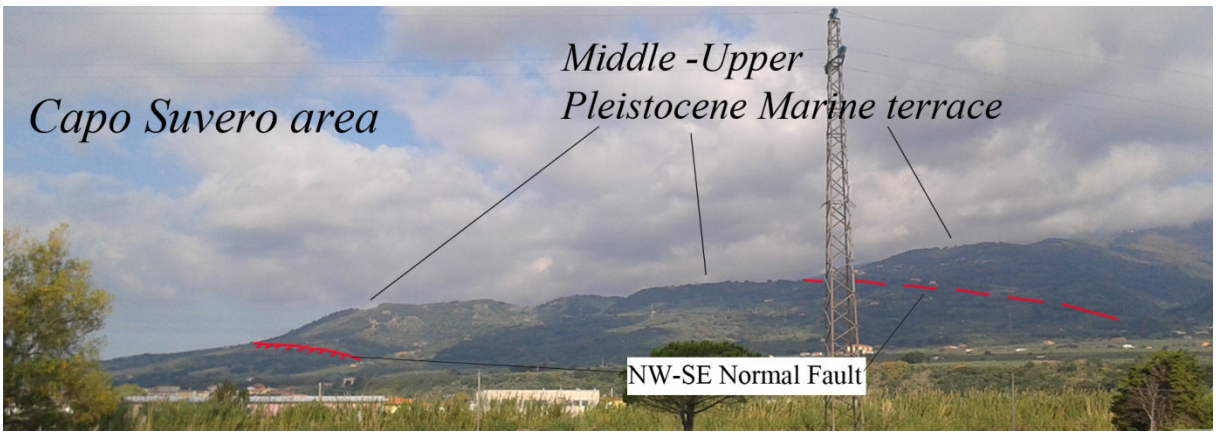

Figure 3.17: Northwestern overview of Catanzaro Trough, showing various order of terraces in the Capo Suvero area, bordered in the inner edge by NW-SE normal faulr.

3.3.5 Late Quaternary sequence

A western part of the Catanzaro Trough is characterized by a widely outcropping Late Quaternary sedimentary sequence. A detailed record (*well logs*) of the Late Quaternary geologic formations have been obtained by several borehole placed within Sant'Eufemia Plain (Fig. 3.18).

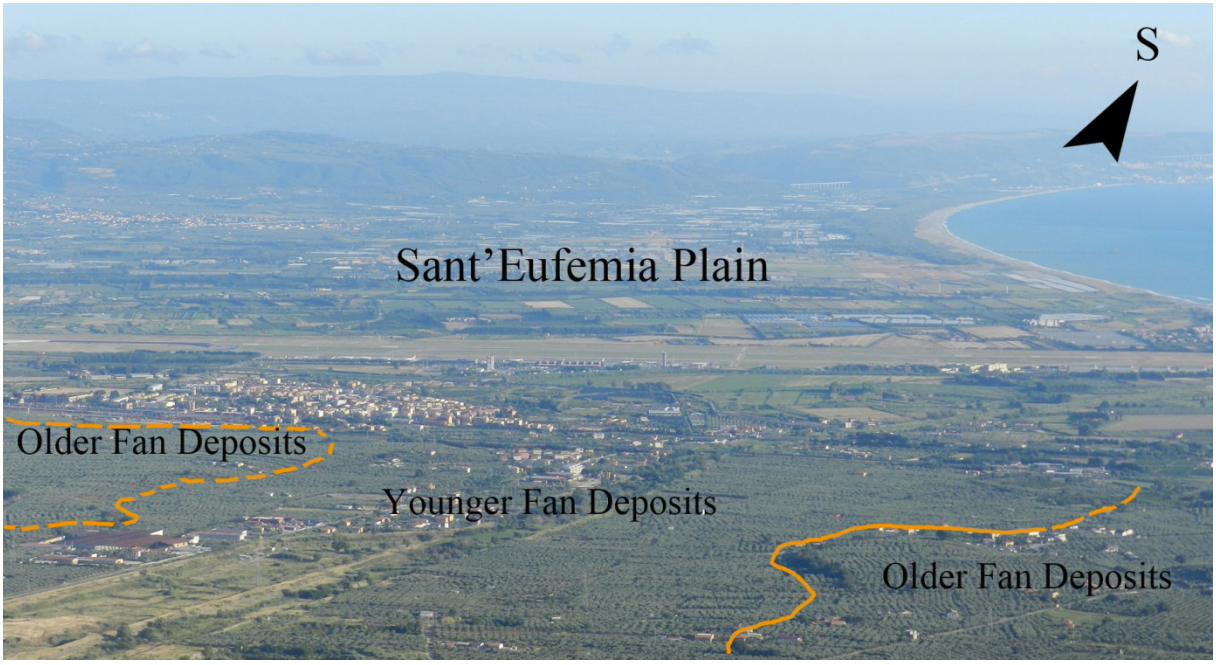

Figure 3.18: N-S overview of Sant'Eufemia Plain, showing two order of fan deposits, related to Upper Pleistocene-Holocene time

The Sant'Eufemia Plain is characterized by alluvial fans. The boreholes show, on average, 60m thick conglomerates and sands deposits, with subordinately silts layers, covering directly Middle Pleistocene clay.

Morphologically we recognized at least two order of fan deposits, mainly developed along the northern edge of the plain (Tortorici et al., 2002). To the south of Capo Suvero area, older alluvial fans is cut by a likely fault escarpment, representing the WNW-ESE normal Zinnavo Fault (Tortorici et al., 2002), which may have subsequently been rapidly buried by younger alluvial fans (Fig. 3.17).

We recognized at least three wide alluvial fans, one of these, the widest, is placed south of Nicastro, reaches the length of about 10 km. Close to the Tyrrhenian coastline, the last two reach the length of about 7 km. All of them are cut newly by very recent fluvial deposits. We integrated these insights with a set of old and new sub-surface data, which we amply treated in the next chapter.

CHAP. 4 Structural data

4.1 Structural analysis

The Catanzaro Trough is characterized by a complex geo-structural history. To gain knowledge of structural features of this region, we focused on analyzing of new structural datasets collected along the onshore segment of Catanzaro Trough. Further, new data, related to the main faults system, have been integrated with the interpretation of aerial photos, collected during photogrammetric surveys conducted in 1983 (scale 1: 33000) and, in 1990 (1:33000) by the Italian Military Geographic Institute (IGM) in Florence.

The collected structural data, related to the brittle elements and classified on the base of kinematics and fault directions, helped us to define the stress field of the whole study area. The distribution of more than 700 structural measurements, organized in about 40 survey stations (Fig. 4.1), have been analyzed and processed by using the DAISY software (Salvini, 2002). To better understand the tectonic evolution of the area data have been organized in *two structural domains*, one of which characterizing the northern portion of Catanzaro Trough: extending from Capo Suvero area to Corace River and the other one represented by the remaining southern domain: extending from Curinga to Girifalco villages (Fig. 4.1).

The statistical distribution of faults, here analyzed, has been further studied through contouring of the fault planes, slickensides and rotational axes (rotaxes).

The obtained datasets gave the opportunity to reconstruct major lineaments of the area. Where the fieldwork study and aerial photo interpretation become lacking, we integrated the acquired datasets by means of onshore seismic reflection profiles, treated widely in the next section.

A synthesis of location of geological and structural map are shown in figure 4.1. within the sketch map, the uncertain faults are marked by dashed red lines. The uncertainty is due to the difficulties to define the lineaments come from poor geological exposure and lack of clear evidence above Upper Pleistocene- Holocene sediments rarely recording the recent tectonic phases.

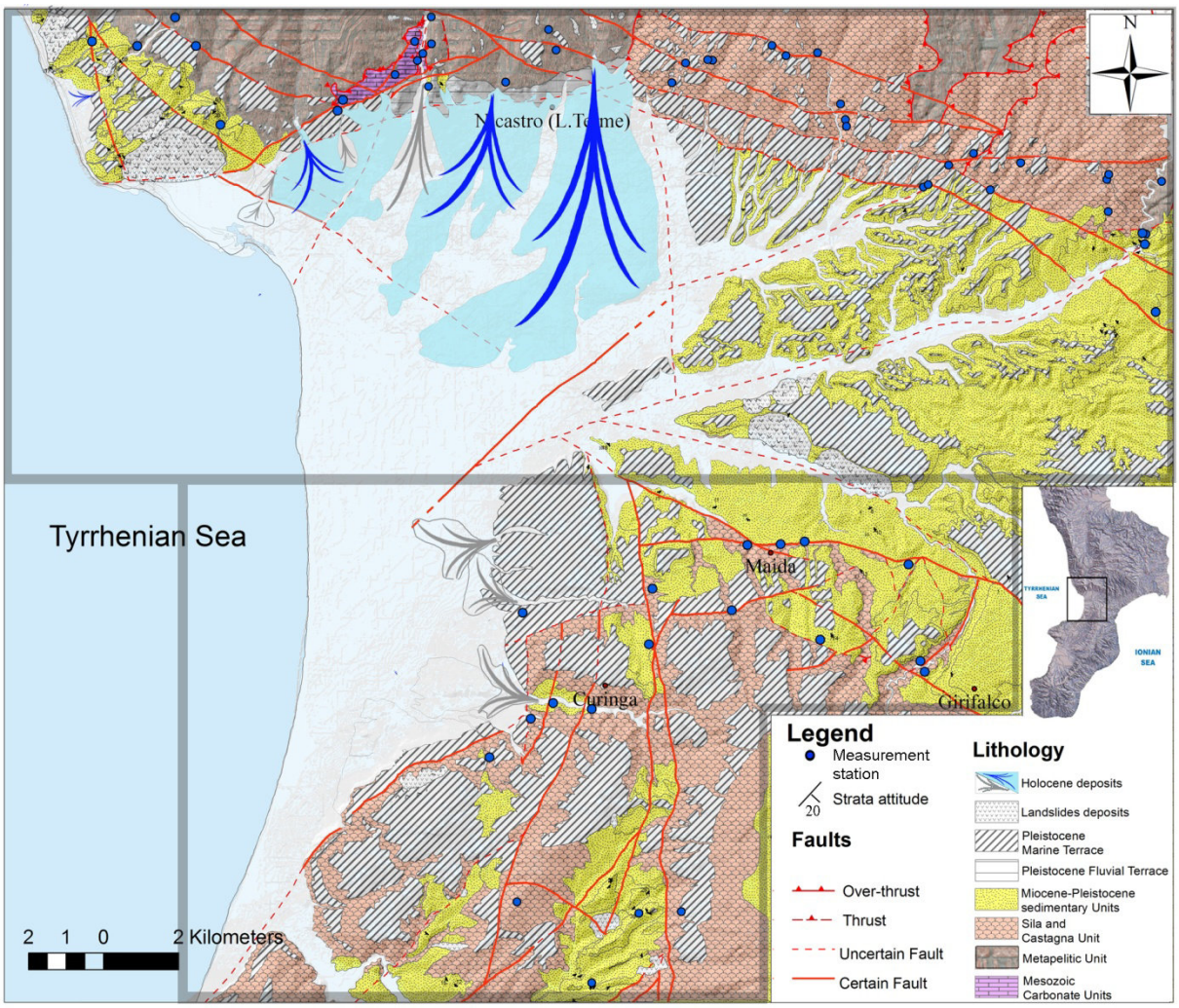

Figure 4.4: Structural and geological sketch map, the datasets have been organized in two structural aerial domains (grey boxes).

4.1.1 Rotational axis (rotaxes)

The rotaxes are structural elements which correspond to the σ_2 axis of a conjugate pair of faults, *andersonian* coniugate faults, used to discriminate between different deformation events (Wise & Vincent, 1965; Salvini & Vittori; 1982, Mattei et al., 1999).

The rotaxes (Fig. 4.2) show in the studied area two main sub-horizontal and sub-vertical clusters, even though we can notice a heterogeneous dispersion of rotaxes. The sub-horizontal rotaxes of normal faults dominate (almost 300 measurements) and are concentrated around the N30 and N70 directions (Fig. 4.2). These clusters are mainly related to N–S and NE–SW normal fault systems, corresponding to an extensional direction (σ_3) mainly WNW-ESE oriented (Fig. 4.2).

Although the number of measurements are less notable than normal faults, the sub-horizontal rotaxes (σ_2) related to reverse faults (Fig. 4.2) show a greater concentration around N45 direction, whereas σ_1 is oriented along NW-SE direction.

The sub-vertical grouping of rotaxes is related to strike-slip faults, but they provide few information about the related conjugate fault systems; therefore, we preferred focused the analysis on the statistical distribution of orientation and kinematics of fault planes, described in the following section.

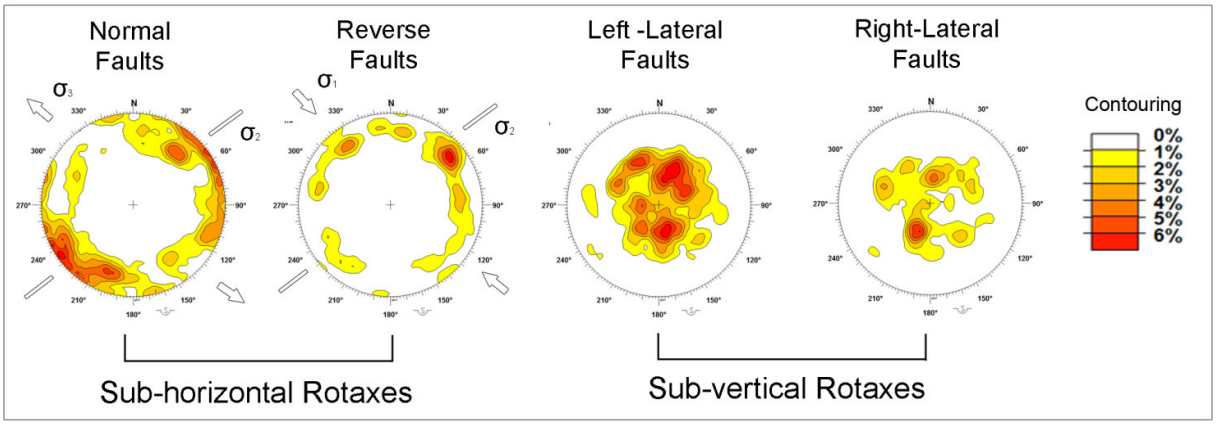

Figure 4.2: Contours of the rotaxes used to discriminate between different deformational events.

4.2 Northern structural domain

The main tectonic lineaments characterizing the northern margin of the area, clearly visible on the macroscale, are represented by transversal faults spanning from NW-SE to ca E-W orientation (Van Dijk et al., 2000; Tansi et al., 2007, Milia et al., 2009). These structural lineaments correspond partially to the southern fault segments, named Lamezia-Catanzaro Fault (*sensu* Tansi et al., 2007), belonging to the three right-stepping *en 'echelon* major S-dipping fault segments.

Along the western portion of the northern area, these transversal fault systems act as high angle tectonic contact between the basement rocks belonging mainly to the Paleozoic Metapelitic and Mesozoic Carbonate units and, the overlying Late Quaternary deposits (Fig. 4.3). These lasts are located widely on the hangingwall of the main faults, causing unfortunately several limitation to define chronologically the kinematics in this margin.

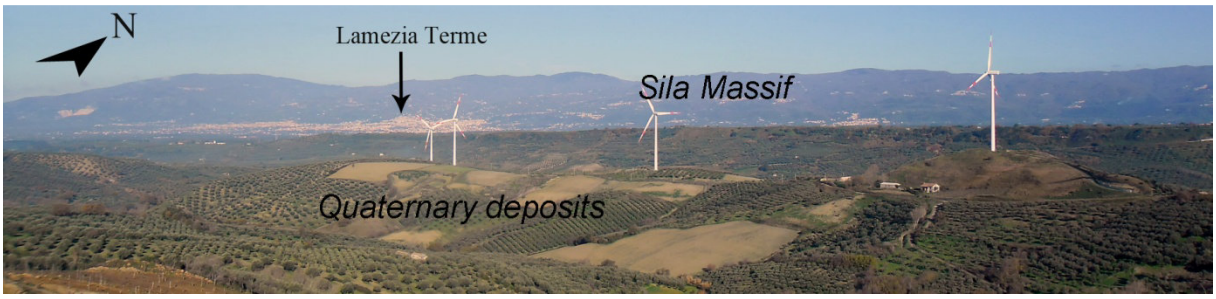

Figure 4.3. Overview of northwestern margin of the Catanzaro Trough.

The geologic features is complicated both by the presence of inversion tectonics, likely due to local transpressional character of the main WNW- ESE faults and, by the activity of Quaternary NE-SW oriented normal faults. These lasts produce the exhumation of buried Early Miocene overthrusting contact between the Metapelitic Units above the Mesozoic Carbonate Unit. This contact outcrop within the Terme di Caronte area, showing a ca E-vergence and a ca W-dipping thrust plane (Fig. 4.4).

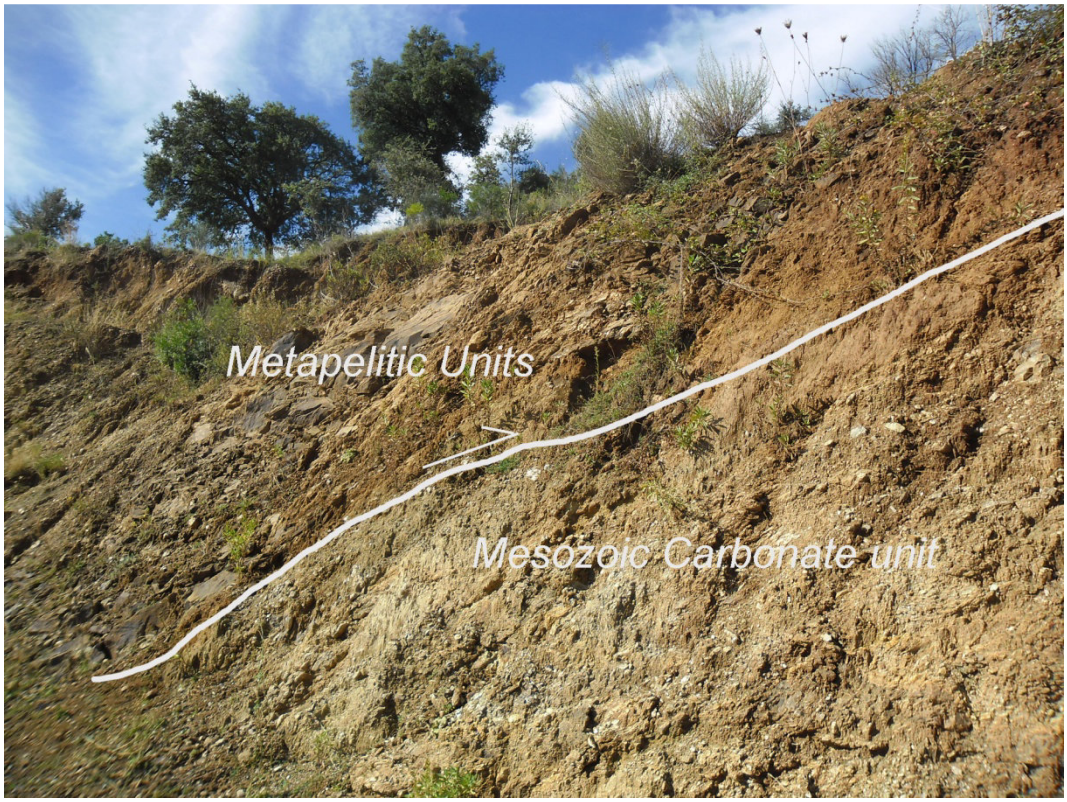

Figure 4.4: Overthrusting contact between the Ophiolitic and Metapelitic units above Mesozoic Carbonate Unit, close to Lamezia Terme town.

Towards eastern part of the northern margin, the WNW-ESE structures show a minor fault offset, indeed, the morphological escarpments, characterized by triangular and trapezoidal facets, become less visible than the western one. The outcropping sedimentary

succession is characterized by Messinian to Late Quaternary age, that allowed us to better analyzed events that influenced this area.

During the first opening phases of the Catanzaro Trough, the bed attitude of the strata show a general S-dipping of former depositional sequences related to Upper Messinian – Pliocene sediments. The Quaternary deposits shows W-dipping layers, in the western side, and E-dipping in the eastern side. This changing occur approximately along the center of the Catanzaro Trough which is characterized by a structural high, acting as a ridge or bedload parting (Longhitano et al., 2013, 2014). This elongated promontory connects the northern with the southern margin of the basin. The lateral continuity is further modified by faults with different direction and age and by the landslides that overturn part of the sedimentary sequences.

4.2.1 Structural data

Structural data analysis of brittle elements, classified on the base of kinematics, i.e. fault directions (DAISY software; Salvini, 2002), allowed to identify several fault sets with different strike and dip. Furthermore, we distinguished two types of substratum dislocated by the faults, that are: the Paleozoic-Mesozoic basement rocks, clearly recording the tectonic events of the Catanzaro Trough; and the Neogene-Quaternary sedimentary deposits that provide clues on chronological evolution of the area.

The northern Catanzaro Through is characterized by above mentioned morphological fault scarp, spanning from NW-SE to E-W direction.

At the mesoscale the structural data document the high distribution of ca. E-W oriented normal faults, widespread in the northwestern portion of the area, clearly offsetting the basement rocks.

As regards sedimentary units, the normal faults show a relative abundance compared with the other kinematics, affecting mainly Messinian to Pliocene deposits (Fig. 4.5). As consequence these lineaments seem to play an important role in the general N-S oriented extensional axis, which drove the Catanzaro Trough opening during late Miocene (see below in figures 4.18b and 4.19b).

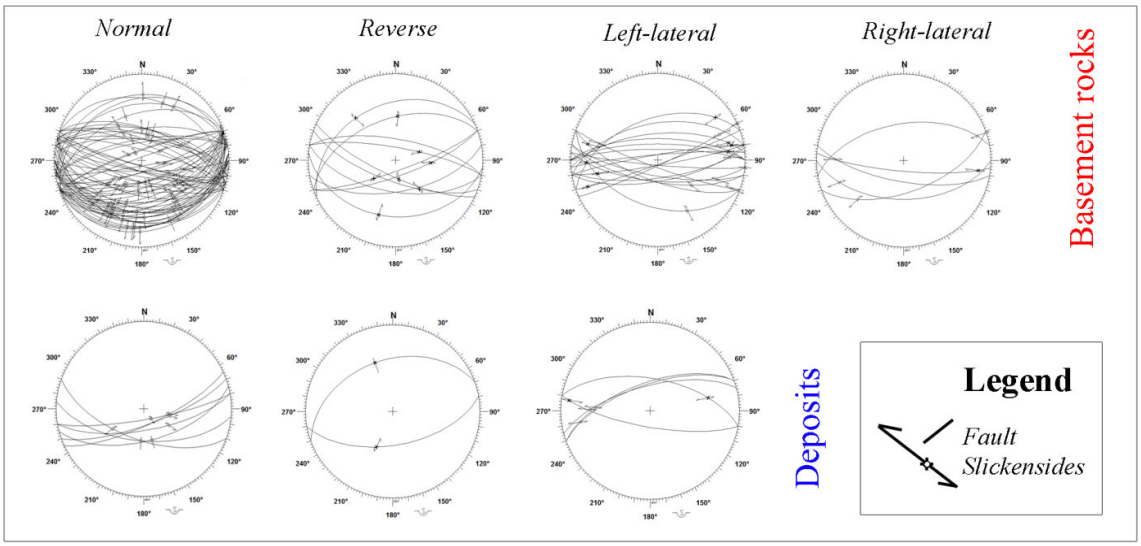

Figure 4.5: E-W faults system classified on the base of the kinematics, direction and type of substrate.

Although at the regional scale, NW- SE fault system represents the boundaries of the transtensional deformation zone. The collected structural data show a poor distribution in terms of structural measurements, both as regards basement rocks and Miocene- Quaternary deposits.

The northern paleostrait deposits are not marked by left lateral faults, at least to the mesoscale, whereas right-lateral strike slip faults affect both basement rocks and deposits (Fig. 4.6).

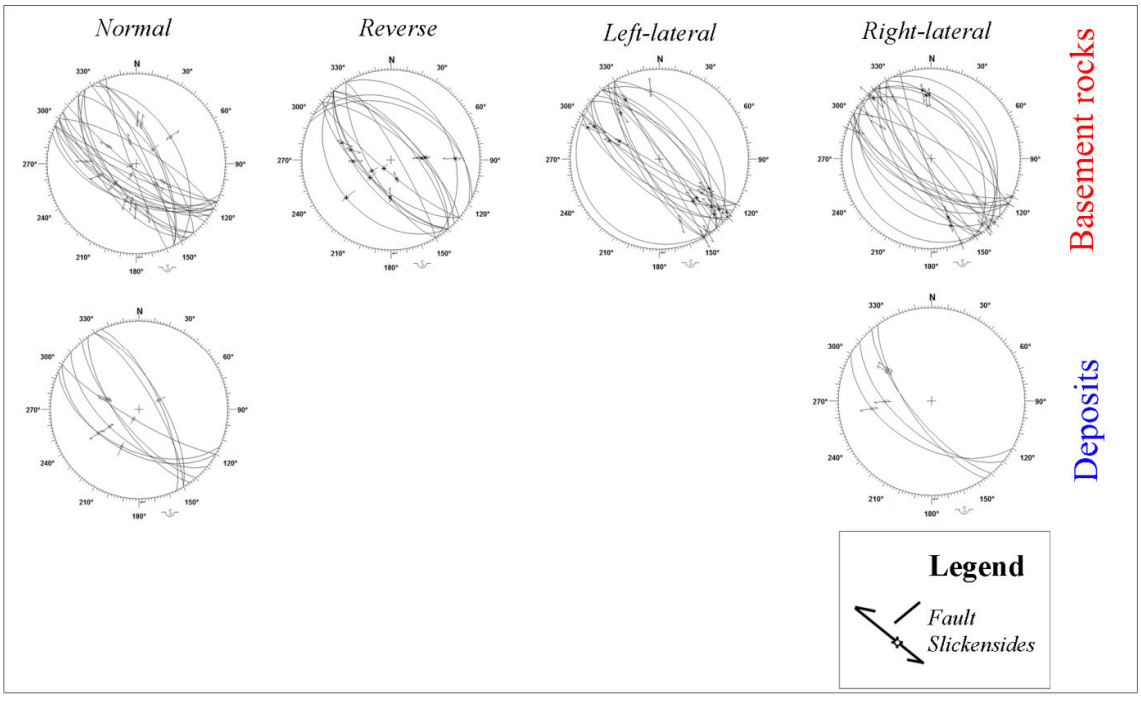

Figure 4.6: NW-SE fault system classified on the base of the kinematics, direction and type of substrate

Although the structural data show a differentiated distribution of faults, the NE-SW oriented faults system represent the more widespread measurements in the northern area (Fig. 4.7).

The NE-SW normal faults, characterized by a significant preponderance of oblique slickensides, usually overprint pre-existing kinematic indicators and former fault system. The WNW-ESE extensional axis driven by the NE-SW normal faults produced a Pleistocene basin subsidence and deepening of the western portion of Catanzaro Trough and the general uplift of adjacent crystalline basement.

Relatively abundant are the left- and right- lateral faults registered both from basement rocks and deposits. The same NE-SW transcurrent faults take on locally transpressional and transtensional features.

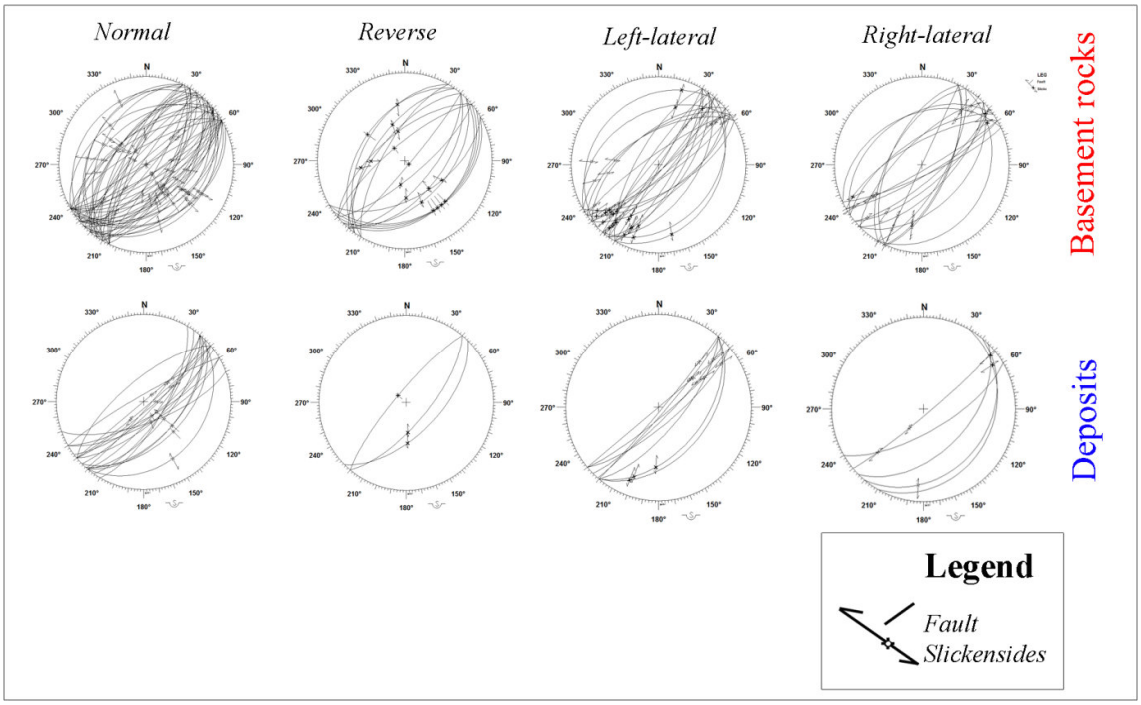

Figure 4.7: NE-SW faults system classified on the base of the kinematics, direction and type of substrate

Close to the Marcellinara area, the Messinian conglomerates are dislocated by syn-sedimentary strike slip faults with a reverse component of motion (Fig. 4.8).

The NE-SW faults represent, especially during the Pliocene age, conjugate structures controlled by the major NW-SE transcurrent system. Within Catanzaro Trough, the NE-SW fault system influence, the ongoing drainage pattern of the main river in the area (the Amato River) and other minor NE-SW orientated streams.

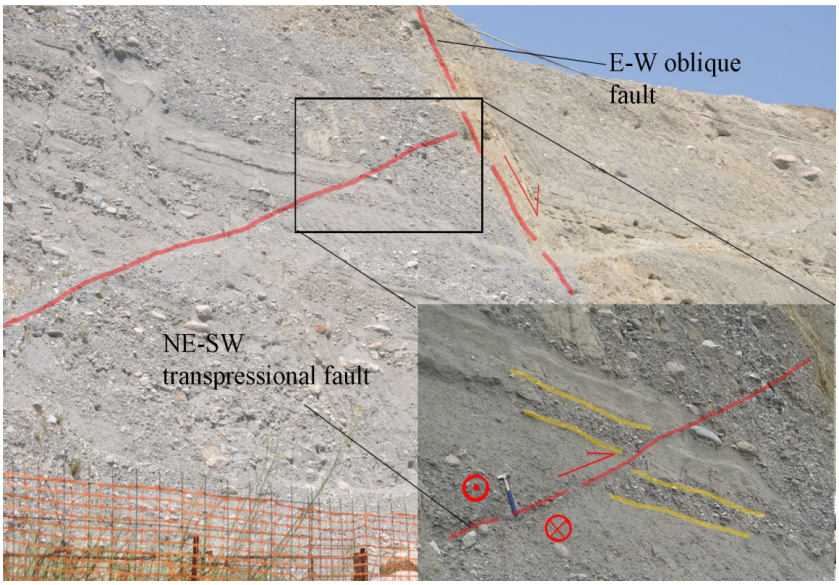

Figure 4.8: NE-SW transpressional faults outcropping above the Messinian conglomerates(visto il basso angolo forse è meglio parlare di thrust

In the northern side of Catanzaro Trough, we measured an high number of N-S faults, affecting both basement rocks and deposits. These structural data have been collected mainly within and close to the Bagni and Corace rivers, which show both of them a N-S stream trend, although two watercourses are placed at a distance of about 20 km from one another, in the western and eastern margin of the study area, respectively. Towards east the Corace River, close to Catanzaro City N-S straight trend. The N-S transcurrent faults collected above sedimentary units shows a relative abundance as regards right lateral faults compared the other (Fig. 4.9).

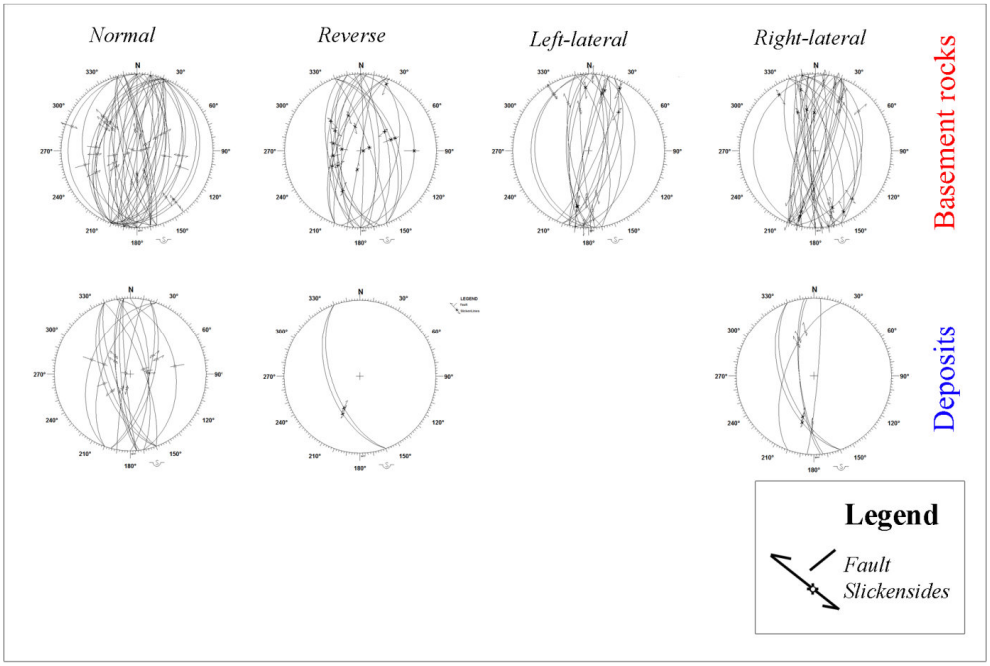

Figure 4.9: N-S fault system classified on the base of the kinematics, direction and type of substrate.

4.3 Southern structural domain

Similar to the northern domain, the main morphological evidence characterizing the area is the NW-SE oriented fault system, represented by the Maida- Punta Staletti system (Ghisetti, 1979). Close to the Maida village the above mentioned lineaments are interrupted by a combination of the NE-SW and N-S trending faults, which represent partially the northward continuation of the Serre Faults (Galli et al., 2007).

Figure 4.10. Overview of southwestern margin of the Catanzaro Trough.

During the Upper Miocene-Pliocene the basin infill undergoes, at the same time, an intense deepening and a drifting towards SE (Van Dijk et al., 2000; Tansi et al. 2007; Tripodi et al., 2013), producing the transgression on the Paleozoic crystalline basement.

Similarly to the northern margin, during Late Pliocene-Lower Pleistocene time, the southern margin undergoes an extensional tectonics superimposed on strike slip kinematics. This tectonics controls the evolution of narrow strait and the connection between the Ionian with Tyrrhenian Sea and the sublittoral sedimentation (Colella & D'Alessandro, 1988; Argnani & Trincardi, 1993; Van Dijk et al., 2000; Chiarella et al., 2011; Longhitano et al., 2012b, 2014).

4.2.1 Structural data

The analysis of southern structural data, classified on the base of the kinematics, direction and type of substratum, have allowed to understand the tectonic evolution of the southern margin of Catanzaro Trough and to compare these results with the same acquired in the northern edge.

Firstly has been analyzed the E-W fault system. Figure 4.11 shows an equal distribution of measurements as regards faults affecting the basement rocks. Whitin this system, we can observe a minor concentration of right lateral faults compared with the normal, reverse and left-lateral kinematics.

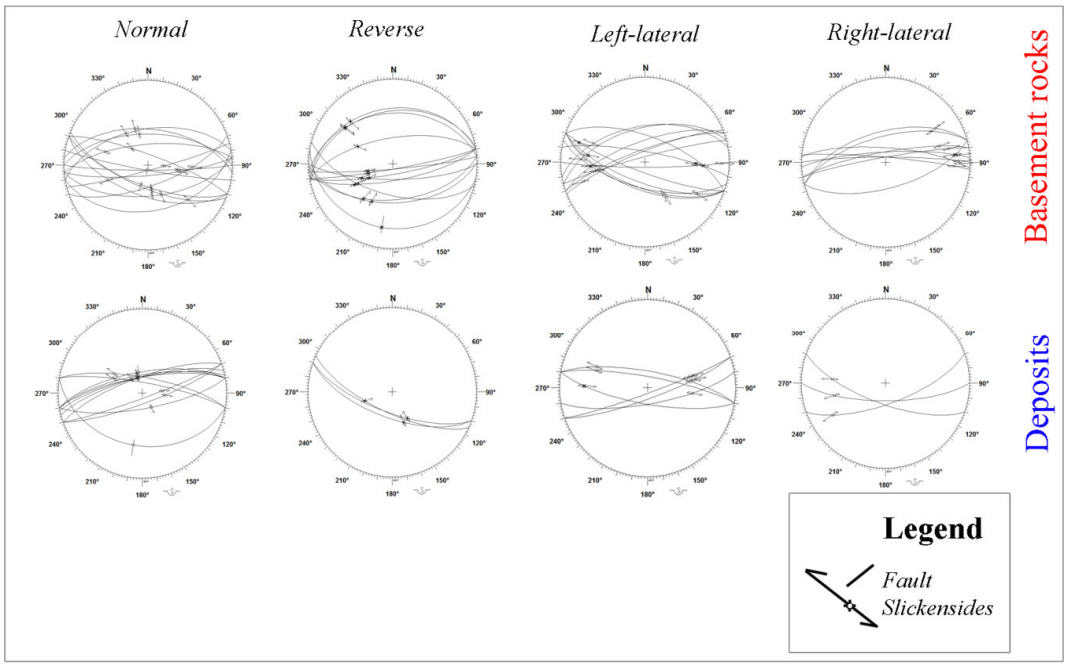

Figure 4.11: E-W faults system classified on the base of the kinematics, direction and type of substrate.

Concerning the structures offsetting the Upper Miocene- Quaternary deposits, we can observe a relative abundance of normal and left-lateral faults, affecting mainly the Messinian-Lower Pliocene conglomerates (Fig. 4.12). We observe that this tectonics affected also the Pliocene marls and more rarely the younger deposits. As observed along the northern border, these lineaments associated with NW-SE transtensional faults are driven by the N-S extensional axis at least during the initial opening stage of the Catanzaro Trough.

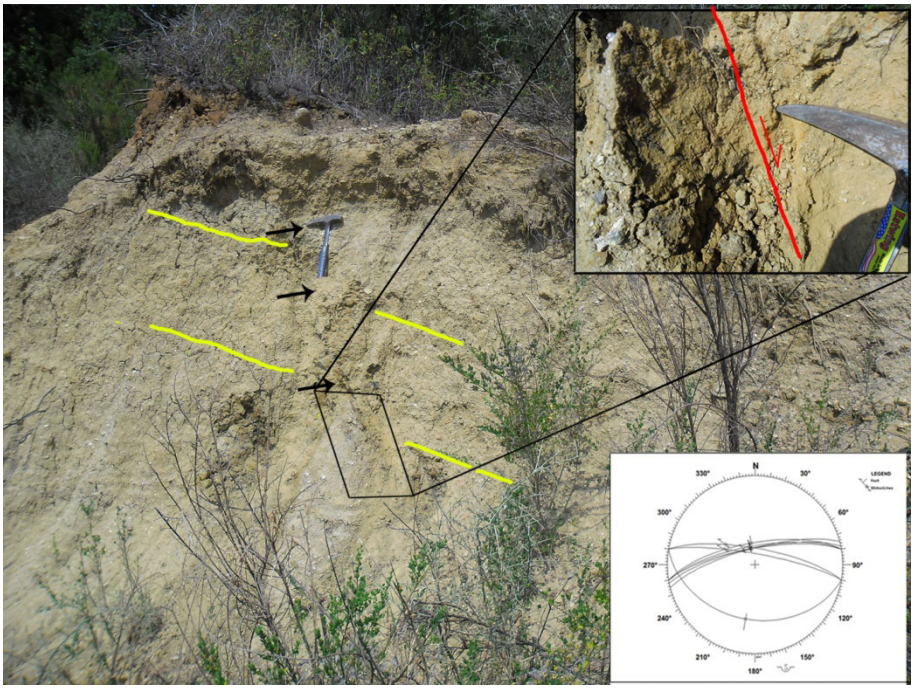

Figure 4.12: E-W extensional faults affecting Messinian- Pliocene conglomerates, black arrows show fault plane and the lower inset show stereographic projection of faults.

In the area we observed, NW-SE faults, showing also an insignificant statistical distribution of fault plane as regards structures affecting the Neogene-Quaternary deposits.

The southern transgressive deposits, similarly to the northern ones are not marked by transcurrent structures, although, here too at the regional scale, NW- SE fault system represents the boundaries of the transtensional deformation zone. The lacking of the data is attributed to later faults activation with different direction which overprints and masks NW-SE kinematics (Fig. 4.13).

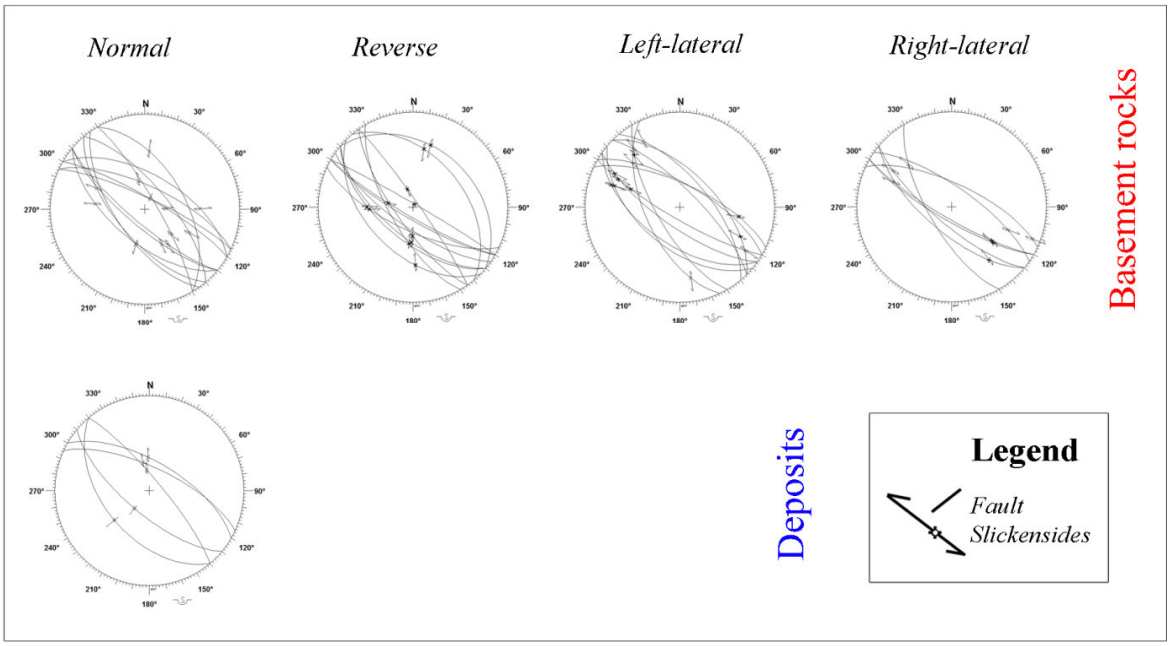

Figure 4.13: NW-SE faults system classified on the base of the kinematics, direction and type of substrate

The outcropping NW-SE fault planes show more than one direction of striation on the slickenside. Cross-cutting relationships are used to define the chronology of kinematics. In the frame of the basin evolution during Pliocene- Lower Pleistocene, were identified a change from transtensional to transpressional/ compressional kinematics of the NW-SE trending faults, as marked by inversion of transcurrent movement (Fig. 4.14).

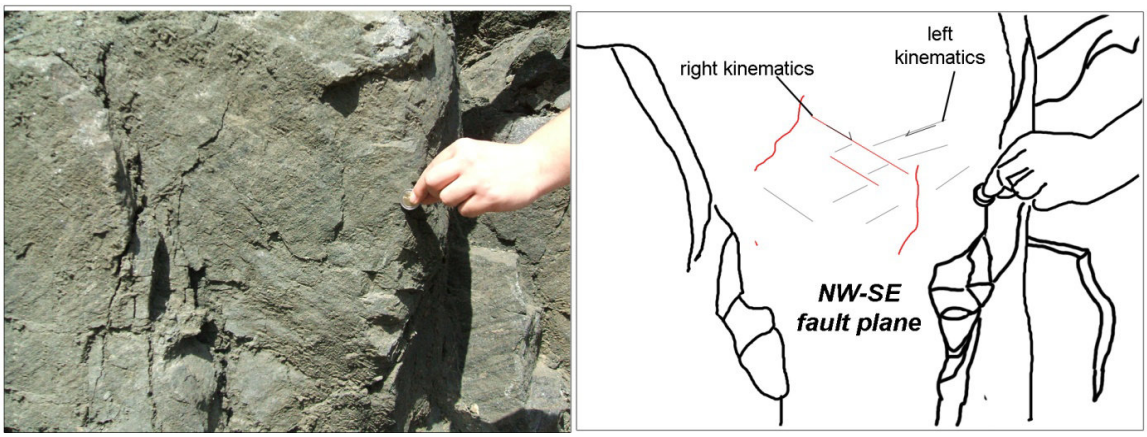

Figure 4.14: Superposition of striations on fault plane. The sketch, on the right shows a NW-SE oriented fault plane with right kinematics (red lines) cutting the left- lateral kinematics (grey lines).

NE-SW fault system represents one of the most widespread structural lineaments in the area, showing an equal distribution as regards the faults offsetting the basement rocks whereas deposits show a relative transcurrent fault planes abundance. Within the transcurrent kinematics we can observe both normal and reverse secondary component of deformation (Fig. 4.15).

NE-SW oriented normal and oblique kinematics overprint widely pre-existing strike slip and low angle faults. At regional scale, the Vibo Valentia Fault and its northern prosecution (Tortorici et al., 2003) represents the morphological evidence of these structural lineaments, which border the inner edges of Middle –Upper Pleistocene marine terraces. This suggests that the NE-SW fault system has been active at least during the Late Pleistocene .

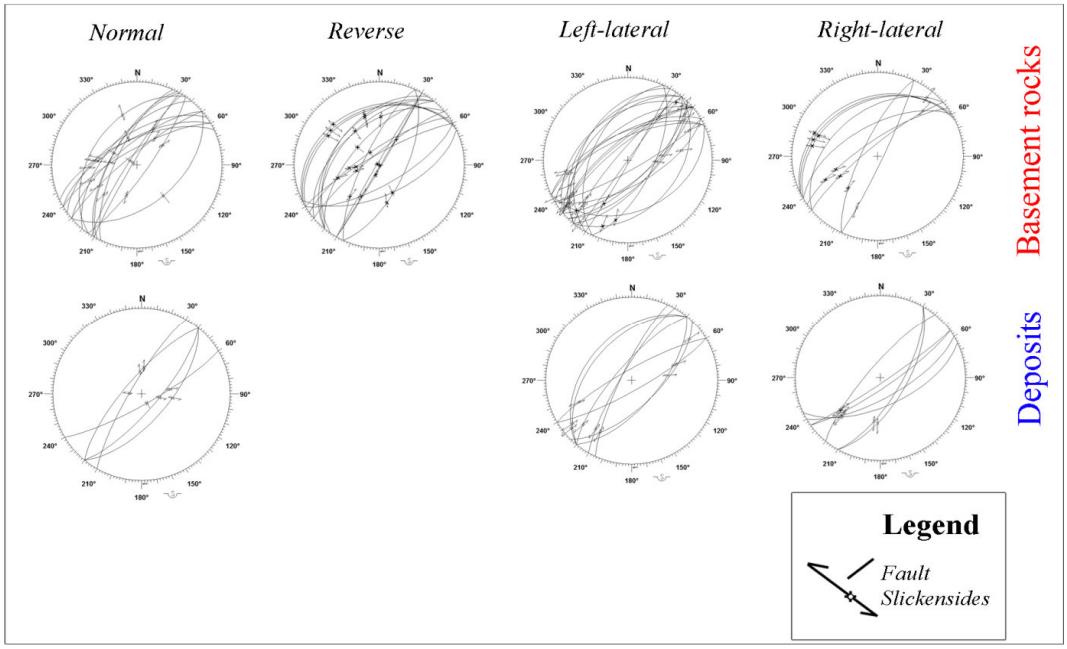

Figure 4.15: NE-SW faults system classified on the base of the kinematics, direction and type of substrate.

Within the southern side of the basin, at regional scale the N-S trending faults are more relevant with respect to the NE-SW ones.

The N-S faults system is characterized by a normal and right lateral fault abundance, as regards measurements affecting basement rocks, whereas deposits show a relative abundance in terms of normal and left-lateral structural lineaments (Fig. 4.16).

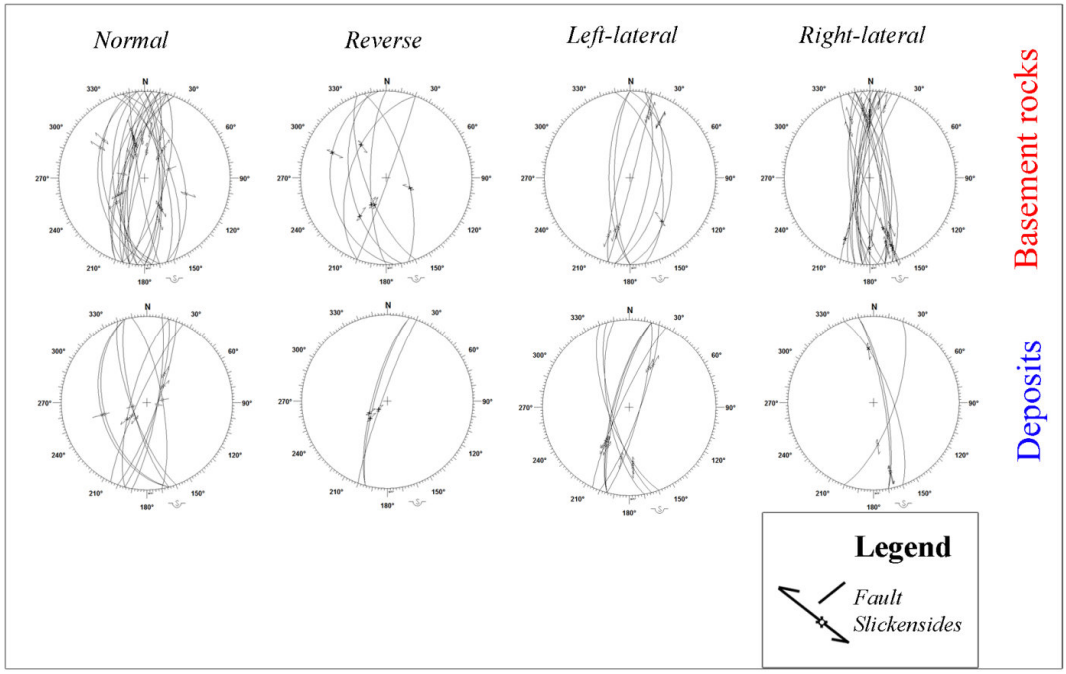

Figure 4.16: N-S faults system classified on the base of the kinematics, direction and type of substrate.

N-S striking normal faults affect mainly the Plio-Pleistocene deposits and, similarly to the above-described NE-SW normal faults bordering the inner edges of Middle –Upper Pleistocene marine terraces.

Close to the Girifalco village, the interaction between NW-SE structural lineaments, morphologically represented by NW-SE trending axial ridges and valleys and, more the recent N-S and NNE-SSW fault systems, strongly increase the tectonic complexity of the area (Fig. 4.17).

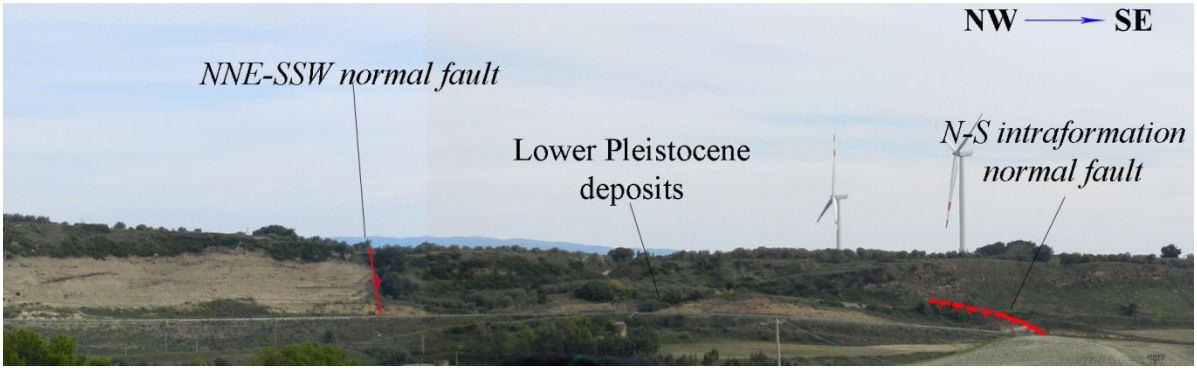

Figure 4.17: Overview of southeastern margin of Catanzaro Trough, showing the two normal fault systems that offset Lower Pleistocene deposits.

4.4 Stress inversion for the Catanzaro Trough

The main goal of the stress analysis is to identify the stress tensor, capable to explain the direction of slip on most of the faults observed. Generally this problem is referred to structural geologists as the inversion problem and can be solved using inversion algorithms. We start with the observed faults and then try to cover some information about the state of stress responsible for them (Zalohar and Viabec, 2007 and references therein).

Tectonic analysis of faults population commonly includes an attempt to determine the main characteristics of stress tensor. The most interesting characteristics are the directions (azimuth, and inclinations) of the three orthogonal principal stresses, assuming that each population of fault measurements corresponds to a single tectonics event, governed by a single regional stress. Faulting commonly uses previous discontinuities as older faults, joints or stratification to nucleate (Angelier, 1979; 1990).

The structural data collected within the Catanzaro Trough have allowed us to provide the analysis of paleo-stresses tensor of the area. The data were organized in three fault population, this selection is based on age of deposits cut by brittle elements:

1. Miocene –Zanclean faults population;
2. Piacezian- Lower Pleistocene faults population;
3. Post lower Pleistocene faults population.

Then the same faults association have been selected also for the basement rocks to obtain the stress inversion to compare with the previous one.

4.4.1 Miocene –Zanclean faults population

The first faults association are represented by the structural data offsetting Miocene-Zanclean deposits (Fig. 4.18). In figure 4.18a we selected NNW-SSE left- lateral and NE-SW

right-lateral associated faults, suggesting that they represent partially a conjugate set. The stereographic projection of the principal stresses derived from application of stress inversion methods (Daisy 4, Salvini, 2002), displays that the cluster indicates a paleo-stress with ca. E-W-trending maximum principal σ_1 axis (P-axis). The principal stress projection acts obliquely, showing a tranpressional feature. The minimum principal σ_3 axis is NNW-SSE oriented, displaying, hence, an horizontal NNW-SSE extensional axis (T- axis). Similarly to stereographic projection in figure 4.18a, the plot in figure 4.18b show the same NNW-SSE T-axis, even though, in this case the paleo-stress is characterized by a vertical σ_1 axis, obtained by stress inversion of E-W normal faults.

The last plot in figure 4.18c, we have obtained the stress inversion by reverse faults that show the same σ_1 axis tranpressional feature imaged in figure 4.18a, namely WSW-ESE oriented maximum principal axis.

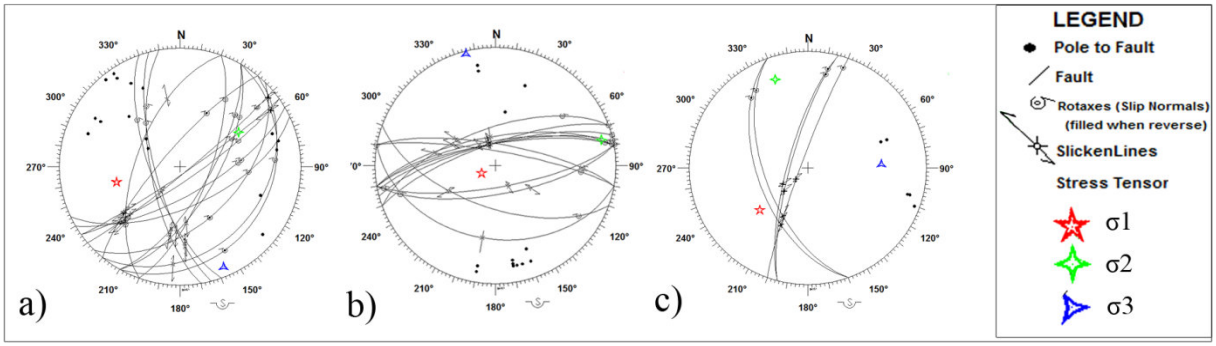

Figure 4.18: a), b), c) Stereographic projection of the Miocene –Zanclean associated faults with stress field of faults (Schmidt's net, lower hemisphere).

If we consider the same faults association selected from basement rocks, we can observe a similar distribution of stress axes (Fig. 4.21). The difference between two selection concerns the N-S oriented reverse faults: these selected faults are the result of the same σ_1 axis orientation (see also figure 4.18c), figure 4.19c shows a P-axis with a more sub-horizontal feature than the previous one.

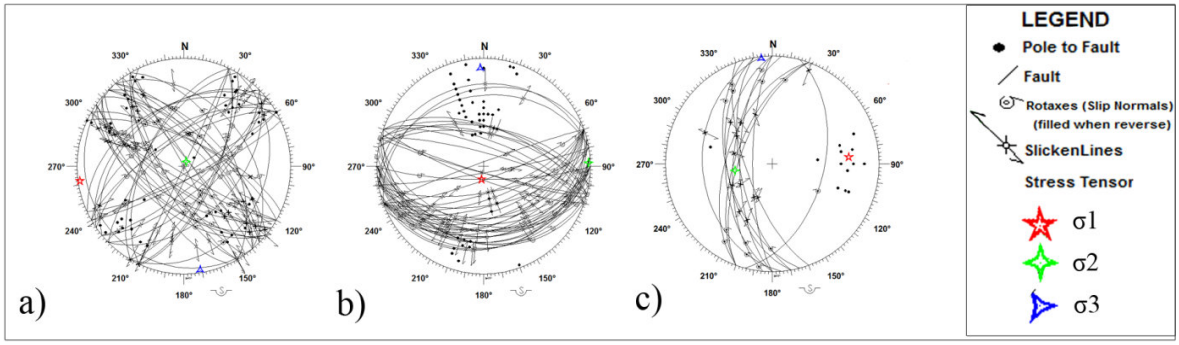

Figure 4.19: a), b), c) Stereographic projection of the basement rocks selected faults with stress field of faults (Schmidt's net, lower hemisphere).

4.4.2 Piacezian- Lower Pleistocene faults population

The fault association, related to the Piacezian- Lower Pleistocene deposits (Fig. 4.20), shows two fault population, both of them are the outcome of a ca. N-S oriented maximum principal axis (σ_1), and a ca. NW-SE oriented minimum principal axis (σ_3). This paleo-stress distribution define an oblique compression ca. N-S oriented, and an NW-SE oriented oblique extension. The stress inversion in the first plot (Fig. 4.20a) has been obtained by the combination of NE-SW right lateral faults with NNW-SSE left lateral fault, whereas in the second plot (Fig. 4.20a) the analysis come from NE-SW reverse faults.

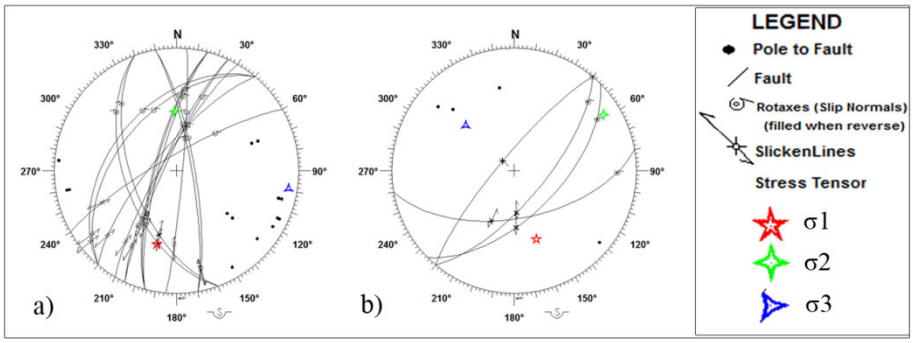

Figure 4.20: a), b) Stereographic projection of the Piacezian- Lower Pleistocene associated faults with stress field of faults (Schmidt's net, lower hemisphere).

Figure 4.21 shows two selected faults population, in this case we considered NW-SE right-lateral and NE-SW left-lateral associated faults, similarly for the selected deposits faults. Even here, we can observe the similar distribution for three axes, even though P- and T-axes are turned about 150 degrees in figure 4.21a compared to figure 4.21b. Both of two distribution show sub- horizontal σ^1 axis, passing from NNW-SSE- to NNE-SSW-oriented direction and a ca. horizontal WNW-ESE- to WSW-ENE- oriented σ^3 axis.

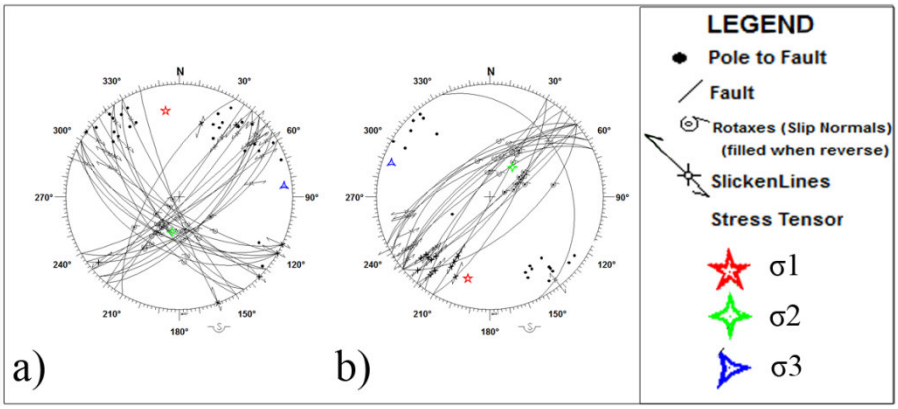

Figure 4.21. a), b) Stereographic projection of the basement rocks selected faults with stress field of faults (Schmidt's net, lower hemisphere).

4.4.3 Post Lower Pleistocene fault population

Finally, both the post Lower Pleistocene and basement rocks faults populations show a vertical attitude of σ_1 together with a horizontal σ_3 trending N280°E, defining, for this domain, a WNW-ESE oriented extensional regime (Fig. 4.22a and b).

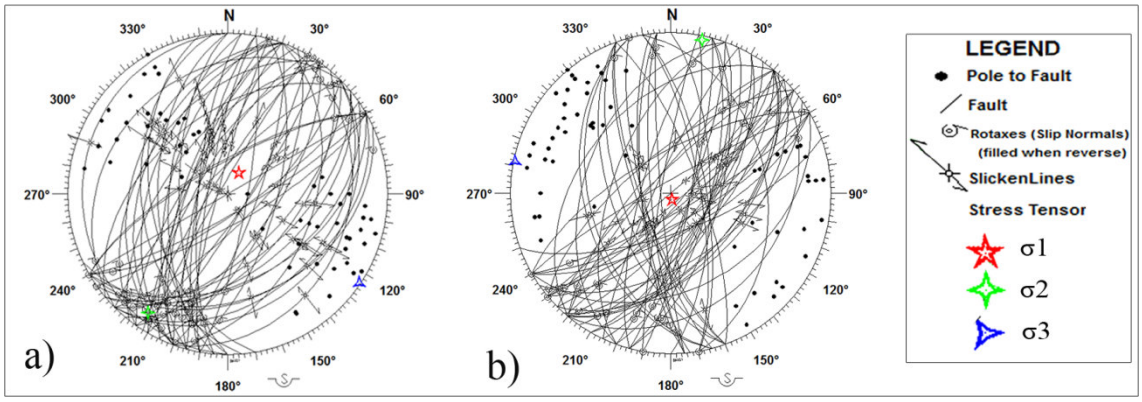

Figure 4.22. a) and b) Stereographic projection of the post lower Pleistocene and basement rocks associated faults with stress field of faults, respectively (Schmidt's net, lower hemisphere).

The results of the stress inversion come from the combination between N-S and NE-SW normal fault association, which clearly dislocated the Middle-Upper Pleistocene marine terraces, as we can see both in the northern and southern border of Catanzaro Trough (see below figure 4. 23 and figure 4. 24).

The northwestern margin of the Catanzaro Trough is affected by NE-SW striking normal faults, SE-dipping, that offset both Early Miocene overthrust and Middle-Upper Pleistocene deposits (Fig. 4.23). These last ones widely outcrop close to the Terme Caronte,

close to Lamezia city. Applying the stress inversion we obtained a WNW-ESE oriented extensional axis (Fig. 4.23).

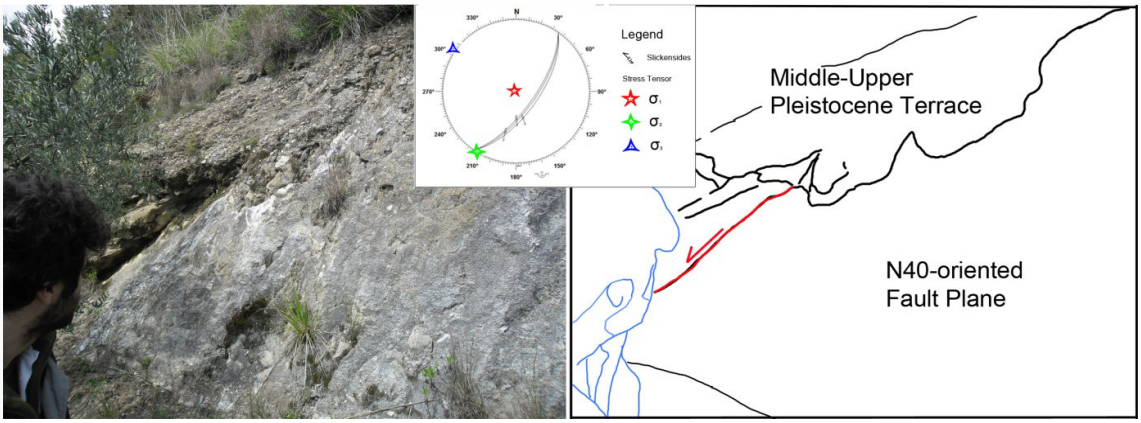

Figure 4.23: N40 oriented normal to oblique faults offsetting Middle Upper marine terrace, the right shows the sketching of the left image: normal faulting is defined by red lines.

The southwestern margin of the Catanzaro Trough is affected by the combined activity of NE-SW (Vibo Valentia Fault) and NNE-SSW oriented normal faults which clearly influence the morpho-tectonic setting of the area. Both of fault systems border the inner edges of Middle-Upper Pleistocene marine terraces, obtaining, here too, a WNW-ESE oriented extensional axis (stereographic projection of fault poles in Figure 4.24c).

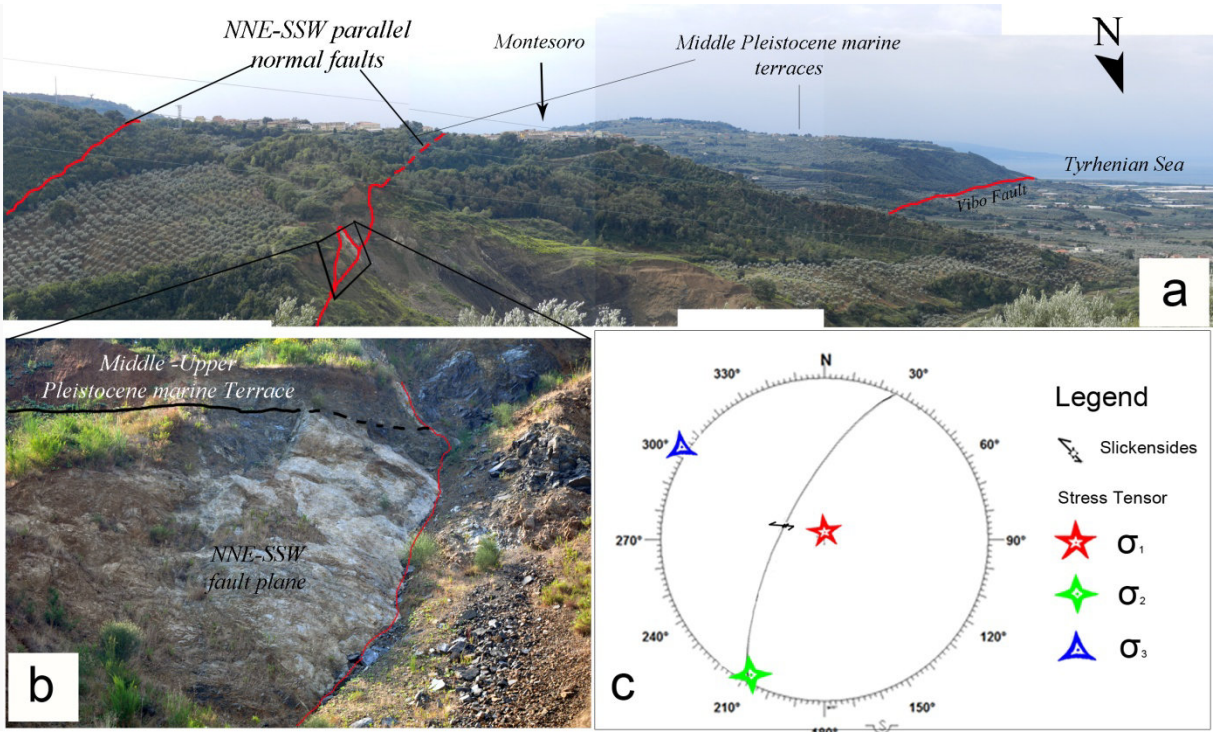

Figure 4.24: a) Overview of southwestern margin of Catanzaro Trough; b) NNE- SSW normal faults, NW-dipping, showing recent activity (evidence of the Pleistocene deposits fault offset); c) stereographic projection of the NNE-SSW fault plane with stress field of faults (Schmidt's net, lower hemisphere).

The NE-SW and N-S normal faults control both the northern and southern margin evolution of these basin, causing locally the Pleistocene split of the on-shore portion of the Catanzaro Trough. This suggests the formation of a graben (as shown by means geophysical data, treated in the next section), that is in agreement with the graben and half-graben systems widespread in the Calabrian Arc, e.g. the Crati and the Mesima grabens, and the Gioia Tauro plain.

CHAP. 5 Geophysical Data

5.1 Geophysical methods

Techniques for the investigation of sub-surface geology have mainly been developed to satisfy the needs of hydrocarbon industries and to mitigate the environmental risk related to faults and volcanoes activities.

The improvement of geophysical methods have produced the development of geology branch concerned with the analysis of stratigraphy, sedimentology and structure in the sub-surface. Amongst the geophysical techniques the most used in the subsurface analysis is the seismic reflection technique. Seismic reflection analysis takes advantage of acoustic properties of rocks that can be picked up by generating a series of artificial shock waves and then recording the returning waves (Dobrin and Savit, 1960; Christensen, 1982; Yilmaz, 2001, Nichols, 2015).

Usually, it all begins with a shot generated, for example, by dynamite explosion (onland) or compressed air in an airgun (offshore). These generate a short, sharp pulse of sound into the ground namely the acoustic wave.

The acoustic wave crossing the rocks is partially reflected when it encounters a boundary between two materials of different density and sonic velocity. Rock hardness (product of density and sonic velocity) is called acoustic impedance. The echoes are called reflections. The stream of reflections arriving and recorded after a time is called trace (Badley, 1985).

The reflection coefficient at the boundary of two rocks is directly dependent of the acoustic impedance. Generally, crystalline or well-cemented rocks bounded by clay-rich or porous rocks can reflect most part of the acoustic wave.

The time taken for an acoustic wave to reach a reflective surface and return is the *two-way time* (TWT), and it can then be related to depth of the reflector at that point.

5.1.1 Acquisition of seismic reflection data

Seismic reflection profiles can be carried out on onshore or offshore. Marine survey is generally more straightforward because the ship can follow a well planned route for the data collection, minimizing also the topographic effect (i.e., depth difference between source and receivers); whereas land-based survey are restricted by topography, access and land use (Mussett, 2003). The source of the energy at the surface is very different, depending essentially from if the acquisition takes place onshore or offshore, in the first case the acoustic

source usually used is generated by a *vibroseis* set-up, whereas in the second case an *airgun*, a device releasing of compressed air with explosive force (Fig. 5.1).

The returning acoustic waves are detected by receivers: these are essentially microphones that are referred to as geophones (onland) and hydrophones (at sea). The pattern of these receivers depends on whether the survey is two-dimensional, a 2-D survey, or three-dimensional, a 3-D survey. A single string containing the receivers spaced 12,5m to 25m, in marine survey is called *streamer,* that can be up to 12 km long (Mussett, 2003).

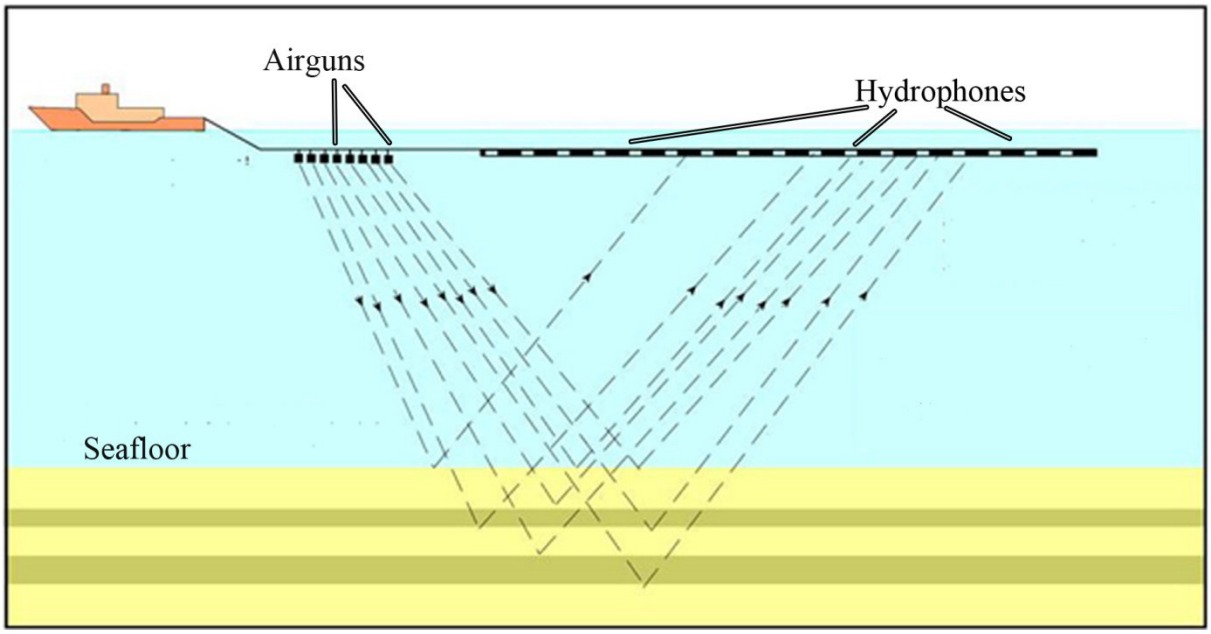

Figure 5.1: Marine seismic reflection surveys imaging a ship which tows airguns. The airguns produce sound waves which are reflected by the strata and detected by hydrophones organized in section within a cable towed behind the vessel.

5.1.1 Processing

Raw data acquired need to be organized and processed in order to image a section of the sub-surface as close as possible to a geological section. The first stage is called *demultiplexing*, during this step the samples recorded in arrival order are separated and reordered producing a time sequence for each sensor. After that *static corrections* or *statics are applied* in order to remove differences amongst source depth and receivers depth (Bradley, 1985). Generally, during the survey the quality control of acquired data is also performed producing a first image named brute stack, i.e., a stack of one choice trace.

A further step of the processing is represented by the *deconvolution*. This algorithm aims to remove the random noise improving the coherent signal revealing only those

reflection that derives from real reflectors. Thus, this step allow to improving the horizontal resolution of a seismic section.

Then the traces are grouped together into families from *common mid points* (CMP) and *common depth point* (CDP) and used to perform velocity analysis. These velocities are used to perform the *normal-moveout (NMO) correction*. The NMO correction allow to remove the effect of offset on the traveltimes flattening horizons. The CMP corrected by NMO can be stacked obtaining a trace from each gather with higher Signal/Noise ratio, thus decreasing noise and increasing real signal. Velocity analysis is important also to discriminate real reflections from other events such as refractions, diffractions and multiples (a coherent noise).

If the reflector has a steep dip, the position of the reflection in the seismic section is displaced downdip and the dip of the reflector is underestimated. To restore the reflections to their correct subsurface positions obtaining a seismic section as close as possible to a geological section, the time migration algorithm is applied to data (Bradley, 1985).

5.2 Seismic data analysis

The western margin of the Catanzaro Trough and its offshore segment was characterized by a complex geo-structural history and represent one of the most seismogenic area of whole Central Mediterranean. To gain knowledge of structural features of this region, multi-scale and multi-disciplinary datasets will be here describe.

The interpretation of geophysical data are focused to the northeastern portion of the Sant'Eufemia Gulf (SE Tyrrhenian Sea) and along western central Calabrian Arc. In the next section we describe the interpretation of following geophysical data:

- *Seismic profiles and wells by ViDEPI project:* interpreted along onshore and offshore Tyrrhenian side;
- *ISTEGE Project data:* Off-shore Multichannel seismic data, high resolution morpho-bathymetry and Chirp profiles acquired aboard the R/V OGS-Explora in the Sant'Eufemia Gulf (Loreto et al., 2012);
- *1-kJoul Minisparker profiles*: Sparker single-channel seismic lines acquired aboard the R/V Bannock (Trincardi et al. 1987).

Layers are constrained assuming a constant seismic velocity of 2200 m/s for Plio-Quaternary sediments (Pepe et al., 2010) and seismo-stratigraphic character (Dumas et al., 1980) of lithologies described in Marta and Marisa wells.

5.3 Seismic profiles and wells by ViDEPI project

In order to bridge the gap of structural and stratigraphic data information, mainly near the coastline, both onshore and offshore area will be analyzed. We used geophysical profiles and wells documentation acquired by Eni s.p.a. (italian oil company) at the beginning of the 80' and available in the frame of the VIDEPI Project (Visibility of Petroleum Exploration Data in Italy). The public technical documents related to the Italian exploration activities were realized by UNMIG-National mining office for hydrocarbons and georesources of Ministry of Economic Development, (*unmig.sviluppoeconomico.gov.it/**videpi/***) (Fig. 5.2).

The documentation concerns expired (public) mining permits and concessions, filed since 1957. The database is updated to 12/31/2014 and allows free-of-charge consultation of the following:

- 2299 final well logs,
- seismic exploration (578 seismic lines of reconnaissance seismic campaigns of the offshore areas + 2 396 2D seismic lines acquired in expired mining permits and concessions),
- technical documentation of the mining permits and concessions (1586 files, 4230 technical reports, 6846 attachments),
- 70 seismic lines of CROP Atlas project,
- paper documents;

We have interpreted nine crossing seismic profiles made available in the frame of the this project (Fig. 5.2). Map in Figure 5.2 shows four seismic section (blue lines): CZ-329-78V; CZ-326-78V; CZ-325-78V; CZ-376-87V and five seismic section (yellow lines): ER-77-502; ER-77-504; ER-77-3023; ER-77-3030; ER-77-3028, distributed along the onshore and offshore Catanzaro Trough, respectively.

In spite of low quality, these seismic profiles have provided together with Marta and Marisa wells good constraints in terms of sismo-stratigraphy inside the Catanzaro Trough basin (Fig. 5.2a).

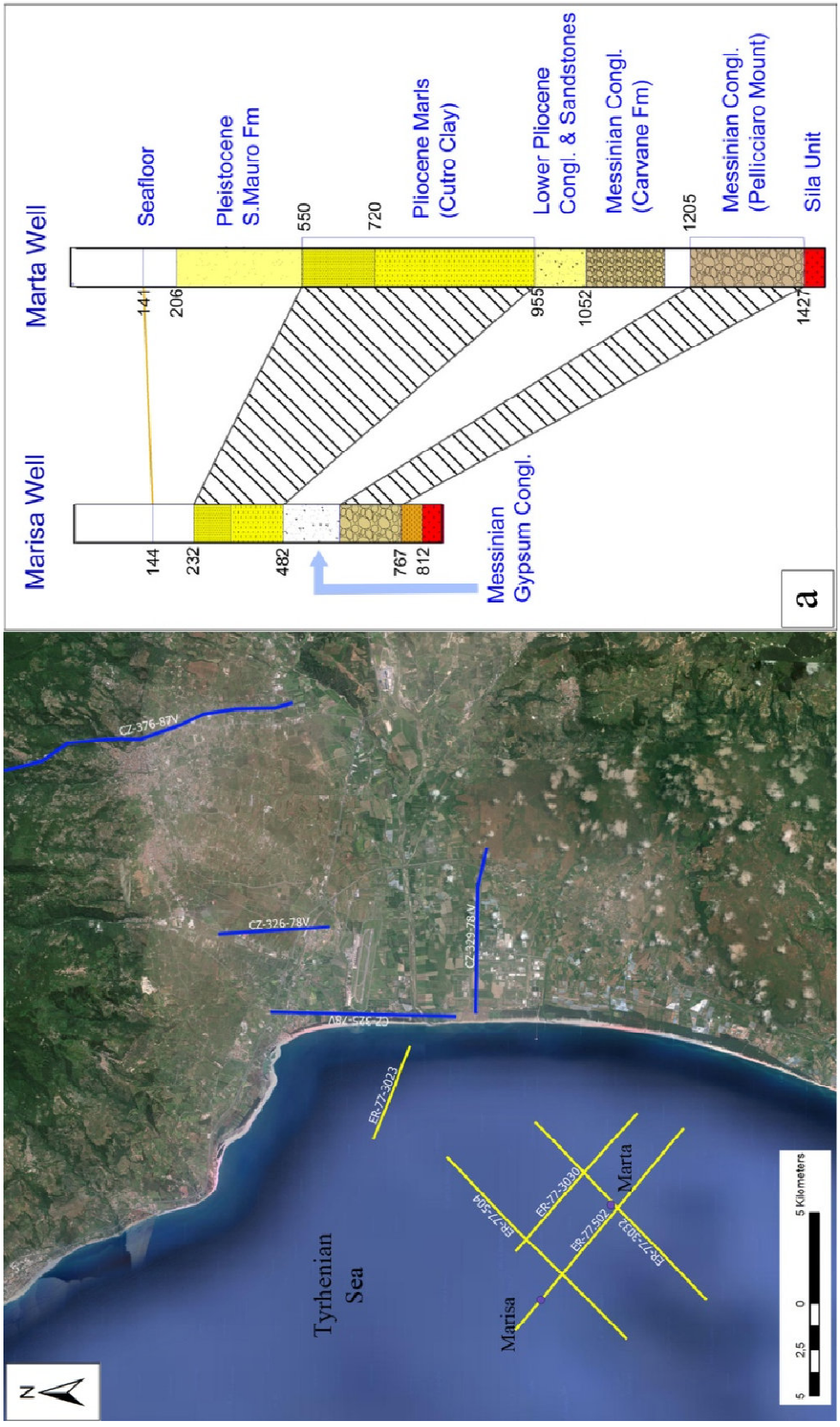

Figure 5.2: Map showing the location of ViDEPI seismic lines, blue and yellow lines represent onshore and offshore seismic profiles, respectively. The base mape is derived from Google Earth, a) Stratigraphic columns derived by ENI wells

5.3.1 Onshore ViDEPI seismic data

Figure 5.3 images the W-E oriented CZ-329-78 mcs ViDEPI profile. This profile shows the Miocene unit, which top corresponds to a high amplitude and very continue seismic reflector, covered by a more stratified even if poorly continue sedimentary unit and corresponding to the Plio-Quaternary deposits. These units are characterized by numerous discontinuities and fault-controlled dislocations, mainly with normal and sporadically inverse kinematic. Amongst shot points 160 – 190, thickness increase of Plio-Quaternary sediments and the evident dislocation of the Miocene reveal the activity of a W-dipping normal fault (Fig. 5.3). This newly identified normal fault, here named *San Pietro Lametino Fault*, is NE-SW oriented (derived by unpublished ViDEPI profiles and Vigor well data, Fig. 5.3).

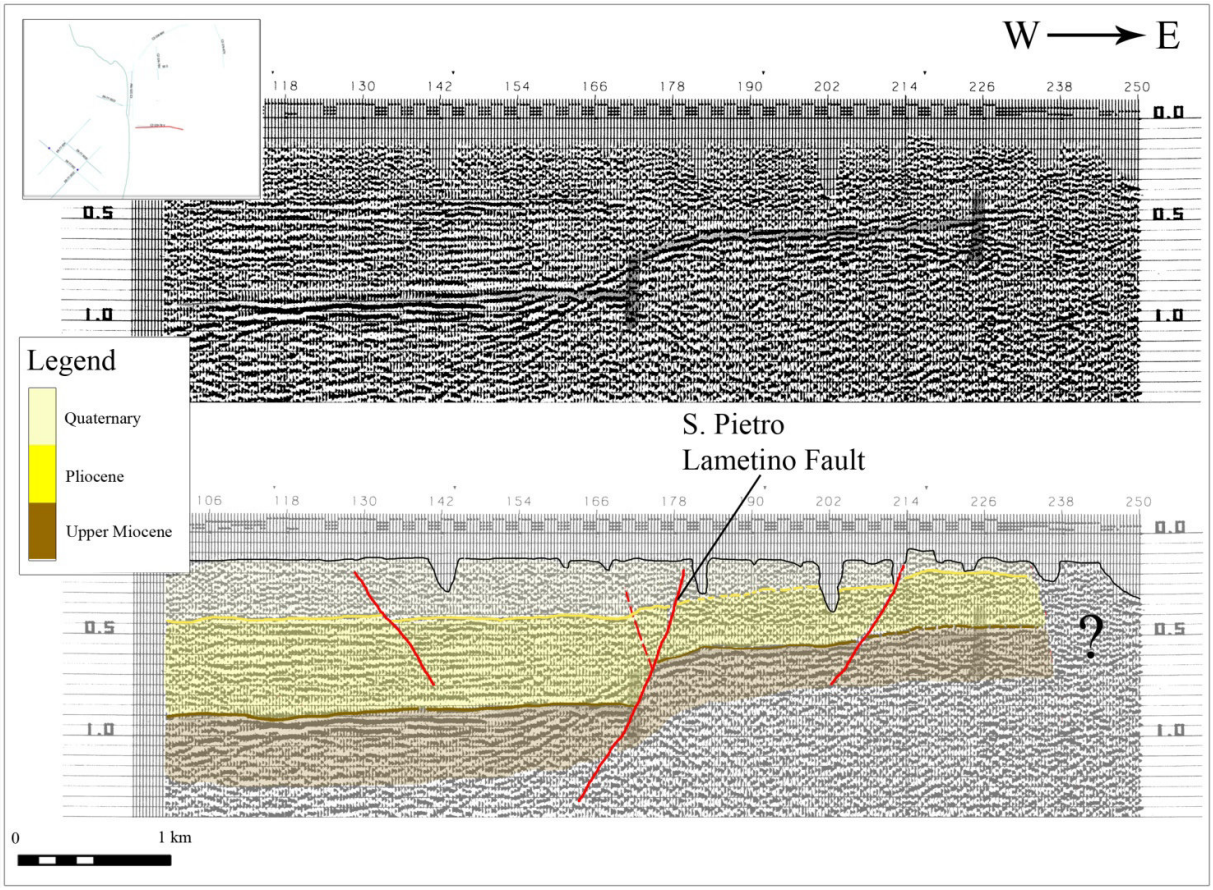

Figure 5.3: CZ-329-78 ViDEPI seismic profile (above) and the same with the interpretation (below). Brown line marks the top of Miocene; Yellow line marks the Plio-Pleistocene transition.

In the same way we have interpreted two N-S oriented seismic profiles: CZ-326-78V and CZ-325-78V, which image a quasi-continuous Messinian- Quaternary sedimentary succession characterizing the onshore Catanzaro Trough. Both lines show in the southern portion the presence of reverse faults responsible of bended layers, clearly visible underneath

the top of Messinian. CZ-326-78V, placed to ca. 4 km far from the shoreline, displays gently folding above the Miocene top and a thinner Pliocene deposits as compared with CZ-325-78V profiles, which is located close to the shoreline and further south-west than the previous one (Fig. 5.4).

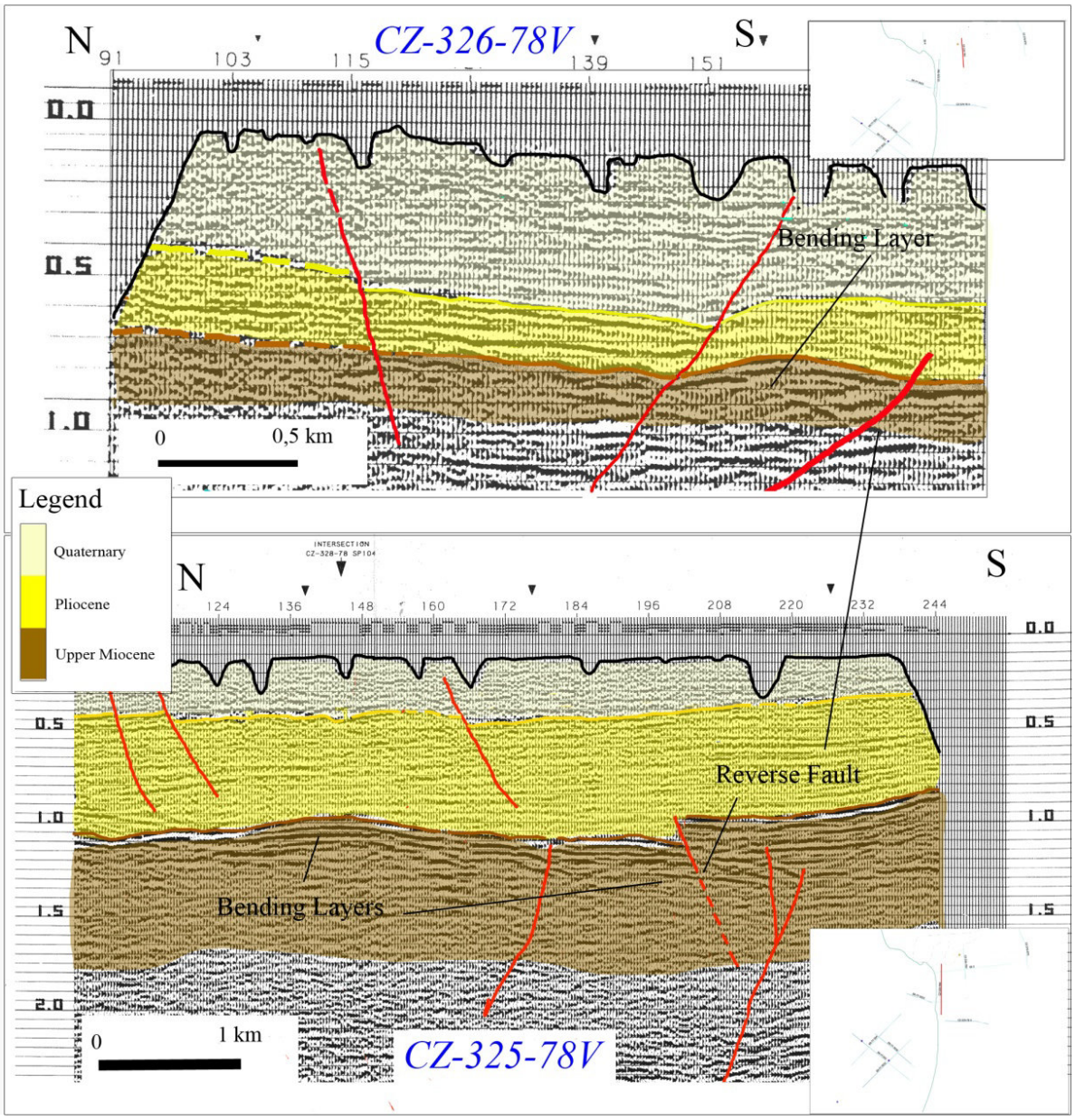

Figure 5.4: CZ-326-78V (above) and CZ-325-78V (below) Videpi seismic profiles

5.3.2 Offshore ViDEPI seismic data

Similarly to the previous section, we have interpreted two parallel offshore ViDEPI seismic profiles, ER-77-502 and ER-77-3028, both oriented WNW-ESE (Fig. 5.5). The well-stratified Plio-Quaternary sequences lie at the top of the Miocene, which is represented by a

highly reflective surface due to the strong acoustic contrast between conglomerates (of Messinian) and marls (of Pliocene). The two seismic profiles display a deformation decreasing towards the coastline, indeed the Upper Miocene-Pliocene sediments are highly deformed in the northwestern part (amongst shot points 100 - 190, ER-77-502) forming a gentle anticline confined within Lower Pliocene; whereas in the southeastern part only slightly folding are detectable (Fig. 5.5; *Transpressional/ compressional faults*). Both of them describe a NNE-SSW-oriented compressional system.

ER-77-502 and ER-77-3028 ViDEPI mcs profiles show amongst shots 178-200 and 20-40, respectively, a normal fault that controls the deepening of the basin towards the onshore (Fig. 5.5), both of them reach 1600 ms of depth and the ER-77-3028 line seems to displace even a deep horizon interpreted as a *basal unconformity*. Based on a previous work (Loreto et al., 2013) and on multichannel seismic profiles, we can state that the two structures are part of the NE-trending *Sant'Eufemia Fault*.

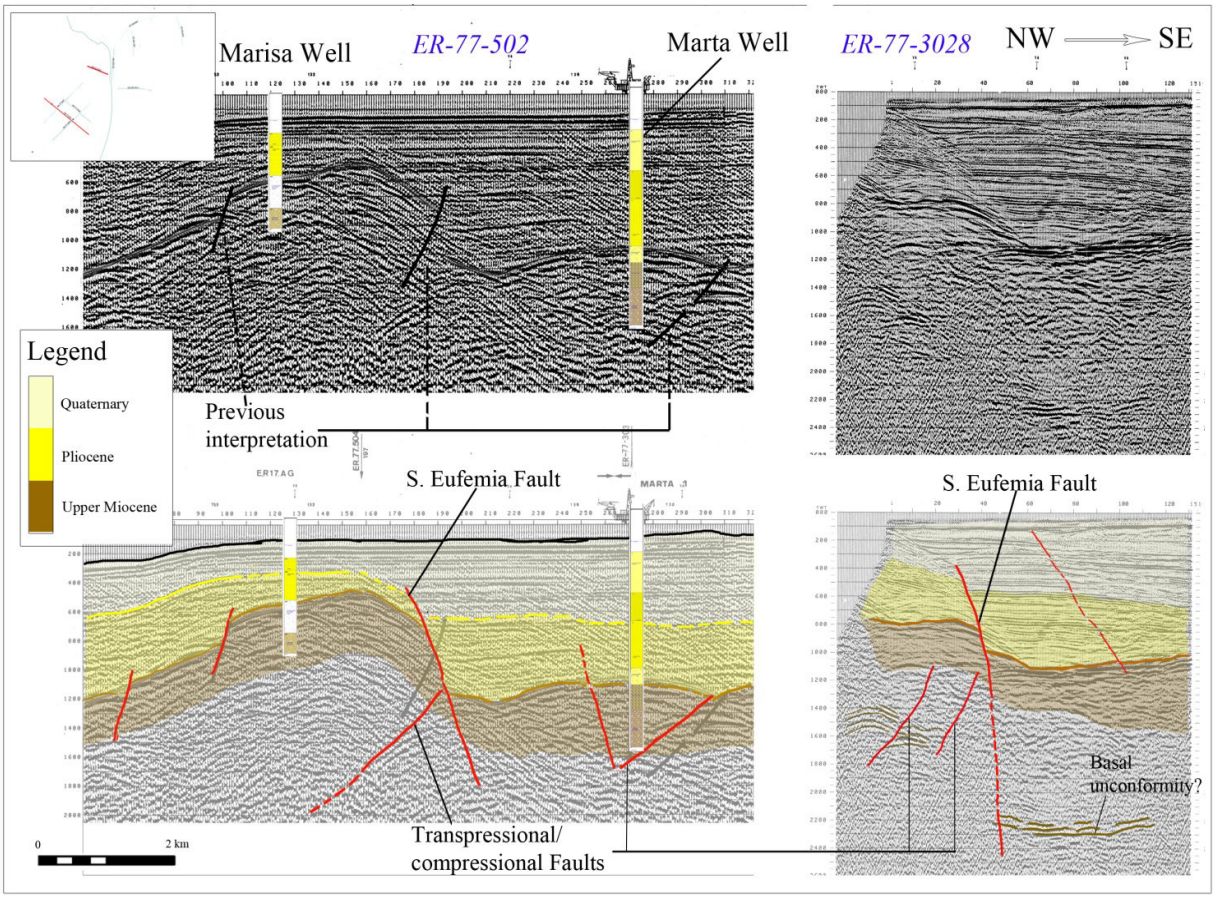

Figure 5.5: Interpretation of two ViDEPI seismic profiles: on the left: ER-77-502 and on the right: ER-77-3028. Brown line marks the top of Miocene; Yellow line marks the Plio-Pleistocene transition.

Further, we have interpreted two ViDEPI seismic profiles, ER-77-504 and ER-77-3028, perpendicularly oriented to the previous one, thus NE-SE oriented.

By means of two ViDEPI wells (Marta and Marisa) we are able to define lithologic features and unconformities characterizing the two reflection profiles: ER-77-504 represents the westernmost seismic profiles, placed on an anticline structure (visible in the transversal profiles in Fig. 5.5). This morphological high is characterized by thinner strata compared with ER-77-3028 which is located, on the contrary, within a down-faulted block closer to the shoreline (Fig. 5.6). Both of two sections show the presence of reverse faults confined beneath the top of Miocene. This compressional kinematics seems to produce a widespread bending of the whole sedimentary succession, locally, interrupted by normal faults that involve the Pliocene (Fig. 5.6).

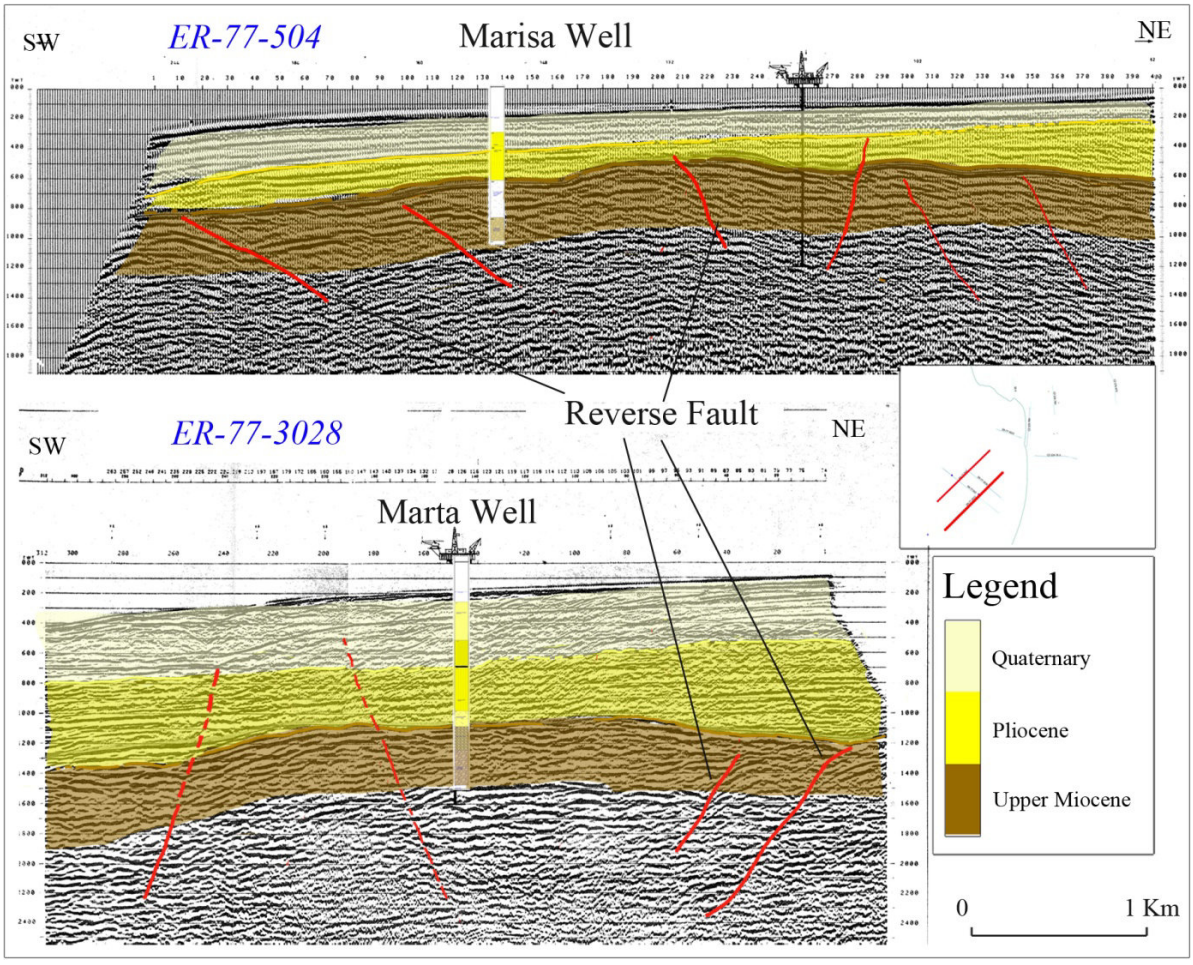

Figure 5.6: NE-SW oriented ER-77-504 (above) and ER-77-3028 (below) ViDEPI seismic profiles.

5.4 ISTEGE Project Data

During the summer 2010 a well-targeted multidisciplinary survey, performed in the frame of the ISTEGE project (Indagine Sismotettonica del TErremoto dell'8 Settembre 1905 (Mw 7.4), was carried out in the Gulf of S. Eufemia on board of the R/V OGS-Explora. During this survey about 330 km of multichannel seismic (MCS) data, 2223 km of sub-bottom chirp profiles, 2231 km^2 of high resolution morpho-bathymetric data, multibeam-derived backscatter data, 12 geological (gravity cores) and biological samples were acquired (Loreto et al., 2012, 2013).

In this thesis work we focused the study on a part of MCS, chirp profiles and high resolution morpho-bathymetry (HRB) (Fig. 5.7). Management and interpretation of seismic profiles were performed by using *Kingdom IHS* software, which has been made available by ISMAR – CNR U.O.S. of Bologna.

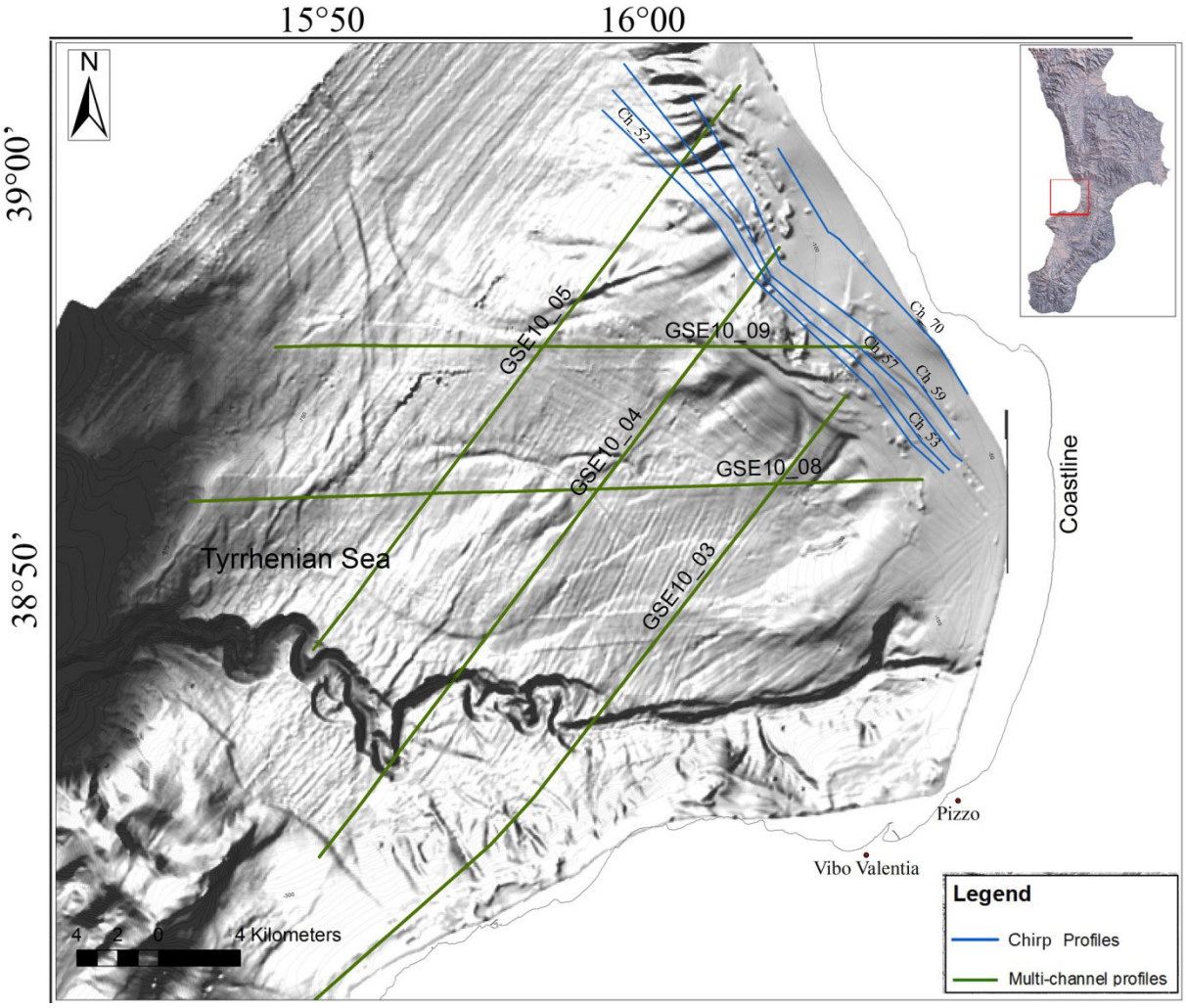

Figure 5.7: Location *ISTEGE Project Data*, blue and green lines represent Chirp and Multi-Channel seismic profiles, respectively, imaged above high resolution morpho-bathymetry.

5.4.1 Multi-Channel Seismic profiles (MCS)

Within the gulf, about 300 km of middle resolution MCS profiles were collected (Loreto et al, 2012). Seismic data were acquired with a 1500 m-long streamer cable, a 120-channel array and a 12.5 m trace interval. The energy source consisted of two GI-guns with a total volume of 8-liters shot every 25 m, with a resulting seismic coverage of 30 for each investigated depth point (Loreto et al., 2013). These data allowed to investigate the entire Plio-Pleistocene sedimentary sequence and the upper part of the Messinian rocks.

Five seismic profiles, part of this dataset, have been used to analysis the tectonics offshore Lamezia plain (see above Fig. 5.7). Further acquisition and processing parameter details in Loreto et al. (2012, 2013).

Figure 5.8 shows two NE-SW oriented MCS lines: GSE10_04; GSE10_05, imaging a S-facing, ca. E-W trending Master Fault (already recognized by Milia et al., 2009) and its antithetic lineaments, deforming differently from the top to the bottom the entire Neogene-Quaternary sedimentary basin.

Here too, as in the ViDEPI seismic lines, the boundary between the Miocene and Pliocene generates a strong acoustic contrast, due to lithology, seismically associated with a high amplitude horizon, represented by Messinian Conglomerate, which is more reflective than Pliocene Marls.

Even though this deformation appear slightly different between the two MCS profiles, both of them show a fault offset, estimated to the top of Miocene layers: 300 ms-thick for GSE10_05 line and 100 ms-thick for GSE10_04. The activity of this normal fault increases up-ward, where it is replaced by folding with associated anticline growth, confined as soon as above the Upper Pliocene- Lower Pleistocene layers (amongst ca. 800 and 1600 ms depth for both of two mcs lines). Therefore an initially extensional/ transtensional mode of fault (William et al., 1989) is replaced by an apparent reversal or transpressional movement as the result of a change of stress field (*Contractional Event* in Fig. 5.8).

Further, we can observe that the tectonic deformation confined between Upper Miocene and Lower Pleistocene produces a Pliocene deposits thickening in the hangingwall with regarding to the same succession in the footwall of Master Fault in both of MCS profiles (Fig. 5.8).

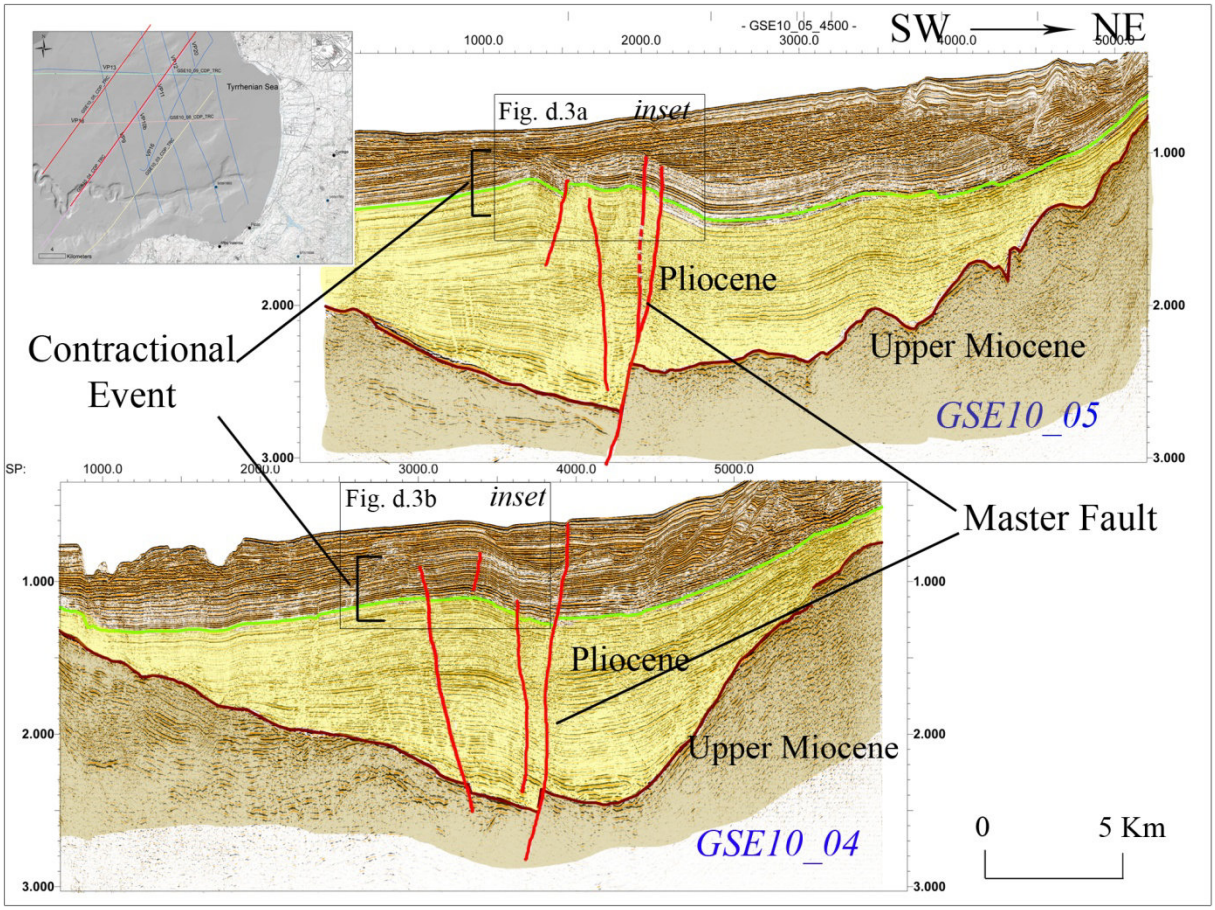

Figure 5.8: MCS profiles acquired in the frame of ISTEGE project, location is marked with a red line in the box. The interpretation has been made by using the Kingdom software (HIS Global Inc.).

Almost perpendicular to the previous MCS profiles, we have interpreted two W-E oriented GSE10_09 and GSE10_08 seismic lines (Fig. 5.9). The two profiles image in the eastern portion, close to the shoreline, a number of slumps likely triggered by the gravitational instability along the internal slope and two *chaotic bodies*, placed within the Pleistocene sedimentary sequence.

GSE10_09 (Fig. 5.9, above) shows a quasi-undisturbed sedimentary succession, which images the whole Pliocene-Quaternary deposits. The southernmost profiles GSE10_08 (Fig. 5.9, below) displays, on the contrary, faulted layers arranged in the central part of the section as structural ridges. The deformation appears confined between the top of Miocene and the seafloor and characterized by a number of faults showing a reverse/transpressional kinematics associated to Plio-Pleistocene strata folding, later replaced then by extensional faulting.

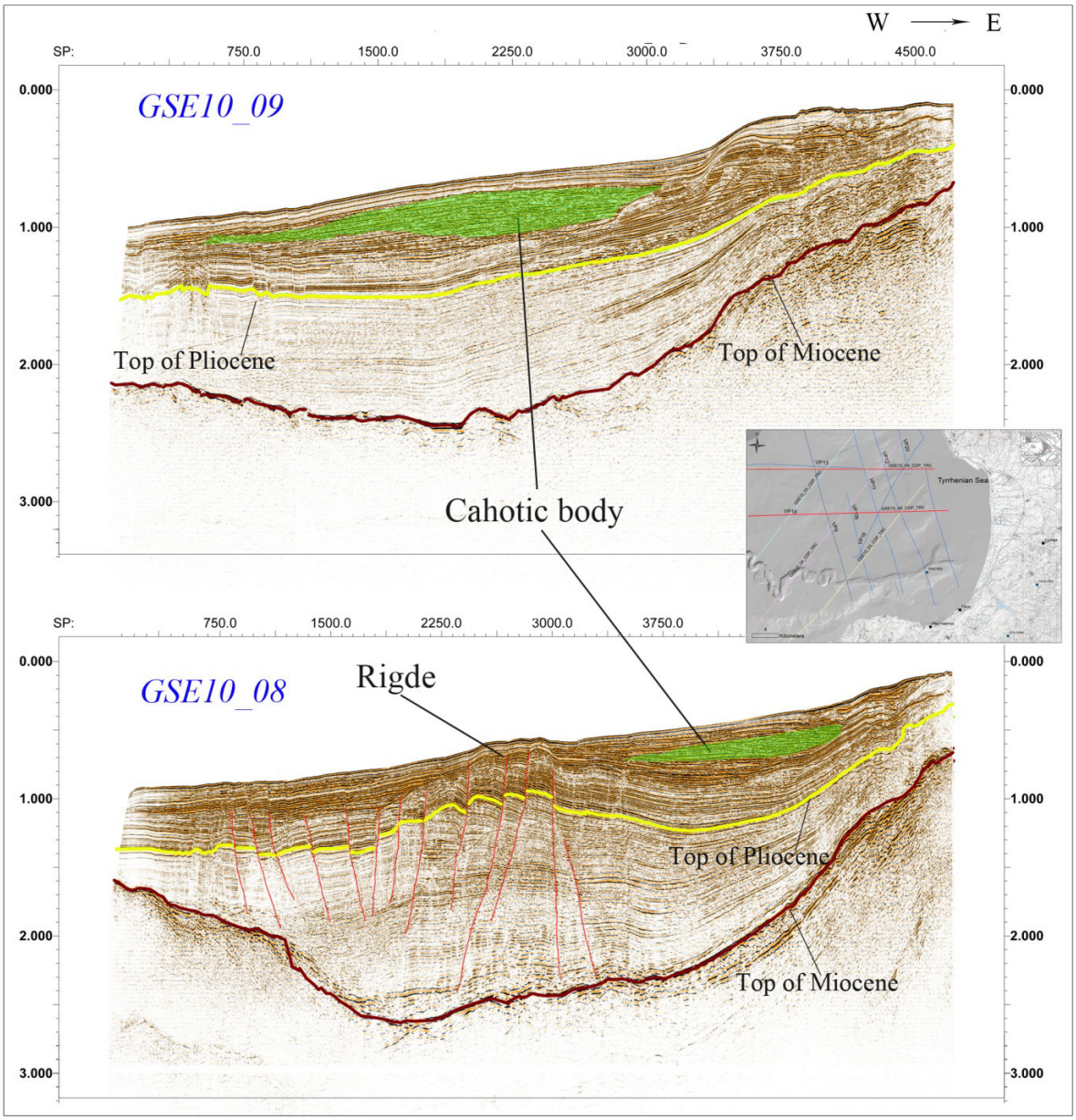

Figure 5.9: GSE10_09 (above) and GSE10_08 (below) Multi-Channel Seismic profiles

5.4.2 Morpho-bathymetric features

High resolution morpho-bathymetric map, performed with a grid cell size of 20 x 20 m, was obtained using two hull mounted multibeam echosounders, the Reson Seabat 8111 (100 kHz) and 8150 (12 kHz). More details about acquisition and processing of multibeam data can be found in Loreto et al. (2012).

By using the HRB we have recognized a number of different features which characterize the Tyrrhenian seafloor morphology (Fig. 5.10): 1) in the eastern portion of Sant'Eufemia Gulf, close to the shoreline, the HRB images two tectonic ridges, which presents a NE-SW orientation. The northernmost one seems to disappear in front of a fault

scarp belonging to the Master Fault, whereas the southernmost ridge is bordered eastward by the Sant'Eufemia fault scarp and to south by the Angitola Canyon (Fig. 5.10).

The Angitola Canyon is the most evident feature of HRB, already shown by Argnani & Trincardi (1988), it is characterized by a ca. W-E-oriented 20 Km-long straight trend near the coastline, becoming suddenly more sinuous westward (Fig. 5.10).

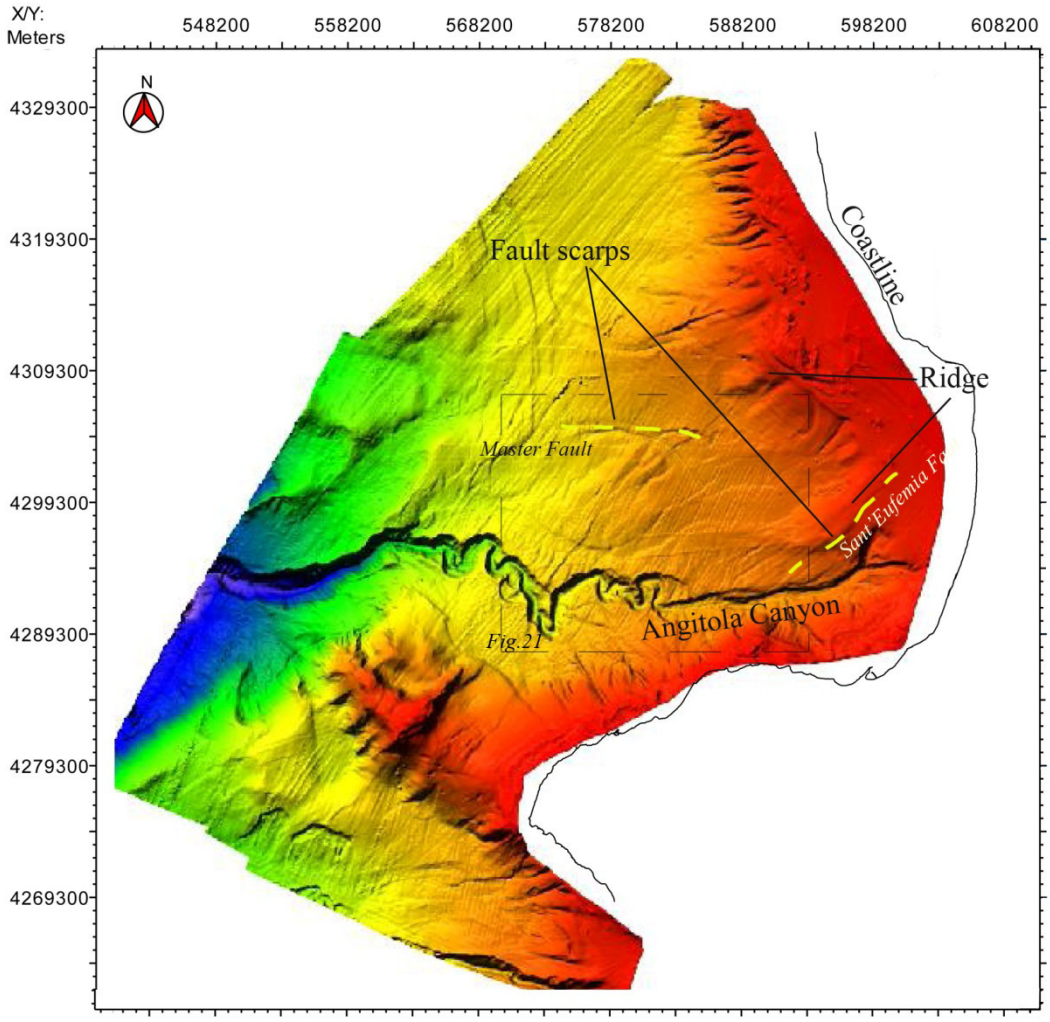

Figure 5.10: High resolution morpho-bathymetric map: yellow dashed lines underlines the fault scarps

5.4.3 Chirp seismic profiles

Chirp profiles allowed us to define the shallow structural and stratigraphic features characterizing the Sant'Eufemia Gulf.

Figure 5.11 images different morphology of the uppermost layers (less than 100m) passing from shelf to slope deposits (Fig. 5.11a), and from deformed (Fig. 5.11b) to undeformed strata. Locally, biogenic structures, small mounts and shallow strata breaks are also detectable (Fig. 5.11c).

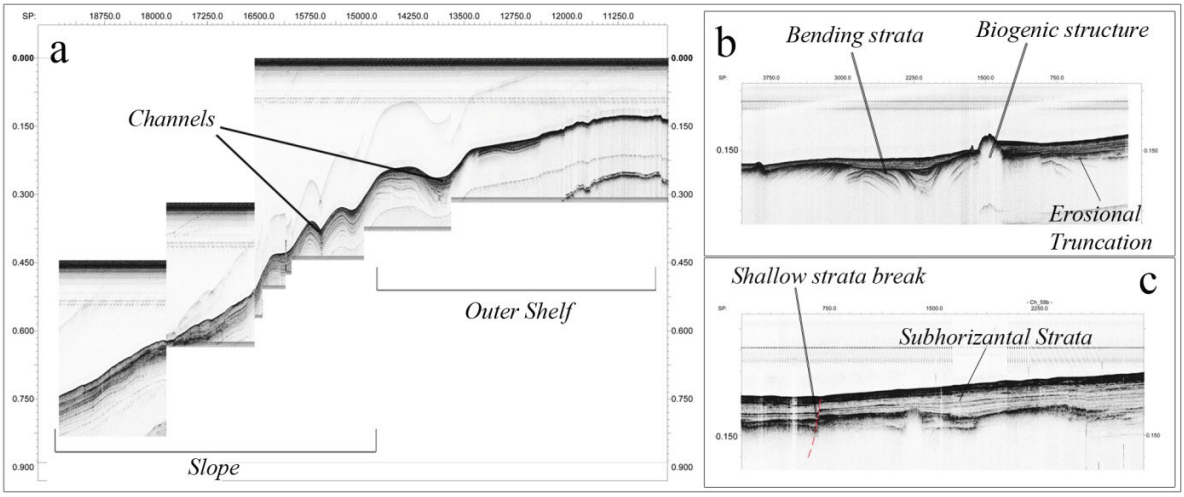

Figure 5.11: Chirp profile located near the Tyrrhenian coastline: a) Ch_57; b) Ch_52; c) Ch_59, the red line indicate the shallow discontinuity associable to a normal fault.

The shallow strata breaks, represents a shallow faults, which are used here to characterized recent activity of the much deeper structural lineaments. Within figure 5.12 Chirp profiles show a number of normal faults offsetting the uppermost layer (less than 100 m-depth) and aligned along the same NE-SW-oriented direction. These faults correspond to the surface continuation of the above mentioned NE-trending Sant'Eufemia Fault. These features demonstrate the recent activity of this structure which was considered one of the best candidate as seismogenic source of the 1905 Calabrian earthquake (Loreto et al., 2013).

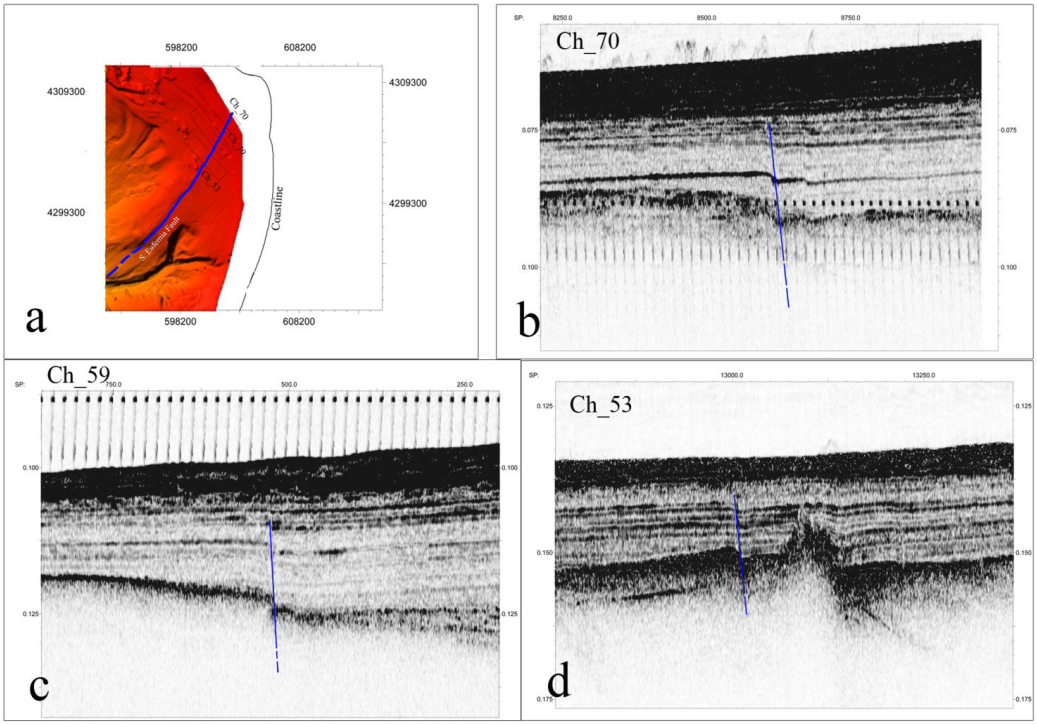

Figure 5.12: a) Location of three chirp profiles, b) Ch_70 c) Ch_59, d) Ch_53 seismic profiles

5.5 Sparker Seismic Profiles

Finally we have interpreted six NNW-SSE striking single-channel seismic profiles (1-kJ Sparker), which were made available by ISMAR- CNR of Bologna and allowed us to integrate the MCS and Chirp profiles, where these data were lacking.

Sparker profiles, collected aboard the R/V Bannock (Trincardi et al., 1987) (Fig. 5.13), were acquired with a broad band of frequencies (100 - 2000 Hz), in order to achieve better acoustic penetration up to 1 sec in TWT. They were fired every 2s, recorded with a 2-s sweep and a band-pass filter of 100 - 600 Hz (Trincardi et al., 1987).

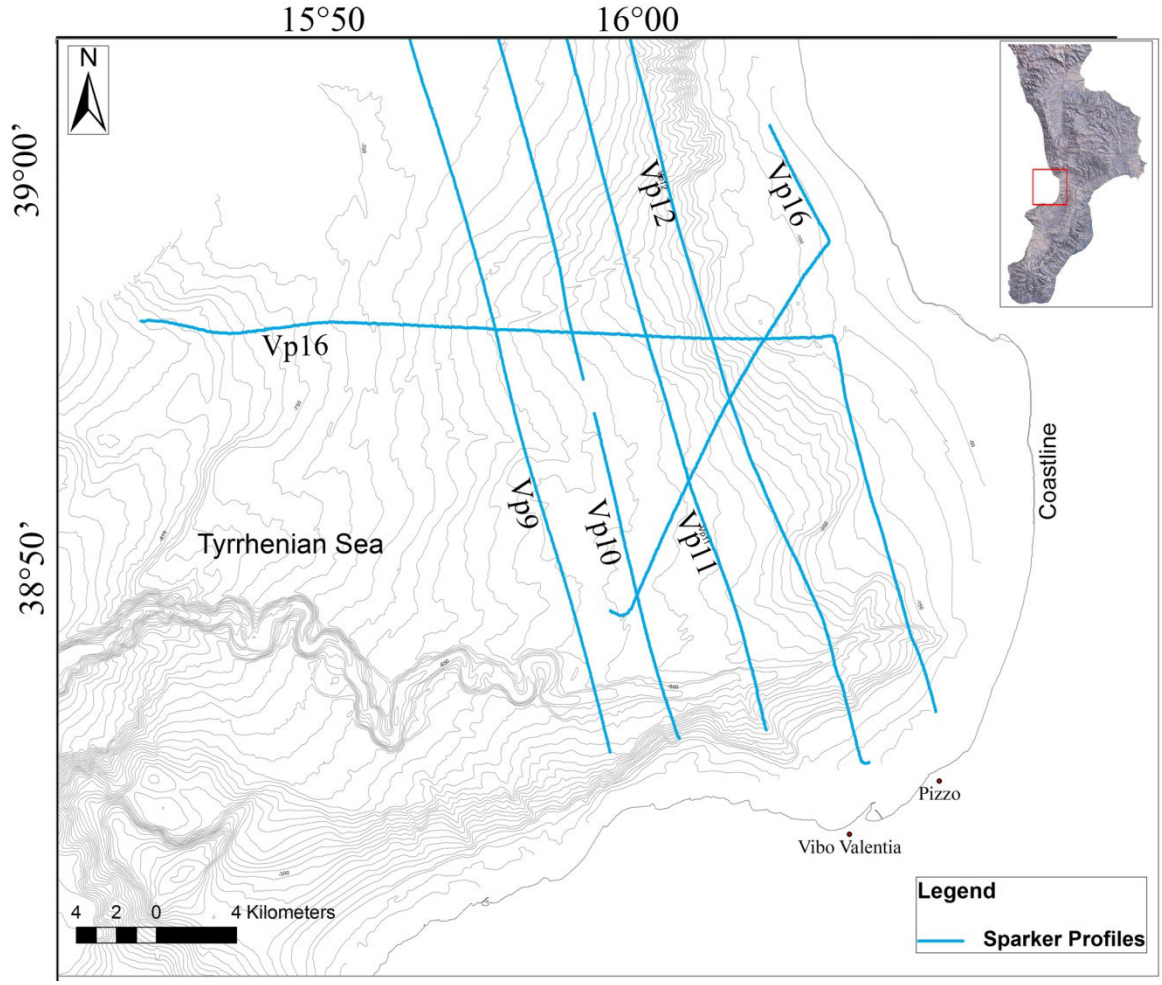

Figure 5.13: Blue lines image *Sparker Seismic Profiles* within the Sant' Eufemia Gulf

Firstly we have focused the interpretation on the two 1 kj Sparker lines (Vp11, Vp12) in the north-eastern margin of Sant'Eufemia Gulf, which show clearly two gentle folds NNE-SSW oriented and almost perpendicularly to the coastline (Fig. 5.14). The folding involves almost entirely the sedimentary sequence, producing a NW-SE oriented shortening, much more evident in the seismic line near the coastline (Vp12 in Figure 5.14) than the other (Vp11 in Figure 5.14).

The two ridges are bordered by two sets of normal faults, causing locally the split of the offshore portion of Catanzaro Trough: Capo Suvero Faults and, Sant'Eufemia and Angitola Faults, respectively. The extensional phase is developed in the study area probably at the later stage of the contractional episode, inheriting in any case the two morpho-tectonic highs.

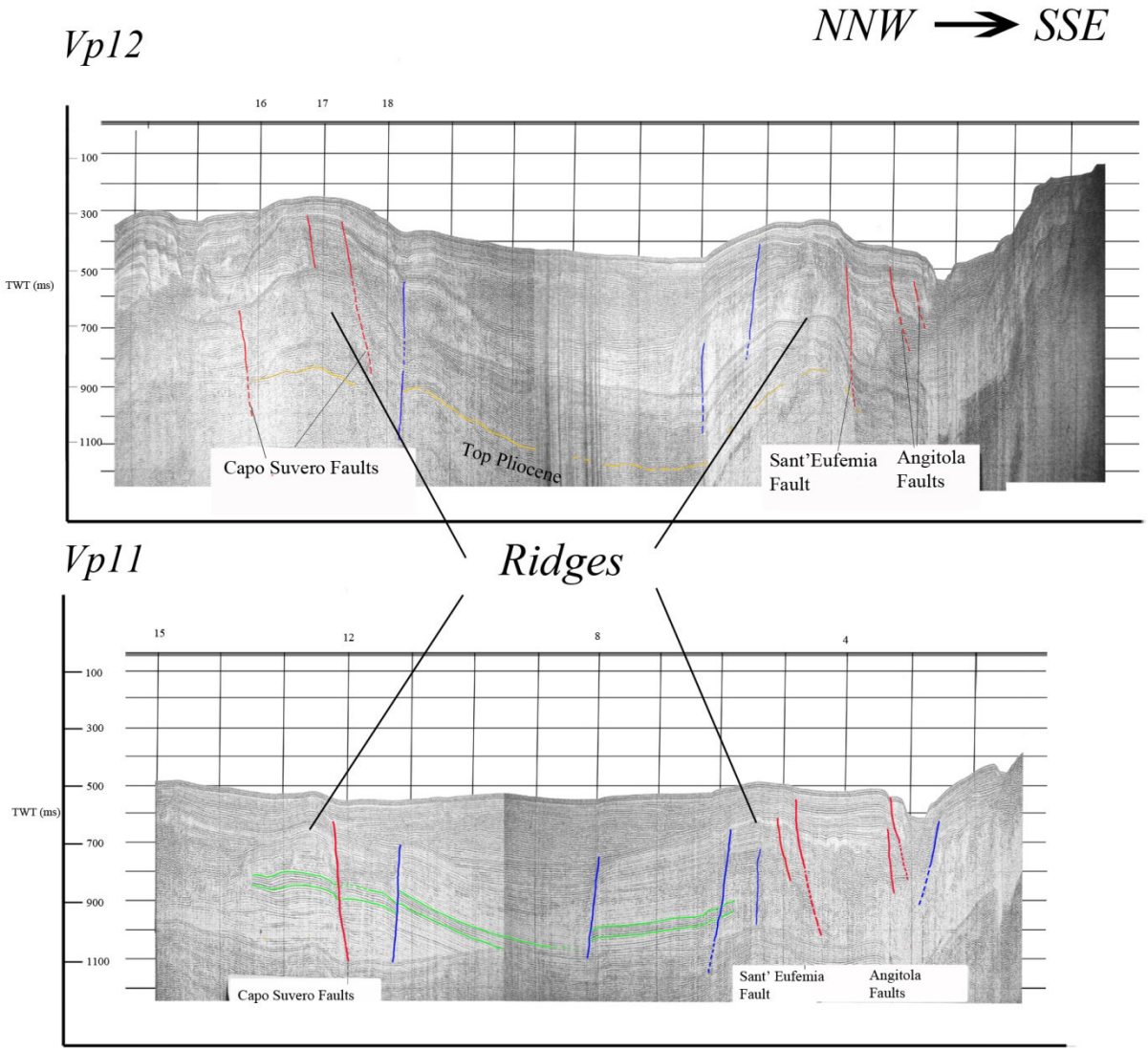

Figure 5.14: a) Sparker 1Kj seismic profiles Vp12, Vp11 arranged as a NNW-SSE trend

In the central part of Sant'Eufemia Gulf, the above mentioned Master Fault creates a sinuous fault scarp, showing on its hangingwall three ridges, which have been described partially in the previous section (GSE10_08 in Fig. 5.9).

Figure 5.15 shows more clearly the existence of these three small ridges with NE-SW elongated shape (black arrows in Fig. 5.15a). Vp9 Sparker seismic cross section (Fig. 5.15b), although not perpendicularly oriented to the ridges, shows sediments of late-Quaternary succession deformed in a sequence of three folds. These event seem replaced in a very recent stage by four normal/transtesional faults that offset the layers up to the seafloor (Fig. 5.15b).

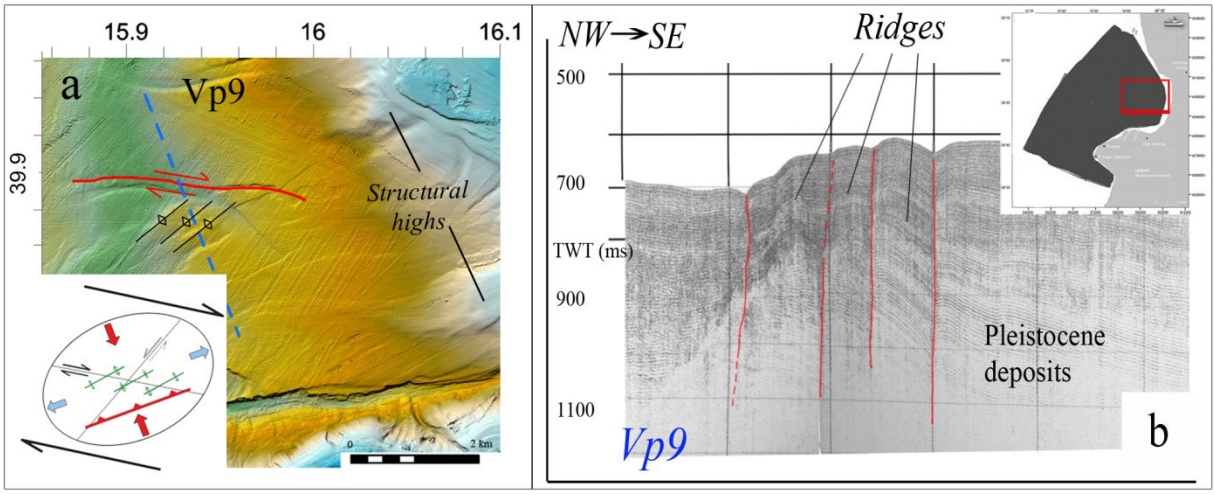

Figure 5.15: High resolution morpho-bathymetric map showing three small ridges, indicated with black arrows. Fault trace and kinematics of Master Fault are represented by red line and red arrows, respectively.

If we compare the three ridges with two elongated structural highs located in the eastern portion of Sant'Eufemia Gulf (Fig. 5.14), close to the shoreline, we can detect some similarities: the same NE-SW ridge orientation, almost similar sequence of folds involved in the Piacezian- Middle Pleistocene tectonic stage and, comparable kinematic change during Middle Pleistocene- Holocene age, passing from transpressional to transtensional kinematics.

The difference is that the three small ridges seem to accommodate movements from strike-slip to oblique, whereas the two northern ridges don't show, at least clearly, any major fault which could justify such change. This even though eastward in the onshore area the presence of similar major faults are widely demonstrated (Van Dijk et al., 2000, Tansi et al., 2007).

CHAP. 6 Active tectonics

6.1 Catanzaro Trough Basin: historical earthquakes and active faults

During the past 20 years, several advances were reached about two topics, faulting and earthquakes, that are become necessarily two strictly linked disciplines (Scholz, 2002).

Calabria is one of the Italian regions with the highest probability of occurrence of major earthquakes (Gasparini et al., 1982; Westaway, 1992; Michetti et al., 2000;, Castello et al., 2006; Basili et al., 2008; Rotondi, 2010; Calò et al., 2012; Presti et al., 2013), as Calabrian Arc region is located within the western Mediterranean subduction system. The area is affected by Ionian slab gravitational roll-back which produces a strong variation of faulting regimes at shallow depth along the local section of the convergent margin.

The study of Catanzaro Trough seismotectonic has been focused to collected data including: historical earthquakes inversion (Sirovich and Pettenati, 2007), some focal mechanisms with well-constrained first-motion (Guerra et al 2006) and all the available crustal focal mechanisms computed for the study region by using waveform inversion methods (Li et al., 2007; D'Amico et al., 2010, 2011; Presti et al., 2013). In this collected data, we also included two new focal mechanisms computed through the CAP waveform inversion method.

The study was integrated by using catalogue *(ITHACA)* and seismic source (DISS):

- ITaly HAzards from CApable faulting (ITHACA) is a database aimed at collecting and analyzing all available information on active tectonic structures in Italy, with particular regard to tectonic processes able to generate natural hazards. The main focus of the project is to better define active capable faults, which are defined as faults that have significant potential for displacement at or near the ground surface (Michetti et al., 2000).
- Database of Individual Seismogenic Sources (DISS) is a georeferenced repository of tectonic, fault, and paleoseismological information expressly devoted, but not limited, to potential applications in the assessment of seismic hazard at regional and national scale (Basili et al., 2008, DISS Working Group; 2010).

6.1.1 Central Calabrian Arc historical earthquakes

During the last few centuries the largest catastrophic earthquakes occurred within or close to the Catanzaro Trough, all reaching the epicentral intensity XI of the MCS (Mercalli–Cancani–Sieberg) scale and magnitude greater than 6.5. Relationships exist between faulting and historical earthquakes, for this reason several authors, with different approach, analyzed and defined the various seismogenic sources, within Catanzaro through. Below, we report some examples of historical earthquakes and active faults in study area (Fig. 6.1).

On the basis of the geometrical relationship between the Highest Intensity Datapoint Distribution (HIDD) of the strongest earthquakes of Calabria and the fault scarp trend (Galli & Bosi 2002), Galli & Bosi (2003) tentatively attributed to the Lamezia-Catanzaro Fault (sensu Tansi et al., 2007), which border the northern margin of the Catanzaro paleostrait, the 1638 shock (March 28, Mw=6.6; Mw is moment magnitude, named Maw in Working Group CPTI, 2004).

On the southeastern side of Catanzaro Trough, confined discontinuously from the Stalettì-Squillace-Maida Fault (Ghisetti, 1981), some epicenters of strong historical earthquakes fell along its trace indicating a possible activity of the above-mentioned structure (Galli et al., 2007). Even though poor known, one of the most catastrophic events is represented by the 4 April 1626 earthquake (Fig. 6.1), with epicenter in Girifalco village (I = IX MCS; Baratta, 1907). The second catastrophic event is that occurred in the 28 March 1783, even this occurred likely along Stalettì-Squillace-Maida Fault (Fig. 6.1). This represents the fifth and last important shock of the 1783 sequence that severely damaged the towns of Borgia and Girifalco (Baratta, 1901). It may have reached an intensity of XI (according to Boschi et al. 1995) and a magnitude somewhat greater than 6.5. However, this shock appears to have been deeper than the previous ones (Jacques et al., 2001).

The southwestern margin of the study area is influenced by the activity of Serre Faults (Tortorici et al., 2000, Galli et., 2007). These structures are supposed to be responsible for the earthquakes of 5 November 1659, 7 February and 1 March 1783. To support the evidence of its possible recent activity, some morphological indication, i.e. scarp and trapezoidal and triangular facets, and paleosismological data have been studied (Galli et 2007; Tortorici et al., 2000; Ghisetti, 1981; Jacques et al., 2001). The 1659 earthquake (Baratta, 1901), which shows I_0=X, (Boschi et al. 1995); corresponding to Me=6, was probably due to slip on the central Serre Faults (Fig. 6.1). This event probably ruptured the 10 km-long central segment of the fault (Jacques et al., 2001).

The 7 February 1783 earthquake was located in the southeastern part of the Mesima Basin, at the western foot of the Serre Mountains, and have reached an intensity of X or slightly more (Boschi et al. 1995) and a magnitude of at most 6.5.

Finally, the event of 1 March 1783 represents the fourth shock which struck an evidently smaller area near Polia (Baratta 1901), about 20 km north of the February 7 epicentre; the estimated magnitude was Mw=5.9 (CPTI2, 2004) with I=IX MCS. This earthquake is indicatively located on the hangingwall of Serre Faults, about 20 km towards west of the epicenter 28 March 1783 (Jacques et al., 2001, Graziani et al., 2006).

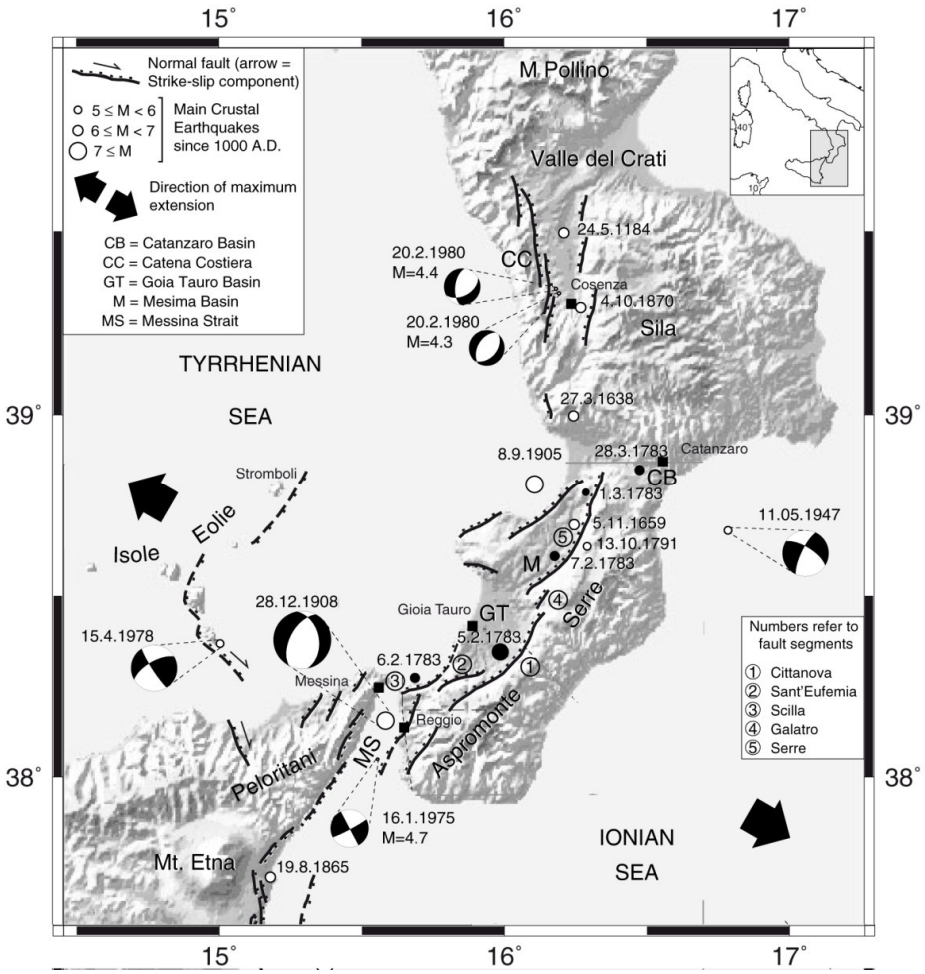

Figure 6.1: Seismotectonic map of the Calabrian Arc. The events of the 1783 earthquake sequence are represented as black dots (modified from Jacques et al., 2001).

The 8 September 1905 earthquake (Fig. 6.1), Mw = 7.0 (Gruppo di Lavoro CPTI04, 2004; Guerra et al., 2006; Rovida et al., 2011), it has been for long time debated both as regards the possible seismogenic fault and its epicentral location (see Loreto et al., 2013 and references therein).

Looking for the seismogenic fault of 1905 earthquake, various authors hypothesized diverse seismogenic sources: the NE-SW trending normal faults system, NW-dipping, named Vibo Valentia Faults by Tortorici et al. (2003), which border the northwestern edge of Serre Massif. The associated 1905 earthquake was defined from the analysis of the historical earthquakes documents, from published seismic catalogues, and Pleistocene marine terraces ages.

Platanesi and Tinti (2002) studied three theoretic tsunamis produced by three potential sources, namely Capo Vaticano fault, Vibo Valentia Fault and Lamezia Fault, they hypothesized that the most probable seimogenetic source of 1905 event could be the *Capo Vaticano Fault*.

Cucci and Tertulliani (2006) used terraces ages, aerophotogrammetry, topographic analysis and Boxer algorithm to evaluate the localization, dimension and orientation of seismic source. They proposed the *Coccorino Fault* as a likely cause of 1905 earthquake.

Close to the shoreline within the Sant'Eufemia Gulf, Loreto et al. (2013) map the NE-trending S. Eufemia normal fault, which is also proposed as the seismogenic source of the 1905 Calabrian earthquake.

They performed a multidisciplinary survey during the summer of 2010 in the S. Eufemia Gulf aboard the R/V OGS-Explora. Biological and geochemical data, collected to detect hydrothermal activity of potential seismotectonic relevance, and evidence stemming from the analysis of geophysical data (multichannel seismic – MCS, sub-bottom profiles – Chirp and high resolution morpho-bathymetry) allowed them to propose a causative source for this event.

With respect to the epicentral locations of the 1905 event, according to several authors, was located onshore (Rizzo, 1906; Boschi et al. 2000; Guidoboni et al. 2007), whereas Riuscetti and Schick (1974), Camassi and Stucchi (1997), Michelini et al. (2006), and a recent macroseismic study by Rovida et al. (2011) all place the epicenter offshore.

6.2 The 28 March 1783 and 8 September 1905 earthquakes inversion

In addition to the previous study we show an inversion of the 1783 and 1905 macroseismic dataset using the kinematic function (KF) elaborated by Pettenati and Sirovich, (2007) and by Loreto et al. (2012), respectively.

This procedure uses as input the intensity distribution of the macroseismic field (Sirovich, 1996, Pettenati and Sirovich, 2003, Pettenati and Sirovich, 2007), whereas Gentile et al. (2004) and Sirovich and Pettenati (2004) developed the inversion method.

6.2.1 Methods and data

The methodology is based on expressing the radiation from an earthquake in terms of the dimensionless values of a kinematic function KF based on the representation theorem (Aki and Richards, 1980): the method shows that displacement at a given point on the ground-surface far from the fault is proportional to the energy at the source. The KF procedure is unable to discriminate between the results produced by mechanisms which differ by 180° in the rake angle, since in both cases the method returns the same radiation, only with reversed polarities. This ambiguity, which comes in addition to the classic one concerning affecting the focal mechanism solution between fault and auxiliary plane, may be solved only with additional geological information (Sirovich, 1996, Pettenati and Sirovich, 2003, Pettenati and Sirovich, 2007, Loreto et al., 2012).

Due to the fact that the inversion of the KF is a non-linear problem, Niching Genetic Algorithm (NGA) was used. Genetic algorithms provide advantages in terms of global optimization and computational costs over other randomized search schemes (e.g., local optimization), which moreover easily could be biased by the starting conditions. The NGA algorithm is based on routines from the library by Levine (1996). Further details concerning the method can be found in Sirovich and Pettenati (2004) and in Gentile et al. (2004), while the error estimation of each parameter is described by Pettenati and Sirovich (2007).

Loreto et al. (2012) used parameters in Table 6.1 showing the inverted 447 intensity data points.

NGA INVERSION (123 data)	explored range; step	Model 1 (rupture plane) (sub-population 1)	Model 2 (sub-population 3)
PARAMETER		**VALUE ± error**	**VALUE**
Latitude [°] N	±0.35; 0.01	**38.83(±0.06)**	**38.90**
Longitude [°] E	±0.40; 0.01	**16.16(±0.06)**	**16.14**
Strike [°]	0 — 359; 1	**21(±12)**	**110**
Dip [°]	0 — 90; 1	**50(±6)**	**80**
Rake [°]	0 — 180; 1	**270(±6)** (±180)	**-14** (±180)
Depth [km]	6.0 — 24.0; 0.1	**22..9(±1.1)**	**17.0**
Mo [N m 10^{19}]	1.5 – 6.0; 0.1	**5.18(±2.86)**	**5.50**
Length along strike direction [km]	(*)	**40.0**	**12.0**
Length along anti-strike direction [km]	(*)	**15.0**	**45.0**
Mach along strike direction	0.50 — 0.99; 0.01	**0.85 (±0.11)**	**0.70**
Mach along anti-strike direction	0.50 — 0.99; 0.01	**0.83(±0.09)**	**0.70**
Vs [km sec^{-1}]	3.50 — 3.95; 0.1	**3.79(±0.04)**	**3.38**
Fitness		**258.75**	**273.75**

Table 6.1 - Parameters used in the Sant'Eufemia 1905 earthquake inversion (Loreto et al., 2012).

In figure 6.2A intensity points from the data reported by Guidoboni et al. (2007) were interpolated by Natural Neighbor algorithm (Sirovich et al., 2002) within 80 km from the epicenter. Figure 6.2A shows that the intensities distribution is not strongly homogeneous, and that the maximum intensities (>IX-X) are mainly grouped in the Capo Vaticano area (indicated with white dots).

Figure 6.2B shows two fault plane solutions resulting from the KF inversion in Table 6.1; the boxes represent the earthquake focal mechanism resulting from the surface projection of the two modeled sources.

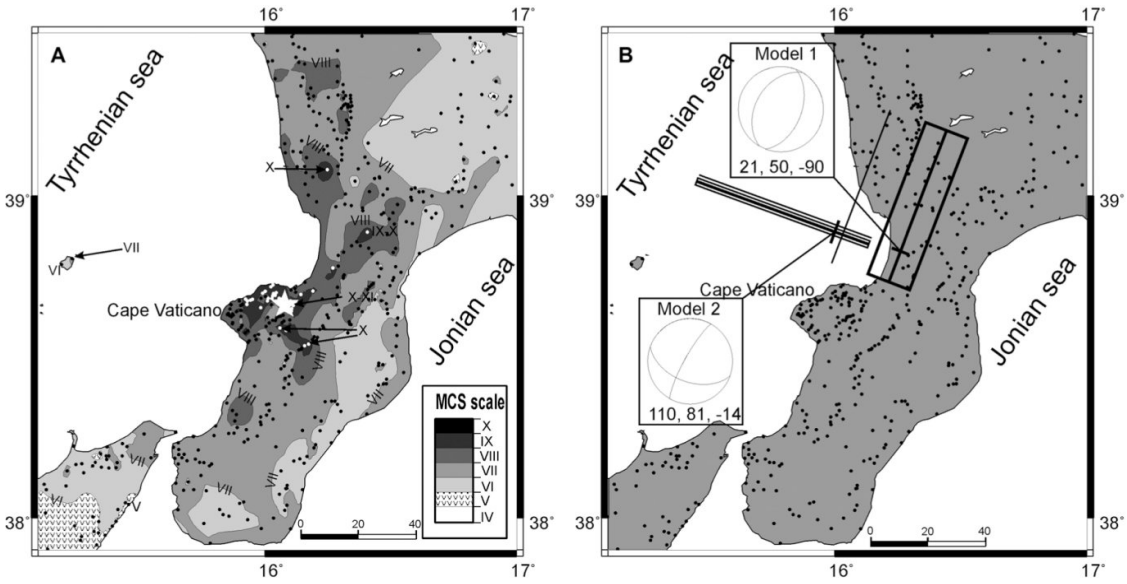

Figure 6.2: 8 September1905 earthquake a) observed intensities interpolated using the Natural Neighbor algorithm (Sirovich et al., 2002); b) intensities of minimum variance model by KF inversion. The white star represents the 1905 macroseismic earthquake epicenter (after Loreto et al., 2012),

The same methodology was used to define the intensity distribution of the macroseismic field for the 28 March 1783 (Fig. 6.3; Sirovich and Pettenati, 2007). It is possible to retrieve geometric and kinematic information about the source of the 28March destructive earthquake by inverting its regional macroseismic intensity patterns (Sirovich et al., 2004). Figure 6.3 shows a fault ca. 45 km-long, with N111° direction, displaying a right lateral kinematics, with reverse component of motion.

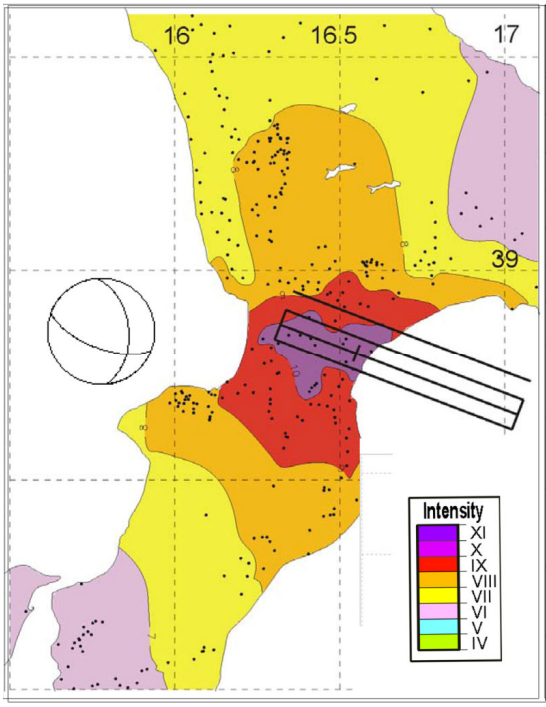

Parametro	Inversione 1 (residuo = 112)
Latitudine N (°)	38.80±0.05
Longitudine E (°)	16.55±0.06
Strike (°)	111±9
Rake (°)	229±12
Dip (°)	65±10
Profondità (km)	20.2±4.8
Vs (vel. Onde S) km·sec^{-1}	3.95±0.10
Mach (Vel. rottura/Vs) direz. lungo lo strike	0.55±0.11
Mach (Vel. rottura/Vs) direz. antistrike	0.85±0.12
Momento sismico $(N \cdot m) \cdot 10^{19}$	8.14±6.4 Magnitudo =7,2 (CPTI04: 6.94M)
Lunghezza(km) direz. lungo lo strike	45.2
Lunghezza(km) direz. antistrike	21.3

Figure 6.3: Location and parameters of the 28 March 1783 earthquake (Sirovich and Pettenati, 2007)

6.3 Focal mechanisms of recent earthquakes

Focal mechanisms of earthquakes are always relevant data in the study of the relationship between earthquakes, seismic faults, and active tectonics (Dziewonski et al., 1981; McCaffrey et al., 1985; Grimison and Chen, 1986; Jackson and McKenzie, 1988; Ekström and Engdahl, 1989; Anderson et al., 1993; Ekström et al., 2005). Focal mechanisms was widely used also in other tectonic studies: definition of orientation of motion along transform faults (Sykes, 1967; Wilson, 1965) or the discovery the main kinematic features of subducting slabs in different areas (Isacks and Molnar, 1971).

A focal mechanism solution (FMS) is the result of an analysis of wave forms generated by an earthquake and recorded by a number of seismographs (Lay and Wallace, 1995; Pondrelli et al., 2006; Scognamiglio et al., 2009). To produce a reasonable FMS, at least 10 records and a good geographically distribution around the epicenter of seismograph stations need. The complete characterization of an earthquake's focal mechanism provides important information, including the origin time, epicenter location, focal depth, seismic moment (a direct measure of the energy radiated by an earthquake), and the magnitude and spatial orientation of the 9 components of the moment tensor. And from the moment tensor, we can ultimately solve the orientation and slip of the fault. For any moment tensor, there are two possible planes. The two planes are called nodal planes, and they are at right angles to one another and intersect along the N axis. One of the planes is the fault surface, and the other is called the auxiliary plane and has no structural significance (Scholz, 2002 and reference therein).

The fault-plane solution or 'beachball' diagram is a product of the moment tensor inversion. The beachball diagram can also be obtained by graphic techniques from a study of P-wave first motions. Consulting the seismogram recording the vertical component at each station, we can evaluate whether the first motion detected was 'up' or 'down', representing compression or extension, respectively (Scholz, 2002, Cronin, 2004).

6.3.1 Seismotectonics of Catanzaro Trough: methods and data

To constrain the active tectonics of the Calabrian Arc region, we collected some seismotectonic data including all the available crustal focal mechanisms computed for the study region by using waveform inversion methods (http://www.bo.ingv.it/RCMT/; http://cnt.rm.ingv.it/tdmt.html; Li et al., 2007; D'Amico et al., 2010, 2011). In the database, we also included three focal mechanisms computed through the CAP waveform inversion method (Presti et al., 2013).

Focal mechanisms estimated with the traditional method of P-wave first motion are usually affected by inherent uncertainties, and they might be unstable because of insufficient azimuthal coverage and are not easily determined for low magnitude events (Lay and Wallace, 1995; Pondrelli et al., 2006; Scognamiglio et al., 2009), whereas waveform inversion methods shows more reliability than the previous one:

1. as regards focal mechanisms determined through *P-wave first motions*, we have selected a number of focal mechanisms derived from the analysis carried out from Guerra et al. (2006) within the southern portion of central Calabrian Arc. The study was focused on the

spatial distribution and focal mechanisms covering the time interval 1988–2005. The earthquake localization (longitude, latitude, depth of hypocenter and origin time) was made up using SIMUL method (Evans et al., 1994), based on P- and S-wave velocity models (Guerra et al., 2006). For the determination of earthquakes focal mechanisms was used FPFIT standard algorithm (Reasenberg e Oppenheimer, 1985), based on first motion arrivals with almost ten polarities for single focal mechanism, even though this condition is not often fulfilled, indeed they used composite focal mechanisms (Guerra et al., 2006 for details).

Guerra et al. (2006) selected 160 seismic events focusing their study only for the 1997 earthquake sequences with low magnitude (Fig. 6.4), dividing the total number of registered events in three period: A for Jenuary, B for June-July and, finally, C for September-October.

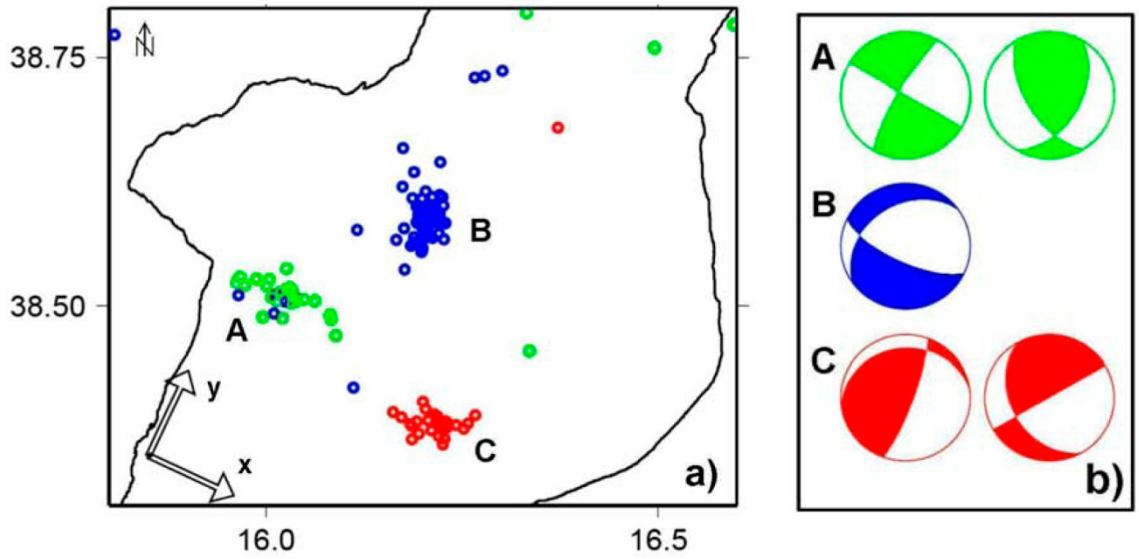

Figure 6.4: a) location of epicenter during 1997 sequences of events; b) Calculated composite focal mechanisms for three sequences of events (modified from Guerra et al., 2006)

The data show three sequences of events: the first one pure left strike slip (A in Fig 6.4b), the second one with normal kinematics (B in Fig 6.4b), whereas the last show ambiguous results, left and right lateral motion (C in Fig 6.4b).

2. The selected *moment tensor solutions* used to reconstruct our database, came from (see Table 6.2):

- the Italian CMT catalog (ItCMT) covering the time interval 1977–2011,
- time-Domain Moment Tensor (TDMT) covering the period 2004–2011;
- Cut and Paste technique (CAP).

The Italian CMT catalog (http://www.bo.ingv.it/RCMT/Italydataset; Pondrelli et al., 2006) has been obtained by merging the existing global CMTs, the Euro-Mediterranean RCMTs, and the solutions computed to extend backward the Euro-Mediterranean RCMT catalog (Pondrelli et al., 2002, 2004). This catalog represents an extension toward smaller magnitudes of the Harvard Centroid Moment Tensor catalog (CMT). The CMT database furnishes robust, stable, and reliable seismic source mechanisms through the analysis of intermediate and long period seismograms recorded at the global scale for earthquakes with M>5 (Presti et al., 2013).

Moment tensors for 4.0≤M≤5.5 earthquakes in the Italian CMT catalog have been computed following the same method that is used to analyze current seismicity for the European-Mediterranean RCMT Catalog (http://www.bo.ingv.it/ RCMT/). The RCMT procedure is based on the inversion of intermediate and long period surface waves recorded at regional and teleseismic distances (Pondrelli et al., 2002, 2004).

The TDMT algorithm performs long-period full waveform inversion for local and regional events with magnitude M≥3.5 (Scognamiglio et al., 2009).

In the CAP method (Zhao and Helmberger, 1994; Zhu and Helmberger, 1996) each waveform is broken up into Pnl (i.e., the first arrivals from a seismic source located in the crust eventually including waves reflected and multireflected from the top of the sharpest discontinuity) and into surface wave, which are weighted differently during the inversion procedure. This procedure is necessary because the selected wave segments are sensitive to different parts of crustal structure and have different amplitude decay with distances. The surface waves, although large in amplitudes, are easily influenced by heterogeneities of the surface crust, whereas Pnl waves are controlled by the average crustal velocity and are therefore more stable. Ground velocity data are preferred to ground displacement mainly because of the use of weak-motion data and because, for earthquakes of magnitude less than 4, there is a high signal-to-noise ratio only at higher frequencies (Presti et al., 2013).

All these features make the CAP method effective for earthquakes over a wide range of magnitudes (down to a minimum of 2.6; D'Amico et al., 2010, 2011; Zhu et al., 2006) as also proven by several tests and comparisons (D'Amico et al., 2010, 2011, Tan et al., 2006, Zhao and Helmberger, 1994).

Table 6.2 shows the methodology applied and input parameters used to compute the focal mechanisms: ID: identity number. Strike, dip, and rake refer to the nodal planes. Mag is the earthquake magnitude with the specific scale (M-Type). Source is the bibliographic source Waveform inversion (Wf Inv). P_Az and T_Az mean azimuth of P- and T-axes, respectively.

P_Pl and T_Pl mean plunge of P- and T-axes, respectively. According to Zoback's (1992), FT is the faulting type, NF: normal faulting, NS: normal faulting with a minor strike-slip component, SS: strike-slip faulting, TF: thrust faulting, TS: thrust faulting with a minor strike-slip component, and U: unknown stress regime (derived from Presti et al., 2013).

ID	Date	O.T.	Lon	Lat	Depth	Strike	Dip	Rake
1	07/09/2005	12:40:33.0	16.32	38,71	16,00	80	90	−42
2	27/09/2005	22:33:09.3	17,1	38,62	29,00	38	79	141
3	30/10/2005	19:09:46.8	15,93	38,83	15.00	208	32	−139
4	16/06/2010	22:39:41.0	16,14	38,83	15.00	109	50	−38
5	15/10/2010	05:21:19.0	16,66	38,87	15.00	287	62	173
6	18/10/2001	11:02:44.0	16,61	39,10	10.00	332	44	−88
7	18/01/2008	13:01:00.0	13.12	39,15	15.05	57	78	−67
ID	**M-Type/Mag**	**Source**	**Method**	**P_az**	**P_pl**	**T_az**	**T_pl**	**FT**
1	Mw=3,06	CAP-BGTA	WfInv	27	28	133	28	U
2	Mw=3,09	CAP-BSSA	WfInv	93	18	350	35	SS
3	Mw=3,05	CAP-BSSA	WfInv	26	58	153	21	NF
4	Mw=4,01	ItCMT	WfInv	119	67	346	16	NF
5	Mw=4,04	ItCMT	WfInv	57	8	148	4	SS
6	Mb=4,01	ItCMT	WfInv	7	88	241	1	NF
7	Mw=3,09	TDMT	WfInv	353	52	129	29	NF

Table 6.2: Database of 7 selected earthquake focal mechanisms for the Calabrian Arc (inspired from Presti et al., 2013). Source is the bibliographic source: Italian Centroid Moment Tensor (ItCMT); Time-Domain Moment Tensor (TDMT); D'Amico et al. (2011) (CAP-BGTA); D'Amico et al. (2010); Li et al. (2007) (CAP-BSSA).

Figure 6.5 show the seven earthquake focal mechanisms selected from: Italian Centroid Moment Tensor (ItCMT); Time-Domain Moment Tensor (TDMT); D'Amico et al. (2011) (CAP-BGTA); Li et al. (2007) (CAP-BSSA); CAP denotes 3 new mechanisms computed with the CAP method (2 CAP-BGTA and 1 CAP-BSSA focal mechanisms, see Tab. 6.2).

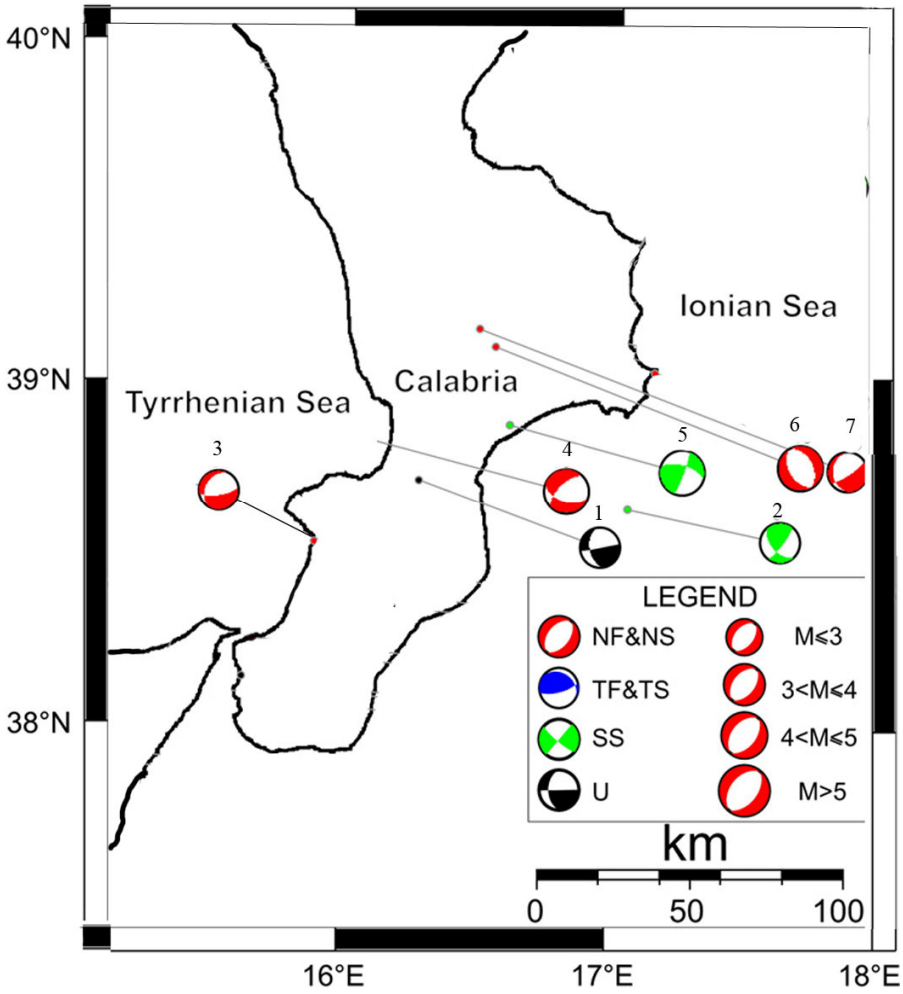

Figure 6.5: Selected crustal earthquake focal mechanisms for the large Calabrian Arc area including Calabria, eastern and western Tyrrhenian Sea, more details in Table 6.1 and in the above paragraph.

6.4 Focal mechanisms of new recent earthquakes

Finally, we included two new focal mechanisms computed through the CAP waveform inversion method (Tab. 6.3; D'Amico et al., 2010, 2011), and provided by Sebastiano D'Amico, researcher at Physics Department of Malta University.

Faulting parameters was obtained from low magnitude events in the central Calabrian Arc. Used velocity models come from detailed 3-D available for the study region (Barberi et al., 2004 and Neri et al., 2011; for more details we refer to D'Amico et al., 2011).

ID	Date	O.T.	Lon	Lat	Depth	Strike	Dip	Rake	M-Type/Mag	Source	Method
1	06/02/2015	19:09	16.44	38,85	11,00	331	76	18	Mw=3,22	CAP-BGTA	WfInv
2	06/02/2015	19:13	16.43	38,85	29,00	38	79	141	Mw=3,09	CAP-BGTA	WfInv

Table 6.3: Database of 2 unpublished earthquake focal mechanisms selected the area, Table 6.2 for details

Two earthquakes focal mechanisms show NW-SE- oriented main fault planes, which are characterized by transpressional kinematics (Fig. 6.6), although the results are not completely stable because of few avalaible stations in the area.

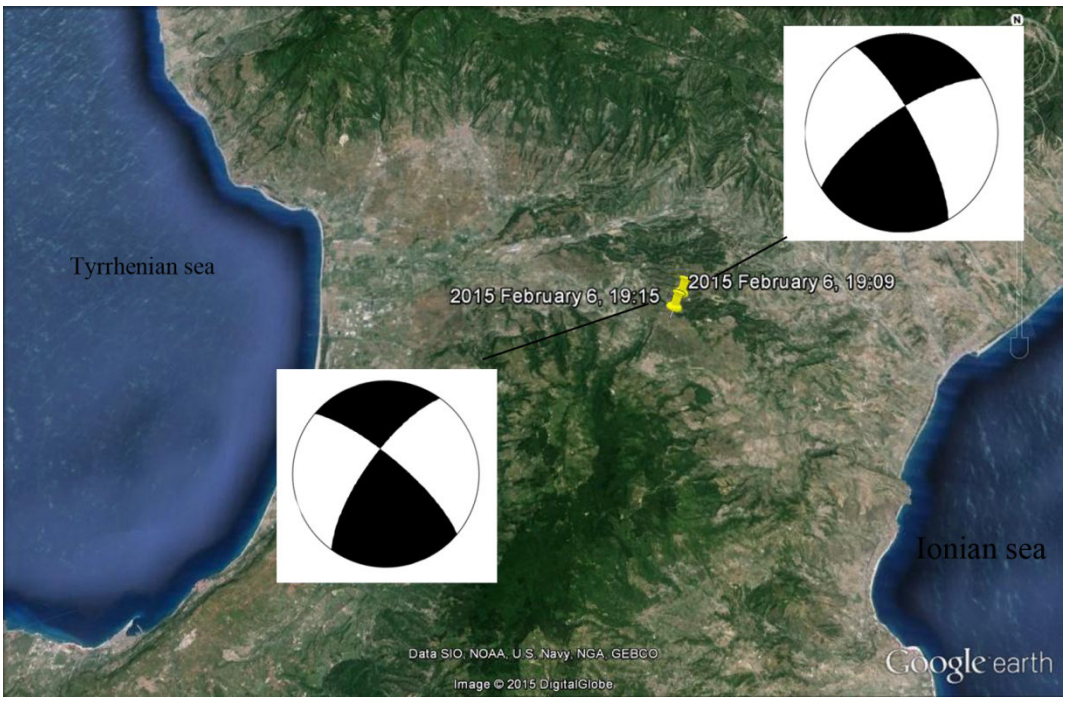

Figure 6.6: Selected crustal earthquake focal mechanisms from recent events with magnitude < 3,5

Discussions and Conclusion

The aim of this work is to define the Plio-Quaternary evolution of the Catanzaro Trough, and the role of transverse and longitudinal faults as part of the differential evolution between northern and southern sector of the Calabrian Arc. Further, the study was focused on the Catanzaro Trough seismotectonic reconstruction related to the analysis of earthquake focal mechanisms available from the existing literature. In these collected data, we also included two new focal mechanisms computed through the CAP waveform inversion method provided by D'Amico from Physics Department University of Malta.

d.1 Plio-Quaternary structural evolution of the western Catanzaro Trough

In order to reconstruct the Plio-Quaternary tectonic evolution of the onshore and offshore Catanzaro Trough, we have combined and analyzed several datasets composed by: geo-structural (more than 700 fault planes, slickensides and rotaxes), and geophysical (multibeam data, multichannel and sparker profiles) data.

Based on the analysis of results, the opening and evolution of the Catanzaro Trough is controlled by different tectonic phases, suggesting that the fault systems reactivation represents a key element to understand the entire evolution of the Southern Apennine system. Combining two datasets, we have recognized at least three tectonic events, classified on the base of age of deposits cut by brittle elements: the earlier tectonic phase, related to Messinian – Zanclean faults population, is well recognizable both onshore and offshore Catanzaro Trough. In the onshore side, evidence of this phase is represented by three fault associations related to this tectonic stage: 1. the NE-SW- oriented right- lateral faults system and ca. NW-SE- oriented sinistral strike slip faults; 2. the ca. E-W-oriented extensional faults; and finally 3. the N-S oriented reverse faults (Fig. 4.18a, b and c, respectively).

The stereographic projections of the principal stresses derived from application of the stress inversion method (Daisy 4, Salvini, 2002) display two results: first, the faults clusters of strike- slip and reverse kinematics indicate an overall paleo-stress with ca. E-W-trending sub-horizontal maximum principal σ_1 axis (P-axis) and an horizontal NNW-SSE extensional σ_3 axis (T- axis). Second, the stress inversion obtained by ca. E-W normal faults show the same NNW-SSE T-axis of the previous faults clusters, even though, in this case the paleo-stress is characterized by a vertical σ_1 axis (Fig. 4.18b). The normal kinematics related to the WNW-

ESE faults system is also highlighted by a morphologically recognizable fault escarpments, partially represented by Lamezia-Catanzaro Fault (LCF, Tansi et al., 2007).

On the Tyrrhenian offshore, the WNW-ESE-oriented ER-77-502 and ER-77-3028 seismic profiles (Fig. 5.5) were interpreted and display a ca. WNW-ESE compressional deformation (NE-SW-oriented ridges, see figure 5.10) decreasing towards the coastline. These deformation is expressed by a gentle anticline confined within the Lower Pliocene deposits. Coherently with onshore structural measurements in figure 4.18c, both profiles are compatible with a E-W-oriented compressional axis.

Towards the center of Sant'Eufemia Gulf we identified also, a SW-facing, WNW-trending Master Fault (Figs. 5.8 and d.1b) acting at least until the Piacezian time that, despite the large offset of 300 ms, eastward rapidly disappears next to the NE-trending ridge related to the activity of reverse/transpressional fault (Figs. 5.5, 5.7, 5.14 and d.1b).

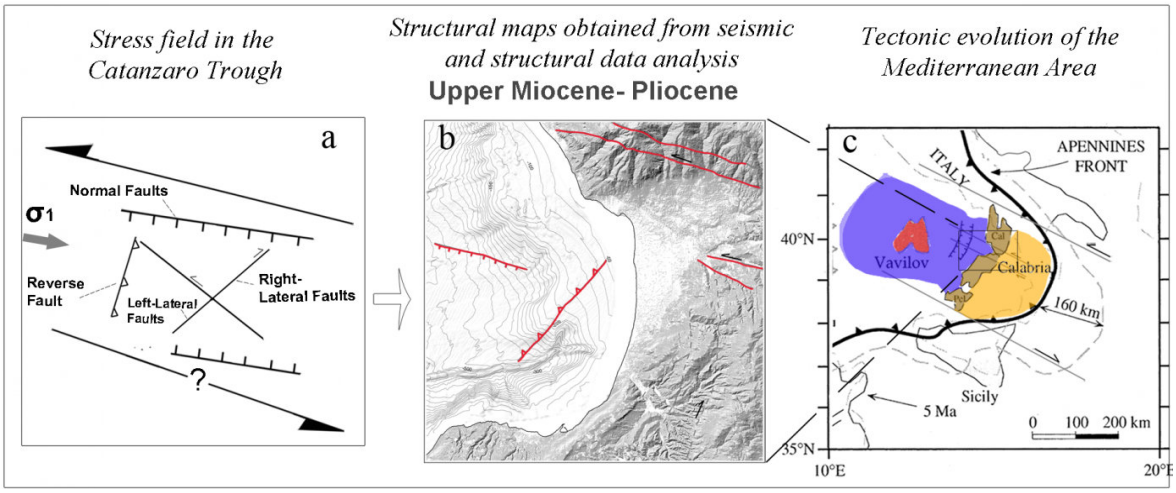

Figure d.1: Earlier tectonic stage reconstruction of Catanzaro Trough and of Southern Apennine system: a) stress field of Catanzaro Trough, b) structural maps resulted by the combination of structural and geophysical datasets, c) tectonic evolution of the Mediterranean area (modified from Gueguen et al., 1998)

The second tectonic phase, within Piacezian- Lower Pleistocene deposits (Fig. d.2a, b and c), is represented by prevalent transcurrent kinematics with oblique reversal component. On the onshore, this phase has been defined combining NE-SW right lateral faults with NNW-SSE left lateral faults, and analyzing the NE-SW reverse faults (Fig. 4.20b). Both faults systems are the outcome of a sub-horizontal maximum principal axis (σ_1), spanning from NNW-SSE to NNE-SSW orientation, and a ca. NW-SE oriented minimum principal axis (σ_3) (Fig. d.2a)

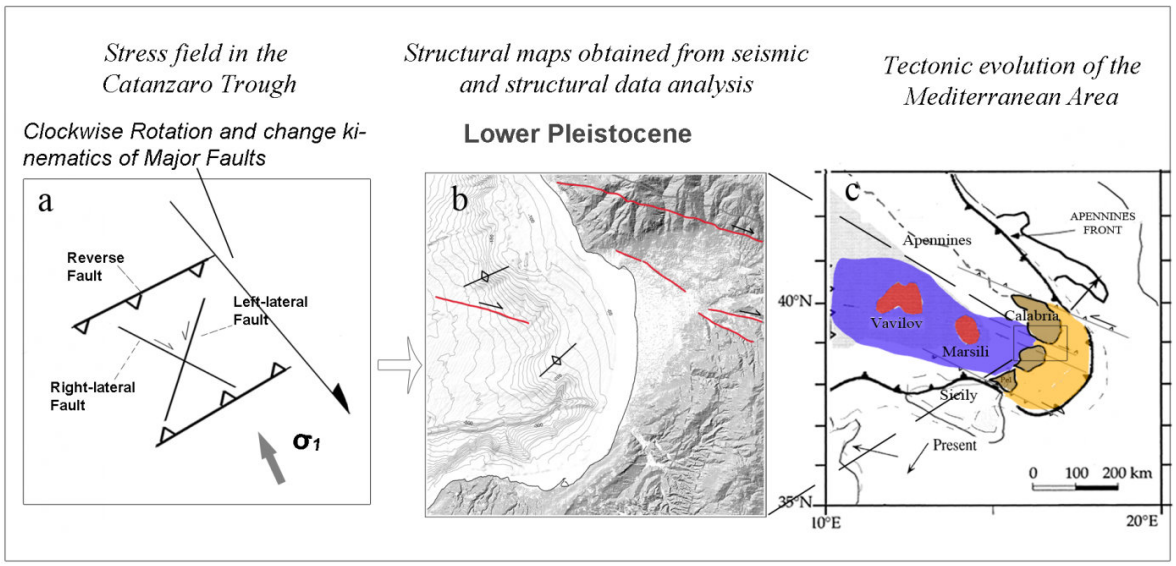

Figure d.2: Second tectonic phase reconstruction of Catanzaro Trough and of Southern Apennine system: a) stress field of Catanzaro Trough, b) structural maps resulted by the combination of structural and geophysical datasets, c) tectonic evolution of the Mediterranean area (modified from Gueguen et al., 1998)

Further, offshore, sediments bordered by the WNW-trending Master Fault show locally a positive tectonic inversion (Figs. 5.8, d.3a and b). Thus, sediments at the hangingwall pass from a extensional, visible in the Miocene-Lower Pliocene time, to transpressive-right lateral kinematics during Piacezian-Lower Pleistocene (Figs. 5.8 and 5.15).

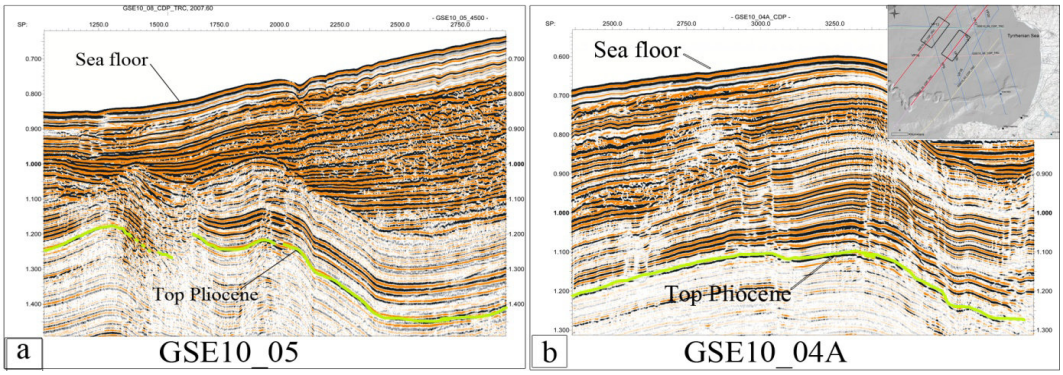

Figure d.3: Evidence of folding (inset in Fig. 5.8) in a) GSE10_05 and b) GSE10_04 details showing a contractional event, confined between Upper Pliocene and Lower-Middle Pleistocene layers.

The development of these fault systems was related to the onset of regional interplate compressive stress northwest oriented and caused by northward motion of the Africa with respect to the Eurasia (Dewey et al. 1989, Mantovani et al., 1992, Mattei et al., 2007, Serpelloni et al., 2010). The compression/transpression events could be related to the flexural down bending of the subducted slab and onset of uplift of thrust belt (Van Dijk and Scheepers 1995, Faccenna et al., 2001).

The third tectonic phase, acting during Middle – Upper Pleistocene (Fig. d.4g, h and i), is characterized by orogenic extension revealed, at least to the mesoscale, by the NE–SW and N–S normal faults systems. These lineaments diffusely dislocate the late Quaternary deposits, and favour the post- contractional uplift of the Calabrian Arc (Ghisetti 1981, Westaway 1993, Faccenna et al., 2001, Tortorici et al., 2003). The event recorded also by the widespread marine terraces, resulted of the interaction between long-term tectonic uplift and Quaternary cycle sea-level changes, distributed along the Tyrrhenian coastline (Monaco and Tortorici 2000, Cucci and Tertulliani 2010, Bianca et al., 2011).

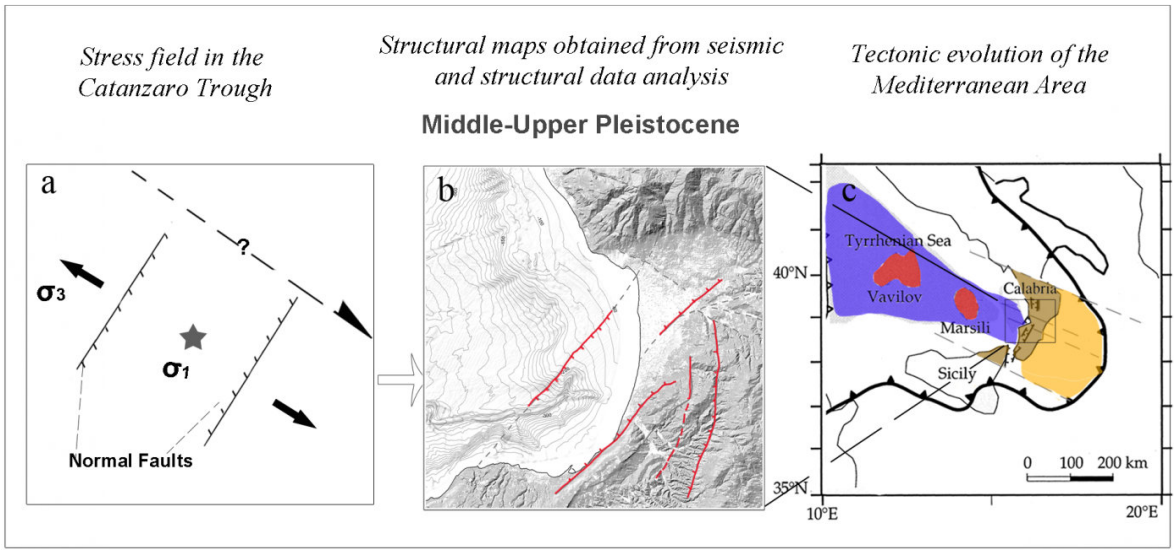

Figure d.4: Third tectonic phase reconstruction of Catanzaro Trough and of Southern Apennine system: a) stress field of Catanzaro Trough, b) structural maps resulted by the combination of structural and geophysical datasets, c) tectonic evolution of the Mediterranean area (modified from Gueguen et al., 1998)

During this last phase, some NE-SW elongated basins were formed within the Catanzaro Trough, one of which is here named *Lamezia Basin* (Fig. d.5a). Lamezia Basin is bounded both to the north and to the south by the above mentioned regional WNW-ESE trending oblique and strike slip fault systems; while laterally is confined by three normal faults that are: the San Pietro Lametino Fault (Brutto et al., 2015), the Vibo Valentia Fault (Tortorici et al., 2002) and the Sant'Eufemia Fault (Loreto et al., 2013) (see figure d.5a for their location).

If the northern termination is clearly identifiable with the LCF system, the southern one is more complex and less constrained. Indeed, it is depicted by a structural high, the Capo Vaticano promontory, southern bordered by the Coccorino and Nicotera Faults system (CF&NF), representing two WNW-ESE trending normal lineaments which could have caused

the Late Quaternary northeast down tilting of the Capo Vaticano Promontory (Pepe et al., 2013).

The NE-trending normal faults control the evolution of the Lamezia Basin, arranged as a graben-like system defining a WNW-ESE oriented extensional axis (Figs. 4.21 and d.4a).

The eastern basin edge is bordered by the W-dipping San Pietro Lametino Fault (SPLF; Fig. 5.3), here identified for the first time, that could represent the northern prolongation of the Vibo Valentia fault system (Monaco &Tortorici 2000), organized as a left-stepping en-echelon segment (*overstepping lineaments*, Peacock et al., 2000). These two segments can form a single and much longer fault (Fig. d.5a; Peacock et al., 2000; Kim et al., 2004; Fossen 2010). The asymmetric displacement between these two faults produces a folded overlap zone, namely relay ramp (Peacock et al., 2000, Fossen, 2010), connecting the two above mentioned overstepping lineaments which acts as transfer zone (Fig. d.5a, b, and c). The uncertain presence of small cracks or secondary faults (*Overstepping Fault* - OF - in Fig. d.5a, b, and c) across the relay ramp suggests that the bounding faults could be connected at depth (Peacock & Parfitt, 2002).

On the western edge, the Sant'Eufemia Fault (SEF) shows a normal kinematics at least since Pleistocene time (Fig. 5.5), even though the fault planes observed during fieldwork show rarely strike slip striations related, likely, to a previous stress field (Fig. d.5a).

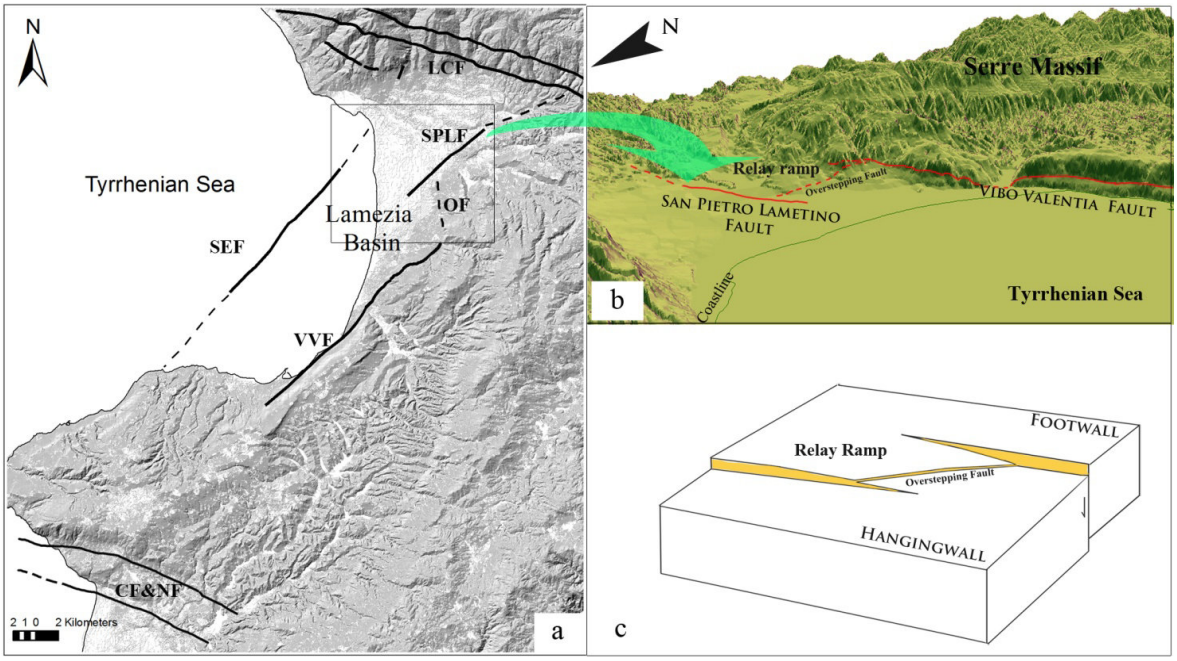

Figure d.5: a) Structural map of Major Faults: (LCF) Lamezia –Catanzaro Fault, (SEF) Sant'Eufemia Fault, (SPLF) San Pietro Lametino Fault, (OF) Overstepping Fault, (VVF) Vibo Valentia Fault, (CF&NF) Coccorino & Nicotera Fault. b) Hillshade of morphological map along Vibo Valentia and San Pietro Lametino Faults, c) Schematic representation of relay ramp (modified after Peacock & Parfitt 2002),

Accordingly, we suggest that the Sant'Eufemia Fault, extending through the whole Sant'Eufemia Gulf, could continue also on-land reaching the morphological northern edge of the Catanzaro Trough and increasing the fault length, previously proposed by Loreto et al. (2013), to more than 30 km. This hypothesis is strongly supported by fault planes recognized close to Caronte Terme (Fig. 4.23), and that can be related to the NE- SW offshore Sant'Eufemia faults on the basis of both direction and kinematics, even though we lost partially the evidence within the Lamezia Basin.

d.2 Reconstruction of Catanzaro Trough seismotectonic

Although the collected seismotectonic datasets coming from: historical earthquakes inversion (Sirovich and Pettenati, 2007), first-motion focal mechanisms (Guerra et al 2006) and waveform inversion methods (Presti et al., 2013 and reference therein), show a contrasting results, considering the avalaible data and the complexity of the studied area I decided to correlate the results obtained by Presti et al. (2013) regarding the whole Calabrian Arc with that one derived from the structural datasets acquired within Catanzaro Trough.

Presti et al. (2013) inverted, for stress tensor parameters, sub-samples of focal mechanisms mainly computed through waveform analyses, using the method of Gephart and Forsyth (1984) and Gephart (1990). The results show a sub-horizontal σ_3 with N304°E trending (Fig. d.6a), defining, hence, a WNW-ESE extensional stress regime for this area closely matching the structural evidence described in previous sections for the recognized last tectonic phase (Figs. 4.23, 24, 25 and d.6b). Accordingly, an extensional stress regime compatible with the post-orogenic WNW-ESE extension affecting the entire Apenninic chain; this is in agreement with the graben and half-graben systems widespread in the Calabrian Arc, e.g. the Crati and the Mesima grabens, and the Gioia Tauro plain.

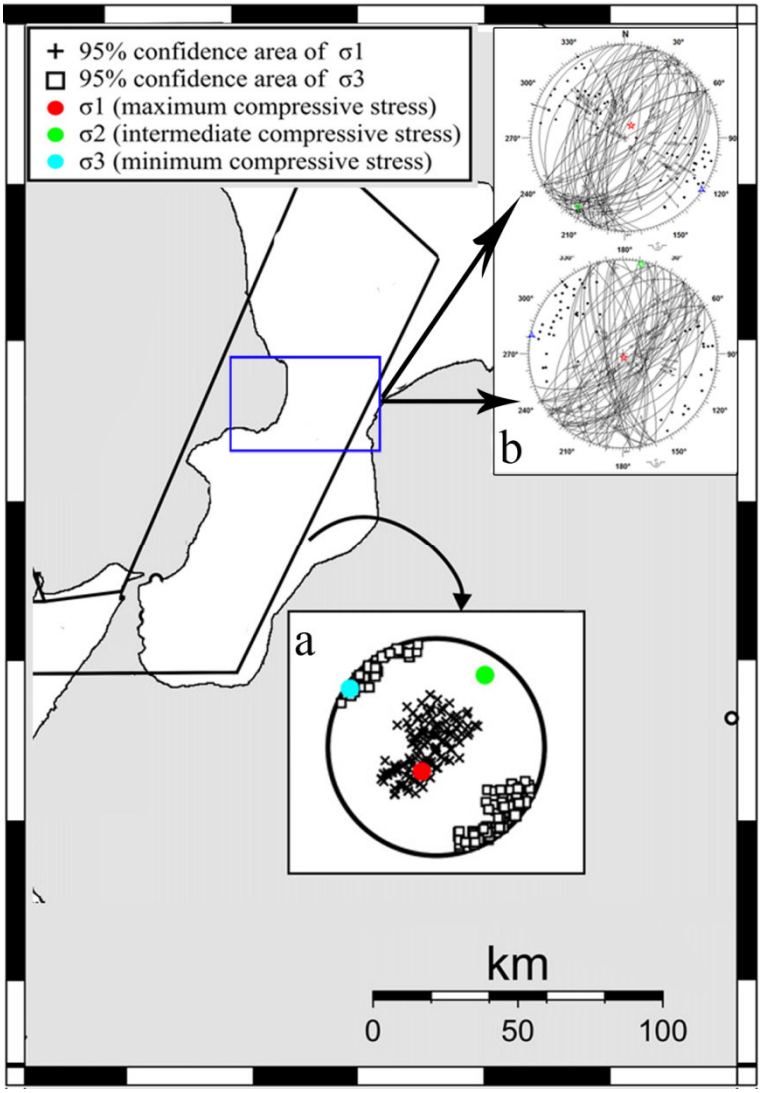

Figure d.6: Orientations of the principal stress axes obtained by inversion of a) the earthquake focal mechanisms from Presti et al., 2013 and b) structural data shown in the present work.

d.3 Concluding remarks

Calabrian Arc is considered at an intermediate evolutionary stage between the still active Aegean subduction system and mature- inactive Gibraltar Arc subduction system (Mattei et al., 2007). In this scenario the Catanzaro Trough is placed amongst two blocks, northern and southern Calabrian Arc. According to Neri et al. (2009), the Ionian slab seems to be detached beneath the northern block, whereas detachment appears not to have occurred to the south one, again.

The combination of geological and geophysical data, acquired along the SE Tyrrhenian Sea facing the Central Calabrian Arc, allowed us to recognize at least three tectonic stages. The first two are characterized by high rate of rotation during Late Pliocene- Lower

Pleistocene. Initially, this tectonic setting favored the development of a sub- horizontal E-W-oriented P-axis, and a ca. N-S-oriented extensional T-axis. Later, during Lower Pleistocene, a change of this stress field is highlighted by the ca. NNE-SSW P-axis and ca. WNW-ESE T-axis orientation.

During Middle Pleistocene age, evidence of vertical axis rotation cessation suggests a first order modification in the kinematics and geodynamic setting of Calabrian Arc (Mattei et al., 2007). On this basis, the last tectonic phase, here recognized, shows two faults association with vertical P-axis and WNW-ESE horizontal extensional axis (Presti et al., 2013), which denote quasi-pure shear.

In conclusion, WNW-ESE oriented faults are responsible for opening of a NW–SE palaeostrait that connected the Tyrrhenian area to the Ionian Sea during multiphase tectonics until early Pleistocene. While NE-SW and N-S fault systems border and control the supposed late Quaternary sub-basin, arranged as Graben Systems (i.e. Lamezia Basin) in response to one of the last extensional stages of Tyrrhenian back-arc basin opening.

In agreement with Jacques et al. (2001), who state that the main destructive earthquake sources bound the NNE-SSW trending steep range fronts (Coastal and Serre Range, Aspromonte and Messina Strait), the NE-SW and N-S trend normal faults play a relevant role as part of recent seismotectonic processes controlling the Late Quaternary geodynamic of the central Calabrian Arc.

Considering these features, the improvement of geological and structural knowledge of the western Catanzaro Trough could provide new insights about the evaluation of the seismic and tsunami hazard in the frame of a new urban development planning and the existing infrastructures safeguarding.

References

Aki K. and Richards P.G.; 1980: Quantitative seismology. Theory and methods. W.H. Freeman & Co., San Francisco, 932 pp.

Amodio-Morelli, L., Bonardi, G., Colonna,V., Dietrich, D., Giunta, G., Ippolito, F., Liguori,V., Lorenzoni, S., Paglionico, A., Perrone,V., Piccarreta, G., Russo, M., Scandone, P., Zanettin-Lorenzoni, E., Zuppetta, A., 1976. L'arco Calabro-Peloritano nell'orogene appenninico Maghrebide (The Calabrian-Peloritan Arc in the Apennine-Maghrebide orogen). Memorie della Societ`a Geologica Italiana 17, 1–60.

Anderson, H., Webb, T., Jackson, J., 1993. Focal mechanisms of large earthquakes in the south-island of New-Zealand — implications for the accommodation of Pacific- Australia plate motion. Geophysical Journal International 115, 1032–1054. http:// dx.doi.org/10.1111/j.1365-246X.1993.tb01508.x.

Angelier, J., 1979. Determination of the mean principal directions of stress for a given fault population. Tectonophysics 56, T17eT26.

Angelier, J., 1990. Inversion of field data in fault tectonics to obtain the regional stress e III. A new rapid direct inversion method by analytical means. Geophysical Journal International 103, 363e376.

Argnani A. & Tricardi F. 1988: Paola slope basin: evidence of regional contraction on the Eastern Tyrrhanian Margin: Societa Geologica ltaliana, Memorie, v. 44, p. 93-105.

Argnani, A., Trincardi F., 1993, Growth of a slope ridge and its control on sedimentation: Paola Slope Basin (Eastern Tyrrhenian Margin), *in* Frostick, L.E., and Steel, R.J., eds., Tectonic Controls and Signatures in Sedimentary Successions: International Association of Sedimeatologists Special Publication 20, p. 467--480.

Atzori, P., Ferla, P., Paglionico, A., Piccarreta, G., Rottura, A., 1984. Remnants of the Hercynian Orogen along the Calabrian-Peloritan Arc, southern Italy: a review. Journal of the Geological Society London 141, 137–145.

Atzori P., Cirrincione R., Del Moro A. & Pezzino A. (1994) - Structural, metamorphic and geochronologic features of the Alpine event in south-eastern sector of the Peloritani Mountains (Sicily), 63: 113–125.

Azzaro, R., Barbano, M.S., Camassi, R., D'Amico, S., Mostaccio, A., Piangiamore, G., Scarfì, L., 2004. The earthquake of 6 September 2002 and the seismic history of Palermo (northern Sicily, Italy): implications for the seismic hazard assessment of the city. Journal of Seismology 8, 525–543.

Balescu, S., Dumas, B., Guérémy, P., Lamothe, M., Lhénaff, R., Raffy, J., 1997. Thermoluminescence dating tests of Pleistocene sediments from uplifted marine shorelines along the southwest

coastline of the Calabria Peninsula (southern Italy). Palaeogeogr. Palaeoclimatol. Palaeoecol. 130, 25–41.

Baratta, M., 1901. I terremoti d'Italia. Arnoldo Forni Editore, Bologna.

Baratta M., 1907: Le nuove costruzioni in Calabria dopo il disastroso terremoto dell'8 settembre 1905 – Boll. Soc. Geol. It., 12, 249-338.

Barberi, G., Cosentino M. T., Gervasi A., Guerra I., Neri G., and Orecchio B., 2004: Crustal seismic tomography in the Calabrian arc region, south Italy. Physics of the Earth and Planetary Interiors, 147, pp. 297–314.

Barone M., Dominici R., Muto F., Critelli S. (2008) - *Detrital mode in late Miocene wedge-top basin northeasten Calabria, Italy: compositional record of wedge – top partitioning*. Journal of sedimentary Research, **78**, 693-711.

Basili, R., Valensise, G., Vannoli, P., Burrato, P., Fracassi, U., Mariano, S., Tiberti, M.M., Boschi, E., 2008. The Database of Individual Seismogenic Sources (DISS), version 3: summarizing 20 years of research on Italy's earthquake geology. Tectonophysics. http://dx.doi.org/10.1016/j.tecto.2007.04.014.

Beccaluva L., Maciotta G. & Spadea P. 1982. Petrology and geodynamic significance of the Calabria–Lucania ophiolites. Rendiconti Società Italiana di Mineralogia e Petrologia 38, 973–87.

Ben Avraham, Z. & Grasso, M. (1990) Collisional zone segmentation in Sicily and surrounding areas in the central Mediterranean. Ann. Tecton., 4, 131–139.

Bianca, M., Catalano, S., De Guidi, G., Gueli, A.M., Monaco, C., Ristuccia, G.M., Stella, G., Tortorici, G., Tortorici, L., Troja, S.O., 2011. Luminescence chronology of Pleistocene marine terraces of Capo Vaticano Peninsula (Calabria, Southern Italy). Quaternary International 232, 114e121.

Boccaletti, M., R. Nicolich, and L. Tortorici (1984), The Calabrian Arc and the Ionian Sea in the dynamic evolution of the central Mediterranean, Mar. Geol., 55, 219–245, doi:10.1016/0025-3227 (84)90070-7.

Booth-Rea G, Azaño'n J-M, Azor A. and Garcıa –Dueñas V., 2004: Influence of strike-slip fault segmentation on drainage evolution and topography. A case study: the Palomares Fault Zone (southeastern Betics, Spain). Journal of Structural Geology, 26, pp . 1615–1632.

Bonardi G., Messina A., Perrone V., Russo M., Russo S. & Zuppetta A. (1980) - La finestra tettonica di Cardeto (Reggio Calabria). Rend. Soc. Geol. It., 3: 3-4.

Bonardi, G., Cavazza,W., Perrone, V., Rossi, S., 2001. Calabria–Peloritani terrane and northern Ionian Sea. In: Vai, G.B., Martini, I.P. (Eds.), Anatomy of an Orogen: The Apennines and Adjacent Mediterranean Basins. Kluwer Academic Publishers, Bodmin, pp. 287–306.

Borsi, S., Hieke Merlin, O., Lorenzoni, S., Paglionico, A., Zanettin Lorenzoni, E., 1976. Stilo Unit and "dioritic-kinzigitic" unit in Le Serre (Calabria, Italy). Geological, petrological, geochronological characters. Bollettino della Società Geologica Italiana 19, 501–510.

Boschi, E.; Ferrari, G.; Gasperini, P.; Guidoboni, E.; Smriglio, G., and Valensise, G., 1995. Catalogo dei Forti Terremoti in Italia dal 461 a.C. al 1980. Bologna, ING-SGA, 970p.

Boschi E., Guidoboni E., Ferrari G., Valensise G. & Gasperini P. (1997) - Catalogo dei Forti Terremoti in Italia dal 461 a.C. al 1990. ING-SGA, Bologna.Boschi et al. 2000

Butler, R.W.H., Mazzoli, S., Corrado, S., De Donatis,M., Di Bucci, D., Gambini, R., Naso, G., Nicolai, C., Scrocca, D., Shiner, P., Zucconi, V., 2004. Applying thick-skinned tectonic model to the Apennine thrust belt of Italy: limitations and implications. In: McClay, K.R. (Ed.), Thrust Tectonics and Hydrocarbon System. AAPG Memoir 82, pp. 647–667.

Caggianelli, A., Prosser, G., Rottura, A., 2000. Thermal history vs. fabric anisotropy in granitoids emplaced at different crustal levels: an example from Calabria, southern Italy. Terra Nova 12, 109–116.

Calò, M., Dorbath, C., Luzio, D., Rotolo, S.G., D'Anna, G., 2012. Seismic velocity structures of southern Italy from tomographic imaging of the Ionian slab and petrological inferences. Geophysical Journal International. http://dx.doi.org/10.1111/j.1365- 246X.2012.05647.x.

Camassi, R., Stucchi, M., 1997. NT4.1.1, un catalogo prametrico di terremoti di area italiana al di sopra della soglia del danno. Gr. Naz. Difesa dai Terremoti, Rapp. Interno, Milano (95 pp.).

Cavazza, W., Blenkinsop, J., De Celles, P.G., Patterson, R.T., Reinhardt, E.G., 1997. Stratigrafia e sedimentologia della sequenza sedimentaria oligocenico–quaternaria del bacino calabro–ionico. Boll. Soc. Geol. Ital. 116, 51–77.

Cavazza, W. & Decelles, P.G. (1998) Upper Messinian siliciclastic rocks in southeastern Calabria (S Italy): Paleotectonic and eustatic implications for the evolution of the central Mediterranean region. Tectonophysics, 298, 223–241.

Cavazza, W. and Ingersoll, R.V. (2005) Detrital modes of the Ionian forearc basin fill (Oligocene-Quaternary) reflect the tectonic evolution of the Calabria-Peloritani terrane (southern Italy). J. Sed. Res., 75, 268–279.

Cello G., De Francesco A. & Morten L. 1991. The tectonic significance of the Diamante-Terranova unit (Calabria, southern Italy) in Alpine evolution of the northern sector of the Calabrian Arc. Bollettino della Società Geologica Italiana 110, 685–94.

Cello G., Invernizzi C. & Mazzoli S. 1996. Structural signature of tectonic processes in the Calabrian Arc, southern Italy: Evidence from oceanic- derived Diamante-Terranova unit. Tectonics 15, 187–200.

Chiarabba, C., De Gori, P., Speranza, F., 2008. The Southern Tyrrhenian subduction zone: deep geometry, magmatism and Plio-Pleistocene evolution. Earth and Planetary Science Letters 268, 408–423. http://dx.doi.org/10.1016/j.epsl.2008.01.036.

Chiarella D. (2011) - Sedimentology of Pliocene-Pleistocene mixed (lithoclastic-bioclastic) deposits in southern Italy (Lucanian Apennine and Calabrian Arc): depositional processes and

palaeogeographic frameworks [unpublished PhD thesis]: University of Basilicata, Potenza, 216 pp.

Chiarella, D., Longhitano, S.G. and Muto, F. (2012a) Sedimentary features of the Lower Pleistocene mixed siliciclastic-bioclastic tidal deposits of the Catanzaro Strait (Calabrian Arc, south Italy). Rend. Soc. Geol. Ital., 21, pp. 919–920.

Christensen, N. I. (1982). Seismic velocities. Handbook of physical properties of rocks, 2, 1-228.

Cianflone, G. and Dominici, R. (2011) Physical stratigraphy of the upper Miocene sedimentary succession in the northeastern Catanzaro Through (Central Calabria, Italy). Rend. Soc. Geol. Ital., 17, 63–69.

Cirrincione R. & Pezzino A. (1991) - Caratteri strutturali dell'evento alpino nella serie mesozoica di Alì e nella Unità metamorfica di Mandanici (Peloritani orientali). Mem. Soc. Geol. It., 47: 263–272.

Cirrincione R. & Pezzino A. (1994) - Nuovi dati sulle successioni mesozoiche metamorfiche dei Monti Peloritani orientali. Boll. Soc.Geol. Ital., 113: 195–203.

Cirrincione R., Fazio E., Fiannacca P., Ortolano G., Pezzino A. & Punturo R. (2008) - Petrological and microstructural constraints for orogenetic exhumation modelling of HP rocks: The example of southern Calabria Peloritani Orogen (Western Mediterranean), in GeoMod 2008, Third International Geomodelling Conference, Firenze, 22–24 September 2008. Boll. Geof. Teor. e Appl., 49, 2: 141–146.

Cirrincione R., Fazio E., Ortolano G., Pezzino A. & Punturo R. (2011) - Fault-related rocks: deciphering the structural–metamorphic evolution of an accretionary wedge in a collisional belt, NE Sicily, Inter. Geol. Rev., DOI:10.1080/00206814.2011.623022.

Colella A., Zuffa G. G., 1988. Megastrati carbonatici e silicoclastici della Formazione di Albidona (Miocene, Appennino meridionale): implicazioni paleogeografiche. Mem. Soc. Geol. It., 41: 791-807.

Colella A., 1995. Sedimentation, deformational events and eustacy in the perityrrhenian Amantea Basin: preliminary synthesis. Gior. Geologia, 57: 179-193.

Colonna, V., Piccarreta, G., 1975. Schema strutturale della Sila Piccola Meridionale (Structural scheme of the Southern Sila Piccola). Bollettino della Societ`a Geologica Italiana 94, 3–16.

Colonna, V., Piccarreta, G., 1977. Carta geologico-petrografica della zona compresa tra Serra Stretta-Carlopoli-Gimigliano-Pianopoli (Sila Piccola, Calabria) (Geological-petrographic map of the area between Serra Stretta-Carlopoli-Gimigliano-Pianopoli (Sila Piccola, Calabria). Sviluppo 9, Arti Grafiche G. Favia, Bari, Italy.

Critelli, S. (1999) The interplay of lithospheric flexure and thrust accommodation in forming stratigraphic sequences in the Southern Apennines foreland basin system, Italy. Rend. Lincei Sci. Fis. Nat, Acc. Naz. Lincei., Ser. IX, 10, 257–326.

Critelli, S., Muto, F., Tripodi, V. and Perri, F. (2013) Link between thrust tectonics and sedimentation processes of stratigraphic sequences from the southern Apennines foreland basin system, Italy. Rend. Soc. Geol. Ital., 25, 21–42.

Cucci, L., Tertulliani, A., 2006. I terrazzi marini nell'area di Capo Vaticano (arco calabro): solo un record di sollevamento regionale o anche di deformazione cosismica? Il Quaternario 19, 89–101.

Cucci, L. and Tertulliani, A., 2010. The Capo Vaticano (Calabria) coastal terraces and the 1905 M7 earthquake: the geomorphological signature of the regional uplift and coseismic slip on southern Italy. Terra Nova, 22(5), 378–389.

Damuth, J.E., 1980. Use of high-frequency (3.5e12 kHz) echograms in the study of near bottom sedimentation processes in the deep sea: a review. Marine Geology 38, 51e75.

D'Agostino, N., Selvaggi, G., 2004. Crustal motion along the Eurasia– Nubia plate boundary in the Calabrian Arc and Sicily and active extension in the Messina Straits from GPS measurements. J. Geophys. Res. 109, B11402. doi:10.1029/2004JB002998.

D'Amico, S., Orecchio, B., Presti, D., Zhu, L., Herrmann, R.B., Neri, G., 2010. Broadband waveform inversion of moderate earthquakes in the Messina Straits, southern Italy. Physics of the Earth and Planetary Interiors 179, 97–106.

D'Amico, S., Orecchio, B., Presti, D., Gervasi, A., Zhu, L., Guerra, I., Neri, G., Herrmann, R.B., 2011. Testing the stability of moment tensor solutions for small earthquakes in the Calabro-Peloritan Arc region (southern Italy). Bollettino di Geofisica Teorica ed Applicata 52 (2), 283–298.

Del Ben A., Barnaba C. and Taboga A., 2009: Strike-slip systems as the main tectonic features in the Plio-Quaternary kinematics of the Calabrian Arc. Marine Geophysical Researches 29, pp. 1–12.

Del Moro, A., Paglionico, A., Piccarreta, G., Rottura, A., 1986. Tectonic structure and post- Hercynian evolution of the Serre, Calabrian Arc, southern Italy: geological, petrological and radiometric evidences. Tectonophysics 124, 223–238.

De Roever E. W. F. 1972. Lawsonite–albite facies metamorphism near Fuscaldo, Calabria (southern Italy), its geological significance and petrological aspects. GUA Paper Geological Sciences 1, 1–171.

Dewey, J.F., Helman, M.L., Turco, E., Hutton, D.H.W. & Knott. S., 1989. Kinematics of the Western Mediterranean, in Alpine Tectonics, eds Coward, M. P. & Dietrich, D., Geol. Soc. Lond. Spec. Publ., 45, 265–283.

Dietrich D. & Scandone P. 1972. The position of the basic and ultrabasic rocks in the tectonic units of the Southern Apennines. Atti Accademia Pontaniana Napoli 21, 61–75.

DISS Working Group; 2010: Database of Individual Seismogenic Sources (DISS), Version 3.1.1: A compilation of potential sources for earthquakes larger than M 5.5 in Italy and surrounding areas. INGV – Istituto Nazionale di Geofisica e Vulcanologia, http://diss.rm.ingv.it/diss/.

Di Stefano *A.,* Lentini *R. (*1995*)* Ricostruzione stratigrafica e significato paleotettonico dei depositi Plio-Pleistocenici del margine tirrenico tra Villafranca Tirrena e Faro *(*Sicilia nord-orientale*).* Studi Geologici Camerti, Volume Speciale 2, pp. 219–237.

Dobrin, M. B., & Savit, C. H. (1960). *Introduction to geophysical prospecting* (Vol. 4). New York: McGraw-hill.

Dziewonski, A.M., Anderson, D.L., 1981. Preliminary reference Earth model. Phys. Earth Planet. Int. 25, 297–356.

Ekström, G., Engdahl, E.R., 1989. Earthquake source parameters and stress distribution in the Adak Island region of the central Aleutian Islands, Alaska. J. Geophys. Res. 94, 15499–15519.

Ekström, G., Dziewonski, A.M., Maternovskaya, N.N., Nettles, M., 2005. Global seismicity of 2003: centroid-moment-tensor solutions for 1087 earthquakes. Phys. Earth Planet. Int. 148, 327–351.

Evans J.R., Eberhart-Phillips D. e Thurber C.H., 1994: User's manual for SIMULPS12 for imaging Vp and Vp/Vs: a derivative of the "Thurber" tomographic inversion SIMUL3 for local earthquakes and explosions - USGS Open-file Report, 94-431.

Faccenna C., Funiciello F., Giardini D. & Lucente P., 2001. – Episodic back-arc extension during restricted mantle convection in the Central Mediterranean. – *Earth Planet. Sci. Lett.*, **187**, 105-116.

Faccenna C., Civetta L., D'Antonio M., Funiciello F., Margheriti L., and Piromallo C., 2005: Constraints on mantle circulation around the deforming Calabrian slab. Geophys. Res. Lett., 32, L06311, doi:10.1029/2004GL021874.

Fazio E., Cirrincione R. & Pezzino A. (2008) - Estimating P-T conditions of Alpine-type metamorphism using multistage garnet in the tectonic windows of the Cardeto area (southern Aspromonte Massif, Calabria). Mineralogy and Petrology, 93: 111-142.

Ferrini, G. and Testa, G. (1997) La successone miocenico superiore della Stretta di Catanzaro, dati preliminari. In: Abstracts of the Gruppo di Sedimentologia del CNR (Ed. S. Critelli), Annual Meeting, 13–17 October, Arcavacata di Rende, CS, pp. 53–55.

Festa V., Messina A., Paglionico A., Piccarreta G. & Rottura A. (2004) - Pre-Triassic history recorded in the Calabria–Peloritani segment of the Alpine chain, southern Italy. An overview. Period Mineral, 73: 57–71.Finetti, I. & Del Ben, A. (1986) Geophysical study of the Tyrrhenian opening. Boll. Geofis. Teor. Appl., 28, 75–156.

Finetti, I., Lentini, F., Carbone, S., Catalano, S., Del Ben, A., 1996. Il sistema Appenninico Meridionale–Arco Calabro–Sicilia nel Mediterraneo Centrale: studio geofisico–geologico. Boll. Soc. Geol. Ital. 115, 529–559.

Finetti IR, Lentini F, Carbone S, Del Ben A, Di Stefano A, Forlin E, Guarnieri P, Pipan M, Prizzon A (2005) Geological outline of Sicily and lithospheric tectono-dynamics of its Tyrrhenian margin from new CROP seismic data. In: Finetti IR (ed) CROP PROJECT: deep seismic exploration of the central Mediterranean and Italy. Elsevier, Amsterdam, pp 319–375.

Fornelli, A., Caggianelli, A., Del Moro, A., Bargossi, G.M., Paglionico, A., Piccarreta, G., Rottura, A., 1994. Petrology and evolution of the central Serre granitoids (Southern Calabria — Italy). Periodico di Mineralogia 63, 53–70.

Frepoli, A., Maggi, C., Cimini, G.B., Marchetti, A., Chiappino, M., 2011. Seismotectonic of Southern Apennines from recent passive seismic experiments. Journal of Geodynamics 51, 110–124.

Galli, P., Bosi, V., 2002. Paleoseismology along the Cittanova fault: implications for seismotectonics and earthquake recurrence in Calabria (southern Italy). Journal of Geophysical Research 107, B3. http://dx.doi.org/10.1029/2001JB000234.

Galli P. & Bosi V., 2003: Catastrophic 1638 earthquakes in Calabria (southern Italy): new insights from palaeoseismological investigation. Journal of Geophysical Research, 108 (B1).

Galli, P., Scionti V. and Spina, V., 2007: New paleoseismic data from the Lakes and Serre faults: seismotectonic implications for Calabria (Southern Italy). Ital. J. Geosci., 126, pp. 347-364.

Gasparini, C., Iannacone, G., Scandone, P., Scarpa, R., 1982. Seismotectonics of the Calabrian Arc. Tectonophysics 82, 267–286.

Gentile F., Pettenati F. and Sirovich L.; 2004: Validation of the automatic nonlinear source inversion of the U.S. Geological Survey intensities of the Whittier Narrows, 1987 earthquake. Bull. Seismol. Soc. Am., 94, 1737-1747.

Ghisetti, F., 1979: Evoluzione neotettonica dei principali sistemi di faglie della Calabria centrale: Bolletino Società Geologica Italiana, 98, pp. 387–430.

Ghisetti, F., 1981. Upper Pliocene-Pleistocene uplift rates as indicators of neotectonic pattern: an example from southern Calabria (Italy). Zeitschrift fur Geomorphologie, 40, pp. 93–118.

Ghisetti F., & Vezzani L. (1982) - Strutture tensionali e compressive indotte da meccanismi protondi lungo la linea del Pollino (Appennino meridionale). Bollettino della Societa Geologica Italiana, 101(3), 385-440.

Govers, R., Meijer, P. & Rijgsman, W. (2009) Regional isostatic response to Messinian Salinity Crisis events. Tectonophysics, 463, 109–129.

Graessner T. & Schenk V. (1999) - Low-pressure metamorphism of palaeozoic pelites in the Aspromonte, Southern Calabria: constraints for the thermal evolution in the calabrian crustal cross-section during the hercynian orogeny. J. Metam. Geol., 17, 157-172.

Graessner, T., Schenk, V., Br¨ocker, M., Mezger, K., 2000. Geochronological constraints on the timing of granitoid magmatism, metamorphism and post-metamorphic cooling in the Hercynian crustal cross-section of Calabria. J. Metamorphic Geol. 18, 409–421.

Graessner T. & Schenk V. 2001. An exposed Hercynian deep continental crustal section in the Sila massif of northern Calabria: Mineral chemistry, petrology and a P–T path of granulite facies metapelitic migmatites and metabasites. Journal of Petrology 42, 931–61.

Grimison, N.L., Chen, W.P., 1986. The Azores-Gibraltar plate boundary —focal mechanisms, depths of earthquakes, and their tectonic implications. Journal of Geophysical Research — Solid Earth and Planets 91 (B2), 2029–2047. http://dx.doi.org/ 10.1029/JB091iB02p02029.

Gruppo di Lavoro CPTI, 2004. Catalogo Parametrico dei Terremoti Italiani, versione 2004 (CPTI04). INGV, Bologna (http://emidius.mi.ingv.it/CPTI/)

Guarnieri, P. 2006: Plio-Quaternary segmentation of the south Tyrrhenian forearc basin. Int. J. Earth Sci., 95, pp. 107-118.

Gueguen E., Doglioni C., Fernandez M., 1998. On the post-25 Ma geodynamic evolution of the western Mediterranean. Tectonophysics, 298, pp. 259-269.

Guerra I., Savaglio A. (2006) 8 settembre 1905: terremoto in Calabria., Università della Calabria.337 pp.

Guerra I. , De Rose C. , Gervasi A. , Neri G. , Orecchio B. , Presti D., 2006 "Attività sismica recente in Calabria Centro-Meridionale", Rende: Università della Calabria" in Guerra I., Savaglio A. (eds) 8 settembre 1905: terremoto in Calabria., Università della Calabria. Cap. 5. pp. 261-288

Guerrera F., Martin-Algarra A., Perrone V., 1993. Late Oligocene-Miocene syn-/-late-orogenic successions in Western and Central Mediterranean Chains from the Betic Cordillera to the Southern Apennines. Terra Nova, 5: 525-544.

Guidoboni, E., Ferrari, G., Mariotti, D., Comastri, A., Tarabusi, G., Valensise, G., 2007. CFTI4Med, Catalogue of Strong Earthquakes in Italy (461 B.C.–1997) and Mediterranean Area (760 B.C.–1500). INGV-SGA.

Kagan, Y.Y., 1991. 3-D rotation of double-couple earthquake sources. Geophysical Journal International 106, 709–716.

Knott, *S. D.*, *1987*, The Liguride Complex of Southern Italy: A Cretaceous to Paleogene accretionary wedge: Tectonophysics, v. 142, pp. 217-226.

Iannace A., Boni M. & Zamparelli V. 1995. The middle-Upper Triassic of the San Donato Unit Auc. (northern Calabria): Stratigraphy, paleogeography and tectonic implications. Rivista Italiana Paleontologia Stratigrafia 101, 301–24.

Iannace A., Vitale S., D'Errico M., Mazzoli S., Distaso A., Macaione E., Messina A., Reddy S.M., Somma R., Zamparelli V., Zattin M. & Bonardi G. (2007) - The carbonate tectonic units of northern Calabria (Italy): a record of Apulian palaeomargin evolution and Miocene convergence, continental crust subduction, and exhumation of HP-LT rocks. Journal of the Geological Society, London, 164, 2007, 1165-1186.

Ietto A. & Barilaro A. M. 1993. L'unità di San Donato quale margine deformato cretacico-paleogenico del bacino di Lagonegro (Appennino meridionale-Arco- Calabro). Bollettino della Società Geologica Italiana 111, 193–215.

Isacks, B., Molnar, P., 1971. Distribution of stresses in the descending lithosphere from a global survey of focal-mechanism solutions of mantle earthquakes. Reviews of Geophysics and Space Physics 9, 103–174.

Jackson, J., McKenzie, D., 1988. The relationship between plate motions and seismic moment tensors, and the rates of active deformation in the Mediterranean and Middle-East. Geophysical Journal International 93, 45–73.

Jacques, E., Monaco, C., Tapponier, P., Tortorici, L., Winter, T., 2001. Faulting and earthquake triggering during the 1783 Calabria seismic sequence. Geophysical Journal International 147, 499–516.

Langone A. , Gueguen E., Prosser G., Caggianelli A. and Rottura A., 2006: The Curinga - Girifalco fault zone (northern Serre, Calabria) and its significance within the Alpine tectonic evolution of the western Mediterranean. Journal of Geodynamics, 42, pp. 140 - 158.

Lay, T., Wallace, T.C., 1995. Modern Global Seismology. Academic Press, San Diego.

Lanzafame G., Spadea P. & Tortorici L. 1979. Mesozoic ophiolites of northern Calabria and Lucanian Apennines (Southern Italy). Ofioliti 4, 173–82.

Lentini F. & Vezzani L. (1975) - Le unità meso-cenozoiche della copertura sedimentaria del basamento cristallino peloritano (Sicilia nord-orientale). Boll. Soc. Geol. It., 94: 537–554.

Lentini F., Carbone S., Catalano S., 1994. Main structural domains of the central Mediterranean Region and their Neogene tectonic evolution. Boll. Geof. Teor. e Appl., 36: 103-125.

Levine D.; 1996: Users guide to the PGAPack parallel genetic algorithm library. Rep. Argonne National Laboratory, ANL-95/18, Argonne, IL, 73 pp.

Li, H., Michelini, A., Zhu, L., Bernardi, F., Spada, M., 2007. Crustal velocity structure in Italy from analysis of regional seismic waveforms. Bulletin of the Seismological Society of America 97, 2024–2039. http://dx.doi.org/10.1785/0120070071.

Liberi, F., Morten, L., Piluso, E., 2006. Geodynamic significance of ophiolites within the Calabrian Arc. Island Arc 15, 26–43.

Longhitano, S.G., Chiarella, D., Di Stefano, A., Messina, C., Sabato, L. and Tropeano, M. (2012b) Tidal signatures in Neogene to Quaternary mixed deposits of southern Italy straits and bays. In: Modern and Ancient Depositional Systems: Perspectives, Models and Signatures (Eds S.G. Longhitano, D. Mellere and R.B. Ainsworth), Sed. Geol. Spec. Issue, 279, 74–96.

Longhitano S. G., Chiarella D. and Muto F., 2014: Three-dimensional to two-dimensional cross-strata transition in the lower Pleistocene Catanzaro tidal strait transgressive succession (southern Italy), Sedimentology. 61, 2136–2171 doi: 10.1111/sed.12138.

Loreto, M.F., F. Zgur, L. Facchin, U. Fracassi, F. Pettenati, I. Tomini, M. Burca, P. Diviacco, C. Sauli, G. Cossarini, C. De Vittor, D. Sandron, and the Explora technicians team 2012. In Search of New Imaging For Historical Earthquakes: A New Geophysical Survey Offshore Western

Calabria (Southern Tyrrhenian Sea, Italy), Boll. Geof. Teor. App., v. 53. http://dx.doi.org/10.4430/bgta0046.

Loreto M.F., Fracassi U., Franzo A., Del Negro P., Zgur F. and Facchin L., 2013: Approaching the potential seismogenic source of the 8 September 1905 earthquake: New geophysical, geological and biochemical data from the S. Eufemia Gulf (S Italy). Marine Geology, 343, pp. 62–75.

McCaffrey, R., Molnar, P., Roecker, S., Joyodiwiryo, Y., 1985. Microearthquake seismicity and fault plane solutions related to arc-continent collision in the Eastern Sunda Arc, Indonesia. Journal of Geophysical Research 90, 4511–4528.

Malinverno, A., Ryan, W.B.F., 1986. Extension in the tyrrhenian sea and shortening in the apennines as result of arc migration driven by sinking of the lithosphere. Tectonics 5, 227–245.

Mantovani, E., Babbucci, D., AIbareIIo, D. and Mucciarelli, M., 1990. Deformation pattern in the central Mediterranean and behavior of the Africa/Adriatic promontory. Tectonophysics, 179: 63-79.

Manzi V., Lugli S., Roveri M. & Schreiber B.C., Gennari, R., 2010. The Messinian "Calcare di Base" (Sicily, Italy) revisited. Geologica Society of America Bullettin. doi:10.1130/B30262.1.

Massari, F., Prosser, G., Capraro, L., Fornaciari, E., Consolaro, C., 2010. A revision of the stratigraphy and geology of the south-western part of the Crotone Basin (South Italy). Ital. J. Geosci. 129, 353–384.

Mattei M., Cifelli F., and D'Agostino N., 2007. The evolution of the Calabrian arc: Evidence from paleomagnetic and GPS observations, Earth Planet. Sci. Lett., 263, pp. 259-274.

Messina A., Compagnoni R., De Vivo B., Perrone V., Russo S., Barberi M. & Scott B. (1991a) - Geological and petrochemical study of the Sila Massif plutonic rocks (Northen Calabria, Italy). Boll. Soc. Geol. It., **110**, 165-206.

Messina A., Russo S., Perrone V. & Giacobbe A. (1991b) – Calcalkaline Late Variscan two micacordierite-Al silicate-bearing intrusion of the Sila batholith (northen sector of the Calabrian- Peloritan Arc, Italy). Boll. Soc. Geol. It., **110**, 365-389.

Messina, A., Russo, S., Borghi, A., Colonna, V., Compagnoni, R., Caggianelli, A., Fornelli, A., Piccarreta, G., 1994. Il Massiccio della Sila, Settore settentrionale dell'Arco Calabro-Peloritano (The Sila Massif, northern sector of the Calabrian-Peloritan Arc). Bollettino della Societ`a Geologica Italiana 113, 539–586.

Michelini, A., Lomax, A., Nardi, A., Rossi, A., 2006. La localizzazione del terremoto della Calabria dell'8 settembre 1905 da dati strumentali. In: Guerra, I., Savaglio, A. (Eds.), 8 settembre 1905, terremoto in Calabria. Università della Calabria, pp. 225–240.

Miyauchi, T., Dai Pra, G., Labini, S.S., 1994. Geochronology of Pleistocene marine terraces and regional tectonics in the Tyrrhenian coast of South Calabria, Italy. Il Quaternario 7, 17–34.

Milia A., Turco E., Pierantoni P.P. and Schettino A., 2009: Four-dimensional tectonostratigraphic evolution of the Southern peri-Tyrrhenian Basins (Margin of Calabria, Italy). Tectonophysics 476, pp. 41–56.

Monaco, C., Tortorici, L., Nicolich, R., Cernobori, L., Costa, M., 1996. From collisional to rifted basins: an example from the southern Calabrian Arc (Italy). Tectonophysics 266, 233–249.

Monaco, C. and Tortorici, L., 2000: Active faulting in the Calabrian Arc and eastern Sicily. Journal of Geodynamics, 29, pp. 407–424.

Muto F. and Perri E., 2002: Evoluzione tettono - sedimentaria del bacino di Amantea, Calabria occidentale. Boll. Soc. Geol. It., 121, pp. 391 - 409.

Neri G, Caccamo D, Cocina O, Montalto A (1996) Geodynamic implications of earthquake data in the southern Tyrrhenian sea. Tectonophysics 258:233–249.

Neri G., Orecchio B., Totaro C., Falcone G., and Presti D., 2009: Subduction beneath southern Italy close the ending: results from seismic tomography. Seismol. Res. Lett., 80, pp. 63-70.

Ogniben, L., 1969. Schema introduttivo alla geologia del confine calabro-lucano (Introductory scheme to the geology of the Calabrian-Lucanian boundary). Memorie della Societ`a Geologica Italiana 8, 453–763.

Ogniben L. (1973) - Schema geologico della Calabria in base ai dati odierni. Geologica Romana, 12, 243-585.Paglionico and Piccarreta, 1976.

Ortolano G., Cirrincione R. & Pezzino A. (2005) - P-T evolution of alpine metamorphism in the southern Aspromonte Massif (Calabria - Italy). Schweiz. Mineral. Petrogr. Mitt., 85-1: 31-56.

Peacock D.C.P. and Parfitt E.A., 2002: active relay ramps and fault propagation on Kilauea Volcano, Hawaii. Journal of Structural Geology, 24, pp. 729-744.

Pepe, F., Sulli, A., Bertotti, G., Cella, F., 2010. Architecture and Neogene to recent evolution of the western Calabrian continental margin: an upper plate perspective to the Ionian subduction system, central Mediterranean. Tectonics 29. http://dx.doi.org/10.1029/2009TC002599. TC3007.

Perri F. & Ohta T. (2014) -Paleoclimatic conditions and paleoweathering processes on Mesozoic continental redbeds fromWestern-Central Mediterranean Alpine Chain. Palaeogeography, Palaeoclimatology, Palaeoecology 395, pp. 144–157.

Perrone, V., 1996. Une nouvelle hypoth`ese sur la position pal´eog´eographique et l'´evolution tectonique des Unit´es de Verbicaro et de San Donato (r´egion Calabro-Lucanienne; Italie): implications sur la limite Alpes-Apennin en Calabre. Comptes Rendus de l'Acad´emie des Sciences Paris 322 (IIa), 877–884.

Pettenati F. and Sirovich L.; 2003: Test of source inversion of the USGS "Felt Reports" of the Whittier Narrows, 1987 earthquake. Bull. Seismol. Soc. Am., 93, 47-60.

Pettenati F. and Sirovich L.; 2007: Validation of intensity-based source inversion of three destructive Californian Earthquakes. Bull. Seismol. Soc. Am., 97, 1587-1606, doi:10.1785/0120060169.

Pezzino A., Pannucci S., Puglisi G., Atzori P., Ioppolo S. & Lo Giudice A. (1990) - Geometry and metamorphic environment of the contact between the Aspromonte - Peloritani Unit (Upper Unit) and Madonna dei Polsi Unit (Lower Unit) in the central Aspromonte area (Calabria). Boll. Soc. Geol. It., 109: 455-469.

Pezzino A., Puglisi G., Pannucci S. & Ioppolo S. (1992) - Due unità cristalline a grado metamorfico diverso in Aspromonte centrale. Geometria dei loro rapporti, ambientazione metamorfica del loro contatto e caratteri petrografici delle metamorfiti. Boll. Soc. Geol. It.,: 111, 69–80.

Piluso E. & Morten L. 2004. Hercynian high temperature granulites and migmatites from the Catena Costiera, northern Calabria, southern Italy. Periodico di Mineralogia 73, 159–72.

Piatanesi, A., Tinti, S., 2002. Numerical modelling of the September 8, 1905 Calabrian (southern Italy) tsunami. Geophysical Journal International 150, 271–284. http:// dx.doi.org/10.1046/j.1365-246X.2002.01700.x.

Pondrelli, S., Morelli, A., Ekstrom, G., Mazza, S., Boschi, E., Dziewonski, A.M., 2002. European–Mediterranean regional centroid-moment tensors: 1997–2000. Physics of the Earth and Planetary Interiors 130 (1–2), 71–101.

Pondrelli, S., Morelli, A., Ekstrom, G., 2004. European–Mediterranean regional centroid-moment tensor catalog: solutions for years 2001 and 2002. Physics of the Earth and Planetary Interiors 145 (1–4), 127–147.

Pondrelli, S., Salimbeni, S., Ekstrom, G., Morelli, A., Gasperini, P., Vannucci, G., 2006. The Italian CMT dataset from 1977 to the present. Physics of the Earth and Planetary Interiors 159 (3–4), 286–303.

Presti, D., et al., Earthquake focal mechanisms, seismogenic stress, and seismotectonics of the Calabrian Arc, Italy, Tectonophysics (2013), http://dx.doi.org/10.1016/j.tecto.2013.01.030

Riuscetti M. and Schick R.; 1974: Earthquakes and tectonics in southern Italy. In: Proc. Joint Symp. Eur. Seismol. Comm. and Eur. Geophys. Sco., Trieste, Italy, September 21, pp. 59-78.

Rizzo, G.B., 1906. In: Clausen, C. (Ed.), Sulla velocità di propagazione delle onde sismiche del terremoto della Calabria del giorno 8 Settembre 1905 (46 pp.).

Roda C., 1964. Distribuzione e facies dei sedimenti neogenici nel Bacino Crotonese. Geol. Rom., 3: 319-366.

Reasenberg P.A. e Oppenheimer D., 1985: FPFIT, FPPLOT AND FPPAGE: FORTRAN computer programs for calculating and displaying earthquake fault-plane solutions - U.S. Geol. Surv., Open-file Report 85-739.

Rossetti, F., B. Goffé, P. Monié, C. Faccenna, and G. Vignaroli (2004), Alpine orogenic PTt deformation history of the Catena Costiera area and surrounding regions (Calabrian Arc, southern Italy): The nappe edifice of northern Calabria revised with insights on the Tyrrhenian-Apennine system formation, Tectonics, 23, TC6011, doi:10.1029/ 2003TC001560.

Rotondi, R., 2010. Bayesian nonparametric inference for earthquake recurrence time distributions in different tectonic regimes. Journal of Geophysical Research: Solid Earth 115, B01302.

Rottura, A., Del Moro, A., Pinarelli, L., Petrini, R., Peccerillo, A., Caggianelli, A., Bargossi, G., Piccarreta, G., 1991. Relationships between intermediate and acidic rocks in orogenic granitoid suites: petrological, geochemical, and isotopic (Sr, Nd, Pb) data from Capo Vaticano (Southern Calabria, Italy). Chem. Geol. 92, 153–176.

Roveri, M., Bassetti, M.A. and Ricci Lucchi, F., 2001. The Mediterranean Messinian salinity crisis: an Apennine foredeep perspective. Sed. Geol., 140, 201–214.

Roveri M., Lugli S., Manzi V. and Schreiber B.C. (2008) – The Messinian salinity crisis: a sequence-stratigraphic approach. GeoActa, Special Publication, **1**, 117-138.

Rovida, A., Camassi, R., Gasperini, P., Stucchi, M., 2011. CPTI11, the 2011 version of the Parametric Catalogue of Italian Earthquakes. Milano, Bologna.

Salvini, F., Vittori, E., 1982. Analisi strutturale della linea Olevano-Antrodoco-Posta (Ancona-Anzio Auct.): metodologia di studio delle deformazioni fragili e presentazione del tratto meridionale. Mem. Soc. Geol. Ital. 24, 337-356.

Salvini, F., 2002. The Structural Data Integrated System Analyzer. Version 3.43b (11/12/2002). Dept. of Earth Sciences, University "Roma Tre", Rome, Italy, Free software available upon request at: http://www.dea.uniroma3.it/begin.htm.

Scandone P. 1982. Structure and evolution of the Calabrian Arc. Earth and Evolutionary Science 3, 172–80.Schenk, V., 1980. U-Pb and Radiometric Dates and their Correlation with Metamorphic Events in the Granulite-Facies Basement of the Serre, southern Calabria (Italy). Contrib. Mineral. Petrol. 73, 23–38.

Schenk, V., 1981. Synchronous uplift of the lower crust of the Ivrea Zone and of southern Calabria and its possible consequences for the Hercynian orogeny in southern Europe. Earth Planet. Sci. Lett. 56, 305–320.

Schlische R. W. and Withjack M.O., 2009: Origin of fault domains and fault-domain boundaries (transfer zones and accommodation zones) in extensional provinces: Result of random nucleation and self-organized fault growth. Journal of Structural Geology, 31, pp. 910–925.

Scholz C.H. 2002 the mechanics of earthquakes and faulring. 2nd ed. 471 pp..

Scognamiglio, L., Tinti, E., Michelini, A., 2009. Real-time determination of seismic moment tensor for the Italian Region. Bulletin of the Seismological Society of America 99 (4), 2223–2242. http://dx.doi.org/10.1785/0120080104.

Selvaggi, G., Chiarabba, C., 1995. Seismicity and P wave velocity image of the southern Tyrrhenian subduction zone. Geophysical Journal International 121, 818–826. http://dx.doi.org/10.1111/j.1365-246X.1995.tb06441.x

Serpelloni, E., Vannucci, G., Pondrelli, S., Argnani, A., Casula, G., Anzidei, M., Baldi, P., Gasperini, P., 2007. Kinematics of the western Africa–Eurasia plate boundary from local machanisms and GPS data. Geophysical Journal International 169, 1180–1200.

Serpelloni, E., R. Bürgmann,M. Anzidei, P. Baldi, Mastrolembo Ventura B., and Boschi E., 2010. Strain accumulation across the Messina Straits and kinematics of Sicily and Calabria from GPS data and dislocation modeling, Earth Planet. Sc. Lett., 298(3–4), pp. 347–360.

Sirovich L.; 1996: A simple algorithm for tracing out synthetic isoseismals. Bull. Seismol. Soc. Am., 86, 1019-1027.

Sirovich L. and Pettenati F.; 2004: Source inversion of intensity patterns of earthquakes: a destructive shock in 1936 in northern Italy. J. Geophys. Res., 109, B10309, doi:10.1029/2003JB002919.

Sirovich L., Pettenati F., Cavallini F. and Bobbio M.; 2002: Natural-Neighbor Isoseismals. Bull. Seismol. Soc. Am., 92, 1933-1940.

Sirovich L. and Pettenati F.; 2004 Sorgenti e meccanismi focali di due terremoti distruttivi del 1783 in Calabria dall'inversione dei piani quotati macrosismici. Conference paper to GNGTS: 26º Convegno , Rome, 13-15 November 2007

Sykes, L.R., 1967. Mechanism of earthquakes and nature of faulting on the mid-oceanic ridges. Journal of Geophysical Research 72, 5–27.

Tan, Y., Zhu, L., Helmberger, D., Saikia, C., 2006. Locating and modeling regional earthquakes with two stations. Journal of Geophysical Research 111, B01306.

Tansi, C., Muto, F., Critelli S., and Iovine G., 2007. Neogene–Quaternary strike-slip tectonics in the central Calabria Arc (southern Italy). J. Geodyn., 43, pp. 397–414.

Tiberti, M.M., Fracassi, U., Valensise, G., 2006. Il quadro sismotettonico del grande terremoto del 1905. In: Guerra, I., Savaglio, A. (Eds.), 8 Settembre 1905: Terremoto in Calabria. Università della Calabria, pp. 181–205.

Tortorici, L., 1982. Lineamenti geologico-strutturali dell'Arco Calabro Peloritano (Geologic-structural lineaments of the Calabrian-Peloritan Arc). Societ`a Italiana di Mineralogia e Petrografia 38, 927–940.

Tortorici G., Bianca M., Monaco M., Tortorici L., Tansi C., De Guidi G. and Catalano S., 2002. Quaternary normal faulting and marine terracing in the area of Capo Vaticano and S. Eufemia Plain (Southern Calabria, Italy). Studi Geologici Camerti, 2, pp. 1 - 16.

Tortorici G., Bianca M., De Guidi G., Monaco C. & Tortorici L. (2003) - Fault activity and marine terracing in the Capo Vaticano area (southern Calabria) during the Middle-Late Quaternary, Quat. Int., 101-102, 269-278.

Turco, E., Maresca, R. and Cappadona, P., 1990. La tettonica plio-pleistocenica del confine calabro-lucano: modello cinematico (Plio-Pleistocene tectonics at the Calabrian-Lucanian boundary: a kinematic model). Memorie della Società Geologica Italiana, 45, pp. 519–529.

Trincardi F. Cipolli M., Ferretti P., La Morgia J., Ligi M., Marozzi, G., Palumbo V., Taviani M. and Zitellini N. 1987. Slope basin evolution on the Eastern Tyrrhenian margin: preliminary report. Giornale di Geologia, ser. 3", vol. 49/2, pp. 1-9.

Trincardi, F., Corregiari, A., Field, M.E., Normark, W.R., 1995. Turbidite deposition from multiple sources: Quaternary Paola Basin (eastern Tyrrenian Sea). Journal of Sedimentary Research 65, 469–483.

Tripodi, V., Muto, F. and Critelli, S., 2013. Structural style and tectono-stratigraphic evolution of the Neogene- Quaternary Siderno Basin, southern Calabrian Arc, Italy. Int. Geol. Rev., 4, 468–481.

Van Dijk, J.P., Scheepers, P.J.J., 1995. Neotectonic rotations in the Calabrian Arc; implications for a Pliocene–Recent geodynamic scenario for the Central Mediterranean. Earth Sci. Rev. 39, 207–246.

Van Dijk J.P., Bello M., Brancaleoni G.P., Cantarella G., Costa V., Frixa A., Golfetto F., Merlini S., Riva M., Torricelli S., Toscano C. and Zerilli A., 2000. A regional structural model for the northern sector of the Calabrian Arc (southern Italy). Tectonophysics, 324, pp. 267-320.

Vezzani, L., 1967. Il bacino plio-pleistocenico di S. Arcangelo (Lucania). Atti Accad. gioenia sci. nat. Catania 18, 207–227.

Yilmaz, Ö. (2001). *Seismic data analysis* (Vol. 1, pp. 74170-2740). Tulsa, OK: Society of exploration geophysicists.

Westaway, R., 1992. Seismic moment summation for historical earthquakes in Italy: tectonic implications. Journal of Geophysical Research 97, 15.437–15.464.

Westaway R., 1993: Quaternary uplift of Southern Italy. Journal of Geophysical Research 98 (B12), pp. 741–772.

Wilson, J.T., 1965. A new class of faults and their bearing on continental drift. Nature 207, 343–347.

Williams G. D., Powell C. M. and. Cooper M. A., 1989. Geometry and kinematics of inversion tectonics. 15. *Geological Society, London, Special Publications* 1989, v.44; pp. 3-15

Wise D.U. & Vincent R.J. 1965. Rotation axis method for detecting conjugate planes in calcite petro-fabric. American Journal of Science. 263, pp. 289-301.

Wortel, M.J.R. & Spackman, W., 1992: Structure and dynamics of subducted lithosphere in the Mediterranean region; Proceedings of the Koninklijke Nederlandse Akademie Van Wetenschappen-Biological Chemical Geological Physical and Medical Sciences, 95, pp. 325–347.

Wortel, R., & Spakman W., 2000. Subduction and slab detachment in the Mediterranean-Carpathian region. Science, 290, pp. 1910-1917.

Zanettin Lorenzoni E., 1982. Relationships of main structural elements of Calabria (southern Italy). N. Jb. Geol. Pal¨aont. Mh., 7: 403-418.

Zecchin, M., Caffau, M., Civile, D., Critelli, S., Di Stefano, A., Maniscalco, R., Muto, F., Sturiale, G. and Roda, C., 2012. The Plio-Pleistocene evolution of the Crotone Basin (southern Italy): interplay between sedimentation, tectonics and eustasy in the frame of Calabrian Arc migration. Earth-Sci. Rev., 115, pp. 273-303.

Zecchin M., Civile D., Caffau M., Muto F., Di Stefano A., Maniscalco M. & Critelli S. (2013a) - The Messinian succession of the Crotone Basin (southern Italy) I. Stratigraphic architecture reconstructed by seismic and well data: Marine and Petroleum Geology, 48, 455-473.

Zecchin, M., Praeg, D., Ceramicola, S., Muto, F., 2015. Onshore to offshore correlation of regional unconformities in the Plio-Pleistocene sedimentary successions of the Calabrian Arc (central Mediterranean). Earth Sci. Rev. 142, 60–78.

Zalohar J., Vrabec M., 2007: Paleostress analysis of heterogeneous fault-slip data: The Gauss method. Journal of Structural Geology, 29, 1798-1810.

Zeck S. E., 1990. The exhumation and preservation of deep continental crust in the northwestern Calabrian arc, southern Italy. PhD Thesis, University of California, Santa Barbara, 277 pp.

Zhao, L.S., Helmberger, D., 1994. Source estimation from broad-band regional seismograms. Bulletin of the Seismological Society of America 85, 590–605.

Zhu, L., Helmberger, D., 1996. Advancement in source estimation technique using broadband regional seismograms. Bulletin of the Seismological Society of America 86, 1634–1641.

Zhu, L., Akyol, N., Mitchell, B., Sozbiliz, H., 2006. Seismotectonics of western Turkey from high resolution and moment tensor determinations. Geophysical Research Letters 33, L07316. http://dx.doi.org/10.1029/2006GL025842.

Zoback, M.L., 1992. First- and second-order patterns of stress in the lithosphere: the World Stress Map project. Journal of Geophysical Research 97 (11), 703–711 (728).

Web sites

http://cnt.rm.ingv.it/tdmt/: Time Domain Moment Tensor Catalogue available from INGV 'Centro Nazionale Terremoti'

http://diss.rm.ingv.it/diss/: DISS Working Group (2015). Database of Individual Seismogenic Sources (DISS), Version 3.2.0

http://emidius.mi.ingv.it/CPTI: CPTI11 the 2011 version of the Parametric Catalogue of Italian Earthquakes.

http://pr5sit.regione.calabria.it// 'Centro cartografico della Regione Calabria'

http://sgi.isprambiente.it/GMV2/: ISPRA-SGI GeoMapViewer

http://storing.ingv.it/cfti4med/: Catalogue of Strong Earthquakes in Italy (461 B.C.–1997) and Mediterranean Area (760 B.C.–1500). INGV-SGA.

http://unmig.sviluppoeconomico.gov.it/videpi/: ViDEPI Project: 'Visibilità dei Dati afferenti all'attività di Esplorazione Petrolifera in Italia'.

http://www.bo.ingv.it/RCMT/Italydataset.html: The Italian CMT (Centroid Moment Tensor) catalogue.

http://www.dea.uniroma3.it/begin.htm: Free software The Structural Data Integrated System Analyzer. Version 3.43b (11/12/2002). Dept. of Earth Sciences, University "Roma Tre", Rome, Italy, Salvini, F., 2002

http://www.socgeol.info**:** Centro di Documentazione della Società Geologica Italiana.

Appendix

Following below we reported poles and slickensides (slicks) contours concerning the structural measurements acquired in the Catanzaro Trough. The data were divided on the base of direction and kinematics, similarly to the chapter 4 the data was divided, in turn, between two aerial domains, the northen and southern, respectively.

a.1 Northern domain

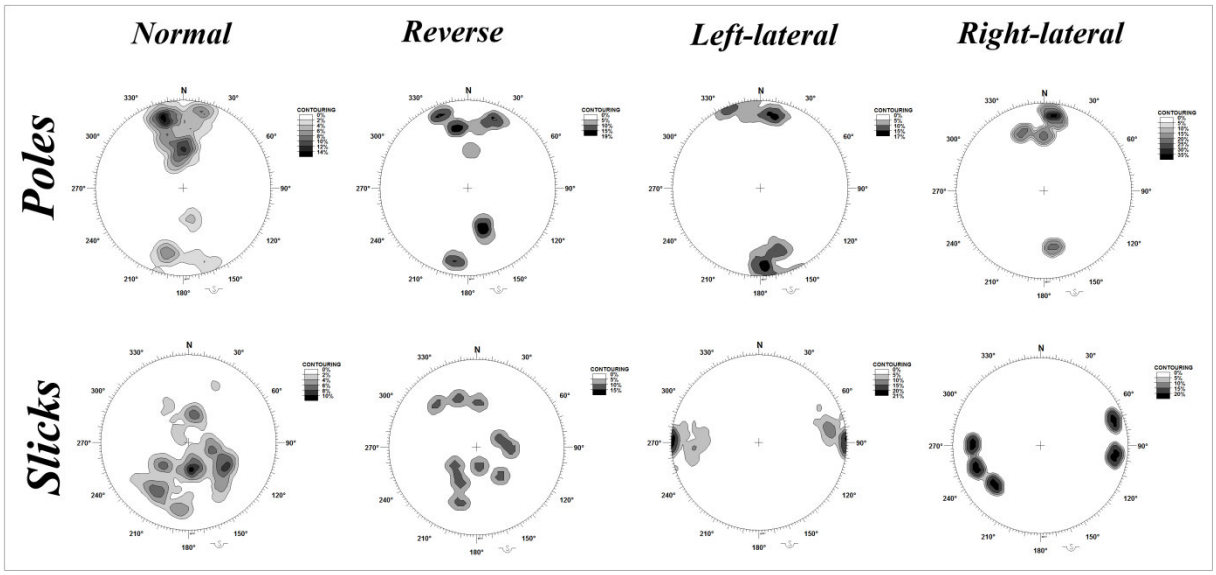

Figure a.1: E-W faults system classified on the base of the kinematics (horizontally arranged), Poles and slicks (vertically arranged).

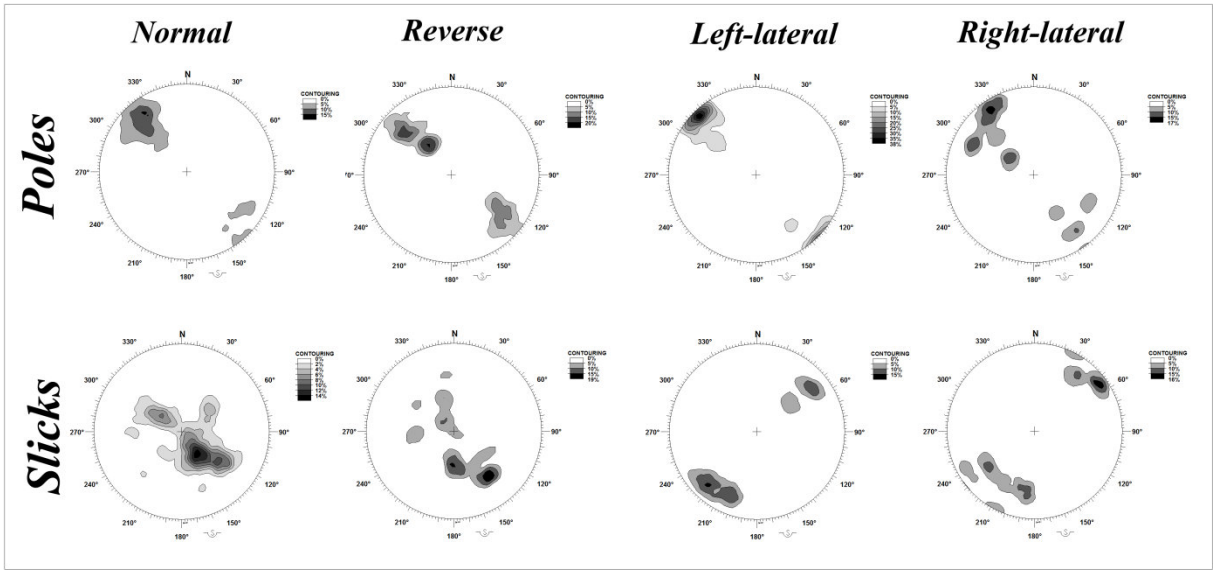

Figure a.2:NE-SW faults system classified on the base of the kinematics (horizontally arranged), Poles and slicks (vertically arranged).

.

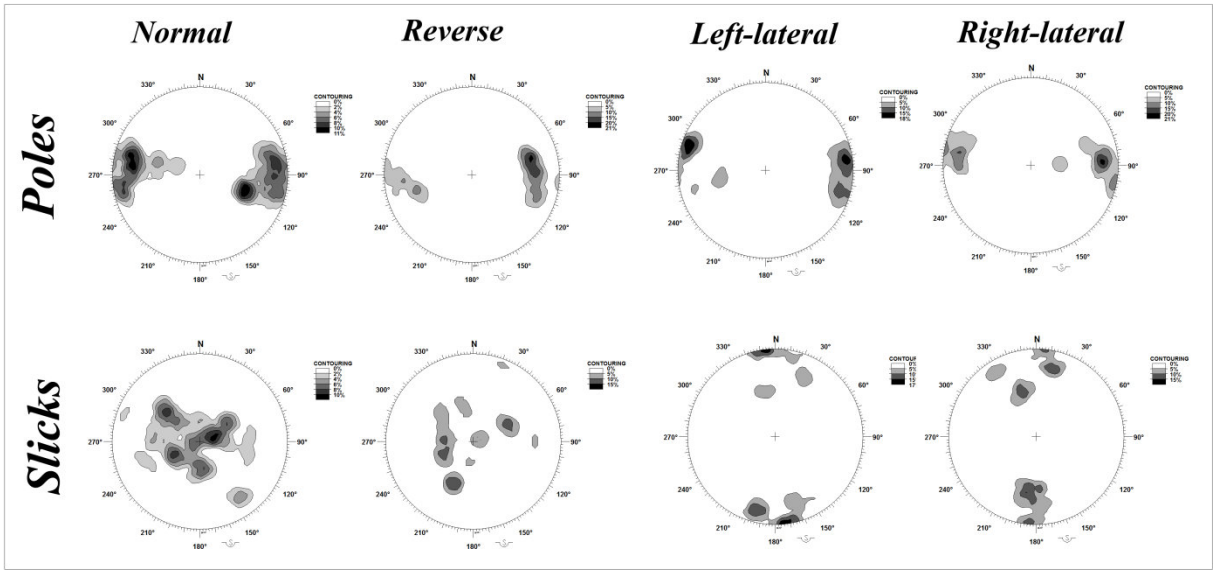

Figure a.3: N-S faults system classified on the base of the kinematics (horizontally arranged), Poles and slicks (vertically arranged).

.

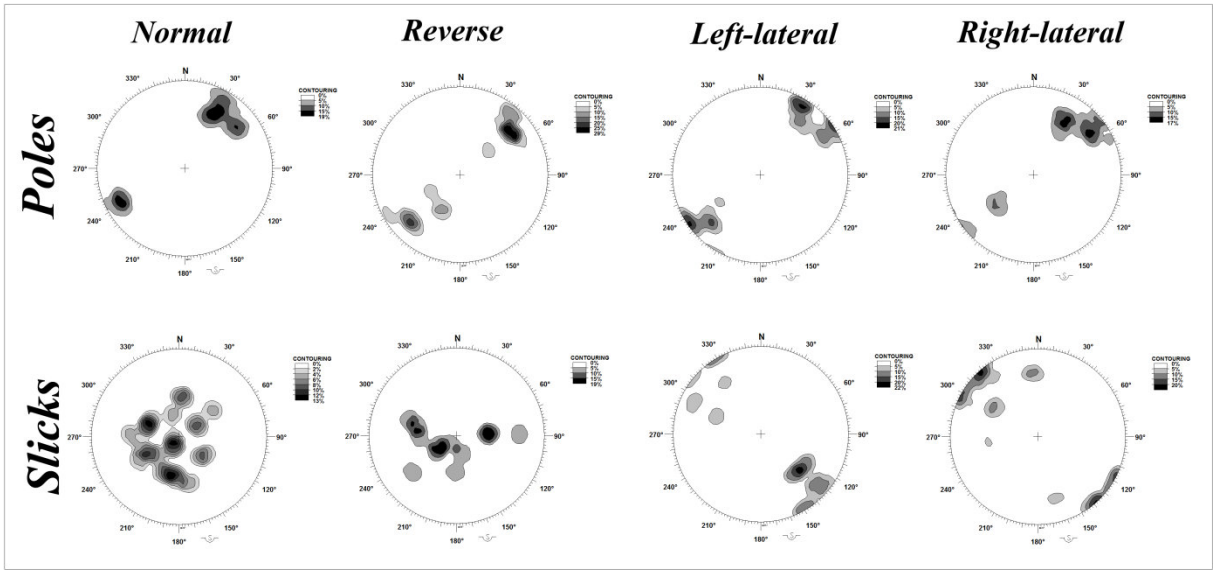

Figure a.4: NW-SE faults system classified on the base of the kinematics (horizontally arranged), Poles and slicks (vertically arranged).

a.2 Southern domain

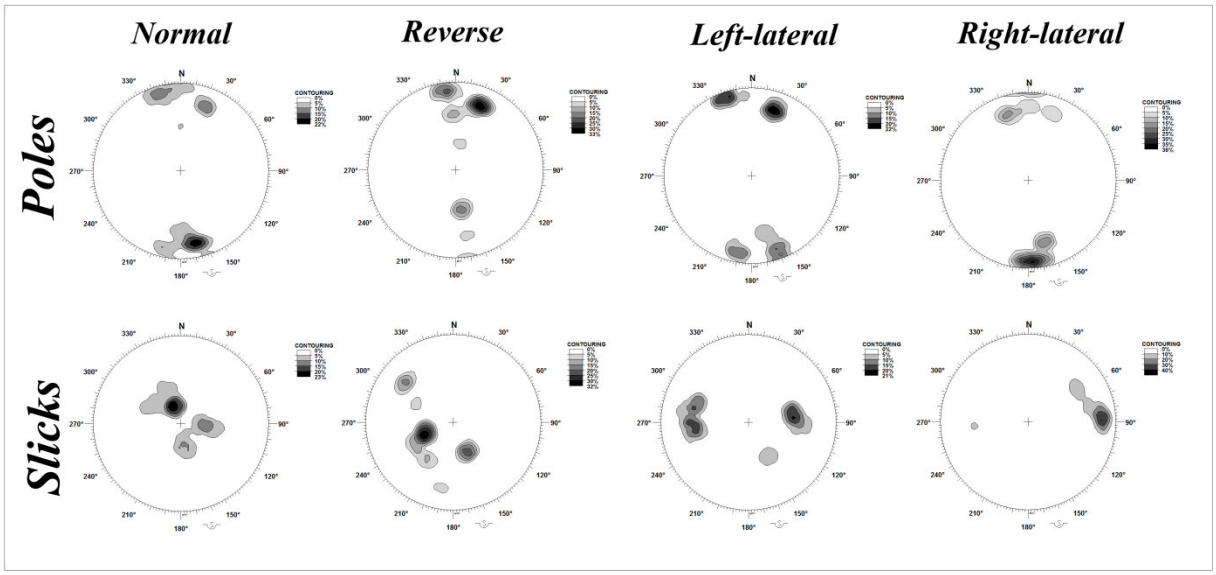

Figure a.5: E-W faults system classified on the base of the kinematics (horizontally arranged), Poles and slicks (vertically arranged).

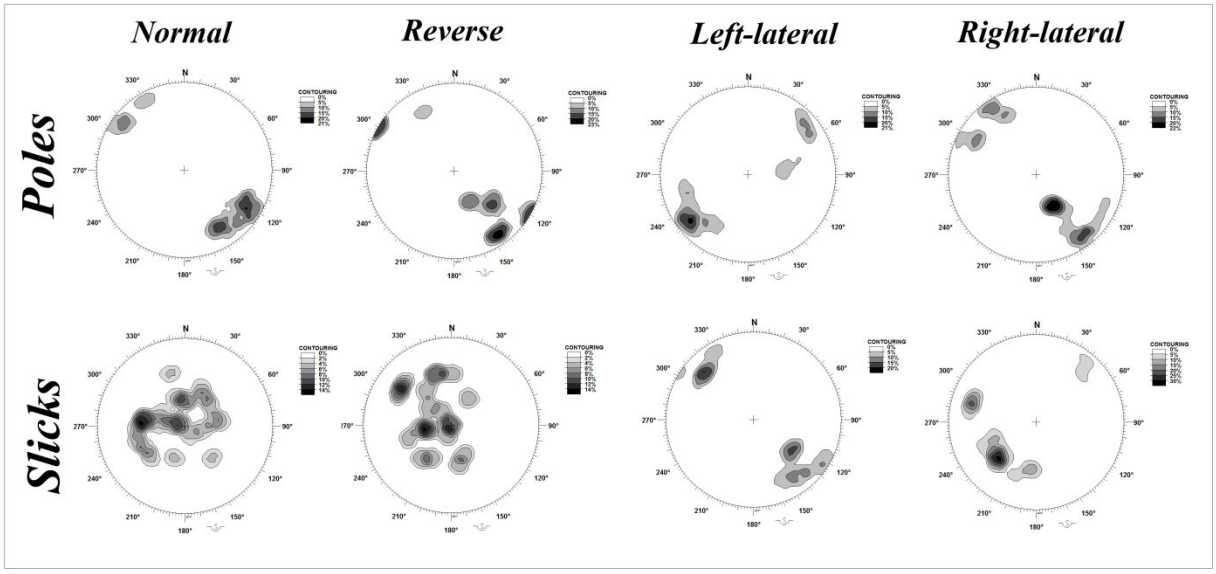

Figure a.6: NE-SW faults system classified on the base of the kinematics (horizontally arranged), Poles and slicks (vertically arranged).

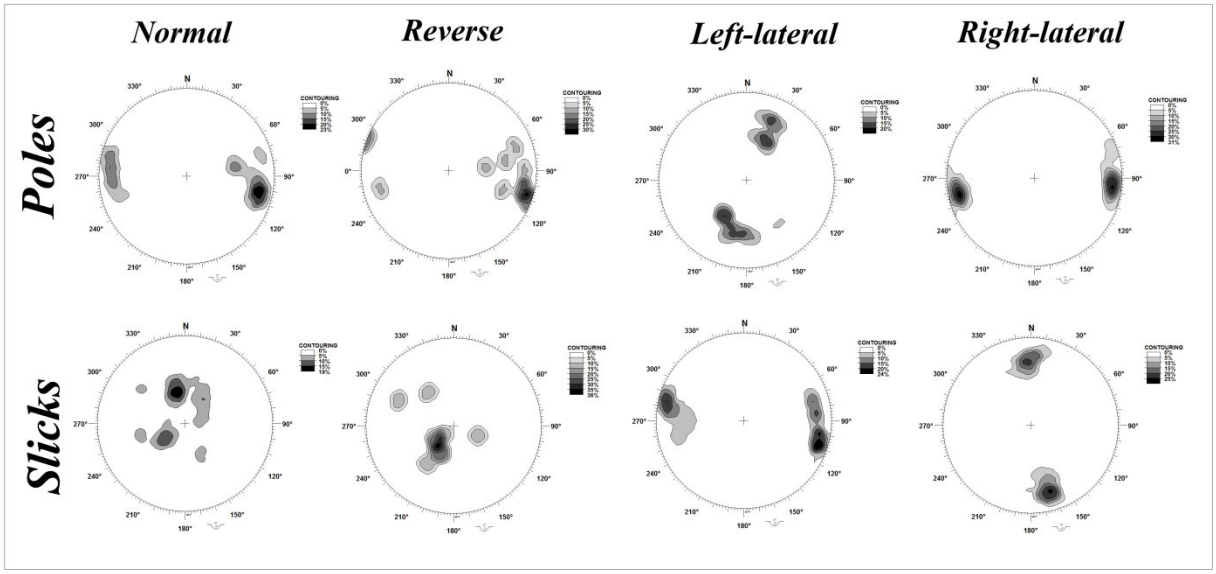

Figure a.7: N-S faults system classified on the base of the kinematics (horizontally arranged), Poles and slicks (vertically arranged).

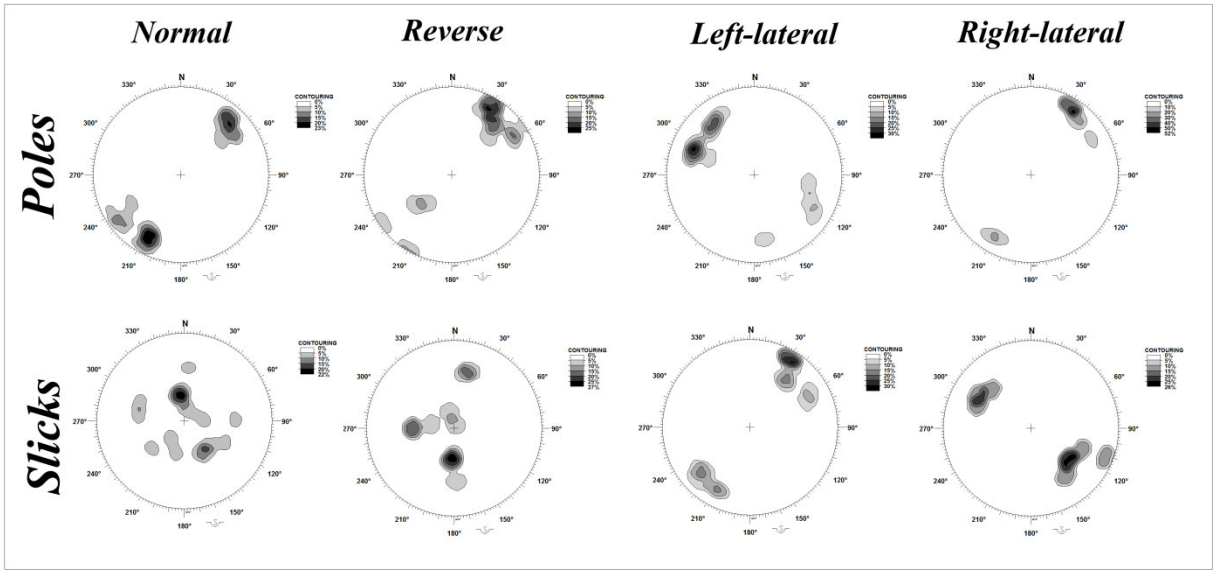

Figure a.8: NW-SE faults system classified on the base of the kinematics (horizontally arranged), Poles and slicks (vertically arranged).